DYNAMIC ON-ROAD MEASUREMENTS OF DRY UNIT WEIGHT AND MOISTURE CONTENT VIA SOIL RESISTIVITY

by

Mohammad H. Sooman

A Dissertation Submitted in

Partial Fulfillment of the

Requirements for the Degree of

Doctor of Philosophy

in Engineering

at

The University of Wisconsin-Milwaukee

December 2024

ABSTRACT

DYNAMIC ON-ROAD MEASUREMENTS OF DRY UNIT WEIGHT AND MOISTURE CONTENT VIA SOIL RESISTIVITY

by

Mohammad H. Sooman

The University of Wisconsin-Milwaukee, 2024
Under the Supervision of Professor Sam Helwany

The current study examines the potential of electrical resistivity, specifically the Wenner four-electrode method, as a non-destructive, efficient, and dependable technique for predicting the in-situ moisture content and dry unit weight of soil during compaction. Although conventional measurement methods are precise, they are frequently time-consuming and labor-intensive, rendering them less effective for real-time field applications. This research establishes a rapid alternative for on-site assessments by establishing an association between critical soil properties, including moisture content, dried unit weight, resistivity values, and the number of compactor passes (compactive effort).

Extensive laboratory testing was conducted on a diverse array of soil types, such as sand, and fat clay, using the standard and modified proctor compaction methodologies. To optimize the number of compactor passes and simulate field conditions, a soil strip container and electrical resistivity meter was designed to accommodate electrode placement and facilitate resistivity measurements. Molds were modified to include vertical apertures. The experiments demonstrated an inverse correlation between soil density and moisture content and electrical resistivity. The rate of electrical resistivity change varied considerably depending on whether the soil was on the dry or saturated side of the optimum moisture content (OMC). The complex interaction between these soil properties was underscored by the observation of a steeper decline in resistivity on the dry side as both density and moisture content increased.

A walk-behind resistivity meter, custom-built, was utilized to measure electrical resistivity. This meter was engineered for dynamic on-road resistivity measurements and is equipped with four cylindrical electrodes that are equally spaced. Field testing confirmed the laboratory results, indicating an important connection between resistivity readings and in-situ moisture content, as well as dry unit weight.

Upon the establishment of a laboratory compaction curve, the study introduces a soil strip method technique for predicting dry unit weight and moisture content in the field using electrical resistivity measurements with the increase of the compactive effort. This method has the potential to be applied to a diverse range of soil types and provides a cost-effective, reliable, and expedited solution for soil compaction monitoring.

In order to accomplish these results, the compaction parameters of sandy soil were assessed using geotechnical-electrical relationships. Two soil types, which were collected and evaluated, were prepared and compacted under conditions that are frequently encountered in geotechnical practice. In order to classify the soil in accordance with the Unified Soil Classification System (USCS), laboratory experiments were implemented, including sieve analysis, liquid limit, and plastic limit. Electrical resistivity measurements were conducted using the Instek GDM-8341 instrument in accordance with ASTM standards, in which the specimens were compacted under varying moisture content, dry density, and compaction efforts. The poorly graded sand was found to have an OMC of 8.5% and an MDD of 120.5 lb/ft^3 under Standard Proctor conditions, and an OMC of 8.0% with an MDD of 132.5 lb/ft^3

under Modified Proctor conditions.

Furthermore, this investigation introduces a soil strip technique that utilizes the relationship between electrical resistivity and the number of passes (compaction effort) of the walk-behind electrical compactor to forecast moisture content and dry unit weight in the field. The findings indicated that soil resistivity is significantly influenced by critical compaction parameters, including moisture content, dry density, and compaction energy, particularly at low moisture content. These results serve to underscore the significance of geotechnical-electrical relationships in the enhancement of the precision and efficacy of soil compaction monitoring.

TABLE OF CONTENTS

LIST OF FIGURES

LIST OF TABLES

ACKNOWLEDGMENTS

I would like to express my deepest gratitude to those who have guided and supported me throughout the course of my research and the completion of this thesis.

First and foremost, I am sincerely thankful to my advisor, Dr. Sam Helwany, for his exceptional guidance, insightful advice, and constant encouragement. His expertise and mentorship have been invaluable in shaping my research. I am also deeply grateful to Dr. Mustafa Al Salah from Caterpillar Inc. for their financial support and valuable insights, which played a crucial role in the success of this research.

I extend my heartfelt appreciation to the Department of Civil and Environmental Engineering at the University of Wisconsin-Milwaukee for providing the resources and support necessary for this study.

Finally, I owe my deepest thanks to my mom and dad for their unconditional love, sacrifices, and belief in my abilities. I am also profoundly grateful to my beautiful lady, soon to be my wife, for her unwavering support, patience, and encouragement during this journey.

To everyone who contributed to this work, in both direct and indirect ways, thank you. Your contributions have been invaluable.

Chapter 1: Introduction

1.1 Background and Motivation

In the field of civil engineering, soil compaction is an essential function, notably in the transportation and infrastructure sectors. It is required for a wide variety of projects, ranging from simple engineering projects to those that are quite complex. There is a strong connection between the quality of the soil compaction and the efficacy and stability of the structures that are produced as a consequence. This, in turn, has an effect on elements such as the amount of time and money required for construction. When it comes to tropical regions, where residual soils are common and present their own unique challenges [1], this is of the utmost importance. In the field of construction, the significance of soil compaction is well-established. This is because soil compaction plays a role in the long-term stability and longevity of structures such as highway embankments, earth dams, and other essential infrastructure [2].

In geotechnical engineering, one of the most important areas of concentration is the development of systems that are both efficient and precise for measuring and monitoring soil compaction. Soil compaction is essential for increasing soil strength, reducing settlement, and enhancing load-bearing capacity, providing a stable foundation for construction projects (Das, 2013). Despite the fact that

traditional approaches are efficient, they tend to fall short when it comes to meeting the requirements of real-time applicability and speed, particularly when applied in field situations. This recurrent challenge highlights the need to develop innovative solutions that can provide adequate soil compaction, which in turn improves the structural integrity and operation of engineered structures [3].

Traditional methods for measuring dry unit weight and moisture content during soil compaction, such as the Standard and Modified Proctor test, face a number of important obstacles. These issues can be broken down into many categories. However, despite the fact that these methods are well recognized in the field of geotechnical engineering, they are both labor-intensive and time-consuming. According to Sharma and Deka (2018), the process of performing several trials in order to develop exact compaction curves can be resource-intensive [4]. This is especially true when dealing with a diversity of soil types over a project area. On top of that, these dynamic compaction methods are not devoid of any shortcomings, which may lead to significant inefficiencies in the laboratory.

The unpredictability that occurs while estimating the optimal moisture content (OMC) is one of the most significant problems that are associated with old approaches. The OMC, which is computed after establishing the moisture content

and dry unit weight curve, might vary for the same soil depending on the curve fitting figure and its position, as Yasun and Abbasi (2018) have pointed out [5]. This introduces uncertainty in the process of determining the appropriate compaction conditions. Because of this irregularity, the process of reaching the required level of soil compaction can be made more difficult, particularly in projects that are substantial in scale.

Additionally, the impact of moisture content on the efficacy of compaction does introduce an additional layer of complexity. Heitor et al. (2012) Research reveals that although compaction energy has a demonstrable influence on soil behavior at low moisture contents, variables such as matric suction become more critical at greater moisture levels. This is the same as the case when the moisture content is higher. This intricacy adds another layer of difficulty to the process of effectively forecasting and regulating the consequences of compaction using standard approaches [6].

Alternative methods have been investigated as a means of enhancing the effectiveness and precision of soil compaction measurements in response to the issues that have been presented. A static compaction approach, for example, is proposed by Sharma and Deka (2018) [4]. This method decreases the amount of

effort and time that is required for dynamic methods. Additionally, Alzabeebee et al. (2021) have presented data-driven models, such as evolutionary polynomial regression analysis, in order to forecast the maximum dry unit weight and the optimal moisture content based on the grain size distribution data [7]. These novel techniques are designed to solve the limits of existing methods, with the goal of delivering solutions that are more reliable and efficient for identifying the parameters of soil compaction conditions.

The purpose of this research is to investigate the use of electrical resistivity measurements as a non-destructive, efficient, and reliable alternative for assessing and monitoring real-time in-situ moisture content and dry unit weight during soil compaction. This research expands on the previous efforts that have been made.

Electrical resistivity has not been unearthed to its maximum potential, which is known for non-destructive approach and simplicity, to evaluate the characteristics of soil compaction as mean to understanding of the conditions under the surface without the requirement for excavation. According to Samouëlian et al. (2005), this approach offers useful insights on the characteristics of the soil under the surface by ascertaining the degree to which the soil is able to conduct electrical current [8]. Because of its capacity to indirectly perceive subsurface conditions, it has gained

popularity over the years in a variety of sectors, including engineering, environmental studies, mining, and archaeology (Azhar et al., 2016). This is due to the fact that it may be used to visualize subterranean conditions [9].

The method begins with the injection of an electrical current into the ground, followed by the measurement of the voltage distribution that is produced as a result. The production of thorough surveys, whether in one, two, or even three dimensions, is made possible by this. These surveys may be conducted in a variety of sizes, ranging from extremely tiny areas to entire regions [8]. According to Chen and Samouëlian, electrical resistivity may provide a wide range of information on the physical characteristics of the soil, including its structure, moisture content, and fluid composition. It also provides a comprehensive image of the geographical and temporal variability of the soil [8][10].

Electrical resistivity is normally non-invasive; however, some researchers have taken it a step further by merging it with standard geotechnical testing equipment. This is an interesting development. For example, triaxial and oedometer tests have been adjusted to incorporate resistivity data. This has made it possible to conduct a more in-depth investigation into the connection that exists between electrical resistivity and important parameters such as shear strength and consolidation [10]. In order

to demonstrate how adaptable this procedure may be, this mix of electrical techniques and traditional testing was used.

In conclusion, electrical resistivity is a method of soil characterization that is not only quick and economical but also non-destructive approach according to Samouëlian [8]. It not only works in conjunction with conventional testing procedures, but it may even be able to take their place in some circumstances. It provides a wider range of data coverage and the capacity to investigate more deeply into the ground [9]. The relationships between electrical resistivity and geotechnical parameters are becoming clearer as research in this area continues to advance. As a result, electrical resistivity is becoming an increasingly significant instrument in the field of geotechnical engineering.

1.2 Problem Statement

In order to ensure the long-term stability and performance of geotechnical constructions, it is very necessary to undertake precise measurements of the factors that govern soil compaction. According to Hassan and Nadhum (2023), proper compaction is an essential component of construction since it not only reduces the likelihood of structural failure but also minimizes the amount of settlement that occurs and increases the load-bearing capacity of the material [11].

The traditional methods of assessing soil compaction parameters, such as the proctor tests, have been shown to have certain drawbacks. Real-time monitoring of compaction operations is made more difficult by the fact that these procedures are frequently labor-intensive, time-consuming, and prone to human error [6][4]. On the other hand, new developments in technology have resulted in the creation of alternate approaches to the control of compaction.

According to Heitor et al. (2012), one of these methods is the utilization of intelligent compaction technologies, which allow for the continuous assessment of soil modulus and degree of compaction while the process of compaction is taking place[6]. The effectiveness of the process of compaction can be increased to its full potential by using this strategy. In addition, Hassan and Nadhum (2023) propose that utilizing geotechnical-electrical correlations as a means of evaluating compaction parameters is yet another unique technique. It has been demonstrated that this approach has high correlation coefficients between soil resistivity and compaction parameters, particularly when the moisture content of the soil is low [11].

In conclusion, whereas traditional methods of monitoring soil compaction characteristics continue to be significant, new technologies are emerging that offer

means to monitor and control soil compaction that are more efficient and accurate. These technological breakthroughs, which include electrical resistivity measurements and intelligent compaction technologies, have the potential to enhance the quality of geotechnical construction projects as well as their efficiency [1], [6], [11], [12].

1.3 Research Objectives

The objective of research is to explore the use of dynamic on-road measurements and continuous monitoring of soil resistivity to accurately predict moisture content and dry unit weight, with a focus on applications in geotechnical engineering and geotechnical projects. Soil moisture content and dry density are critical factors that influence pavement performance under cyclic loading conditions [13]. However, the relationship between soil electrical resistivity and moisture content is complex, as factors such as soil type, dry density, and clay content can impact resistivity measurements [14].

To address this complexity, the research involves extensive laboratory testing to establish an association between soil resistivity and compaction curves. This correlation serves as a baseline for field applications. In the field, soil strip calibration is conducted by measuring electrical resistivity across a range of

compaction efforts, represented by the number of passes of compactor. By comparing the field resistivity values with the laboratory-established benchmarks, it becomes possible to determine the appropriate number of passes needed to achieve the desired compaction level in the field. This approach allows for the real-time prediction of in-situ moisture content and dry unit weight, ensuring that the soil reaches the required strength through optimal compaction.

1.4 Scope and Limitations

Advances in computer modeling and machine learning have greatly expanded the range of electrical resistivity applications in geotechnical engineering. Large datasets from resistivity surveys and laboratory testing may be integrated using techniques like artificial neural networks (ANN), support vector machines (SVM), and genetic programming. These techniques address previous constraints, such as the inability to account for soil heterogeneity, by offering more exact forecasts of soil compaction characteristics such as dry unit weight and moisture content. The use of computational and analytical techniques in this research broadens its reach by providing a more rigorous framework for evaluating electrical resistivity data in complicated and large-scale geotechnical projects.

Despite their benefits, electrical resistivity measurements have limits that must be

addressed. Electrode spacing, soil temperature, mineral composition, and pore fluid conductivity may all have a substantial impact on electrical resistivity measurements. For example, high soil temperatures diminish resistivity owing to enhanced ion mobility, but high mineral content may result in conductivity overestimation, reducing the credibility of findings [15][16]. To address these problems, the scope is limited to the evaluation of resistivity trends under controlled laboratory and soil strip field conditions. This work employs rigorous calibration and established techniques, assuring consistency and accuracy in resistivity measurements over a wide range of soil conditions.

Innovations in electrode design broaden the scope of this study. Electrical Resistivity meter fitted into geotechnical equipment, such as compaction rollers and penetrometers, provide real-time resistivity measurement during dynamic field operations. These innovations overcome the limits of old approaches by allowing for the direct linkage of resistivity and compaction parameters, which improves both efficiency and data quality.

Furthermore, including electrical resistivity is consistent with geotechnical engineering's sustainability aims. Traditional approaches are often resource-intensive and ecologically damaging. In contrast, resistivity methods reduce

material waste and energy usage, lowering the environmental effect of soil studies. This broadens the scope of resistivity measurements to include projects where sustainability is a critical factor.

Electrical resistivity has progressed over time, from subsurface profiling and groundwater detection to its contemporary uses in soil compaction monitoring, slope stability analysis, and seepage detection in earth dams. This growth indicates its versatility and capability to solve the constraints of old approaches, making it a must-have tool in current geotechnical engineering.

1.5 Thesis Organization

This research has ten chapters, each facilitating a thorough investigation of dynamic on-road measurements of electrical resistivity as a technique for evaluating soil moisture content and dry unit weight during field compaction.

By outlining the study's history, motivation, issue statement, research objectives, scope, and limits, Chapter 1 establishes the foundation for the investigation. This chapter offers electrical resistivity as a non-invasive, effective substitute for conventional soil compaction monitoring techniques, which are inefficient due to their labor-intensive nature and inability to deliver real-time findings. A

comprehensive overview of the literature is given in Chapter 2, with particular attention paid to compaction techniques, soil categorization principles, and the incorporation of electrical resistivity in geotechnical engineering. Important methods are examined, such as dynamic measurement systems and the Wenner Four-Electrode Method, and research shortages are noted, especially with regard to real-time resistivity applications for compaction monitoring.

The study's materials are described in depth in Chapter 3, along with how the soils were categorized using geotechnical tests like compaction curves, Atterberg limits, and sieve analysis. Establishing trustworthy connections between resistivity and compaction parameters requires a thorough grasp of the characteristics of the chosen soils, which is ensured in this chapter.

The methodology used is explained in Chapter 4, with special attention to the adjustments made to ASTM and plastic molds to assess resistivity during compaction tests. These developments made it possible to combine electrical resistivity data with conventional compaction techniques, allowing for precise evaluation in a controlled laboratory setting.

Preliminary design of walk-behind electrical resistivity meter and soil strip container

are presented in Chapter 5, which examines the connections between dry unit weight, moisture content, and electrical resistivity for sandy soil. This chapter addresses the effects of density and moisture on resistivity values and highlights the patterns seen in various compaction attempts.

The study shifts to field-scale applications in Chapter 6, which describes the creation and evaluation of a walk-behind resistivity meter. In order to validate the suggested approaches, the chapter compares laboratory results with field data and explains the soil strip tests intended to mimic real-world situations.

The soil strip methodology, a unique method for estimating compaction parameters using resistivity data, is introduced in Chapter 7. This chapter describes the technique's real-world application in field settings and how it might improve the precision and efficiency of soil compaction monitoring in geotechnical projects.

The dissertation is concluded in Chapter 8, which also discusses the study's limits and summarizes the main findings and their contributions to the advancement of geotechnical engineering methods. Future research recommendations are also given, with a focus on areas where advancements could improve the incorporation of electrical resistivity into soil compaction monitoring.

Chapters 9 and 10 include the references cited in the dissertation as well as appendices that include comprehensive computations, graphs, and supporting documentation to support the methodology and research conclusions.

Chapter 2: Literature Review

2.1 Soil Classification and Compaction: Principles and Techniques

The classification of soil is the basic features of geotechnical engineering. These characteristics provide essential insights into the behavior of the soil and its appropriateness for engineering applications. Atterberg limits, which include the liquid limit (LL), the plastic limit (PL), and the plasticity index (PI), are essential characteristics for comprehending the plasticity and consistency of soil. It is common practice to assess the liquid limit by using either the Casagrande cup technique (ASTM D4318, 2017) or the fall cone penetrometer method (BS EN ISO 17892-12:2018). Studies have shown that the fall cone test provides superior reliability for soils that include different proportions of silt and clay [17]. The indicator of plasticity, which is calculated as: $PI = LL - PL$.

A common method for classifying fine-grained soils is the $PI = LL - PL$ equation. Soil classification methods, such as the Unified Soil Classification System (USCS) and the AASHTO Soil Classification System, use Atterberg limits in conjunction with particle size distribution in order to classify soils according to the engineering features that they possess (ASTM D2487, 2017; AASHTO M145, 1993). The United States Geological Survey (USGS) makes use of a plasticity chart, which categorizes soils according to their location in relation to the A-line $PI = 0.73(LL - 20)$,

distinguishing between clays and silts, as shown below in Table 1.

Table 1: Fine-grained classification according to A-line relation.

Soil Type	LL (%)	PI (%)
CL	< 50	> 7
ML	< 50	< 7
CH	> 50	> 7
MH	> 50	< 7

Similarly, the AASHTO system utilizes parameters like the group index (GI), calculated as: $GI = (F_{200} - 35)[0.2 + 0.005(LL - 40)] + 0.01(PI - 10)$**,** Where F_{200} is the percent passing #200 sieve.

This index, in conjunction with particle size distribution, is used to evaluate and classify type of soil (AASHTO M145, 1993). On the basis of the findings of the sieve analysis, the particle size is classified as gravel, sand, silt, or silt/clay. These classifications are determined by the fact that gravel is retained on sieve #4 (4.75 mm), sand passes through sieve #4 and is retained on sieve the number 200 (75 µm), and silt/clay passes through sieve #200 (ASTM D6913, 2017) for USCS. On the other hand, these classifications are determined by the fact that gravel is retained on sieve #10 (2.00 mm), sand passes through sieve #10 and is retained on sieve the number 200 (75 µm), and silt/clay passes through sieve #200 (ASTM D6913, 2017) for AASHTO. There are still difficulties in ensuring that these old procedures are

accurate and consistent, despite the fact that they are frequently employed. As an instance, research by Kodikara has shown that there are disparities in the results of tests as a consequence of variances in technique, which ultimately results in classifications that are inconsistent [1]. According to Faé et al. (2019), developing techniques such as laser diffraction and dynamic image analysis (DIA) provide quicker and more exact particle size analysis in comparison to traditional methods such as sieve and hydrometer [18]. However, the integration of these techniques with regular systems needs more study due to the fact that they are not yet fully developed in the field of geotechnical engineering. These improvements shed light to the need to continue modify soil categorization systems in order to improve the dependability and compatibility of geotechnical engineering processes.

Soil compaction is a key geotechnical engineering procedure that increases soil density by decreasing air spaces using external pressures. This technique not only increases soil strength and bearing capacity, but it also lowers compressibility, making it a necessary step in the building of stable and long-lasting structures. The link between moisture content and dry unit weight is critical for understanding how soil behaves during compaction since both variables have a major impact on total compaction quality [5].

Soil compaction in the field has traditionally been achieved through various methods such as rolling, tamping, or a combination of these techniques, with factors such as water content, layer thickness, and specific compaction effort playing critical roles in determining the final compacted state of the soil [1], [2], [12], [19]. In the laboratory, the resultant connection between moisture content and dry unit weight is often represented by a compaction curve, which assists engineers in determining the ideal soil compaction conditions.

To assess these qualities, laboratory procedures such as the standard and modified proctor tests have been frequently employed. These tests include compacting soil samples in a mold with a certain number of hammer blows to determine the soil's optimum moisture content (OMC) and maximum dry unit weight (MDUW) as shown in Figure 1.

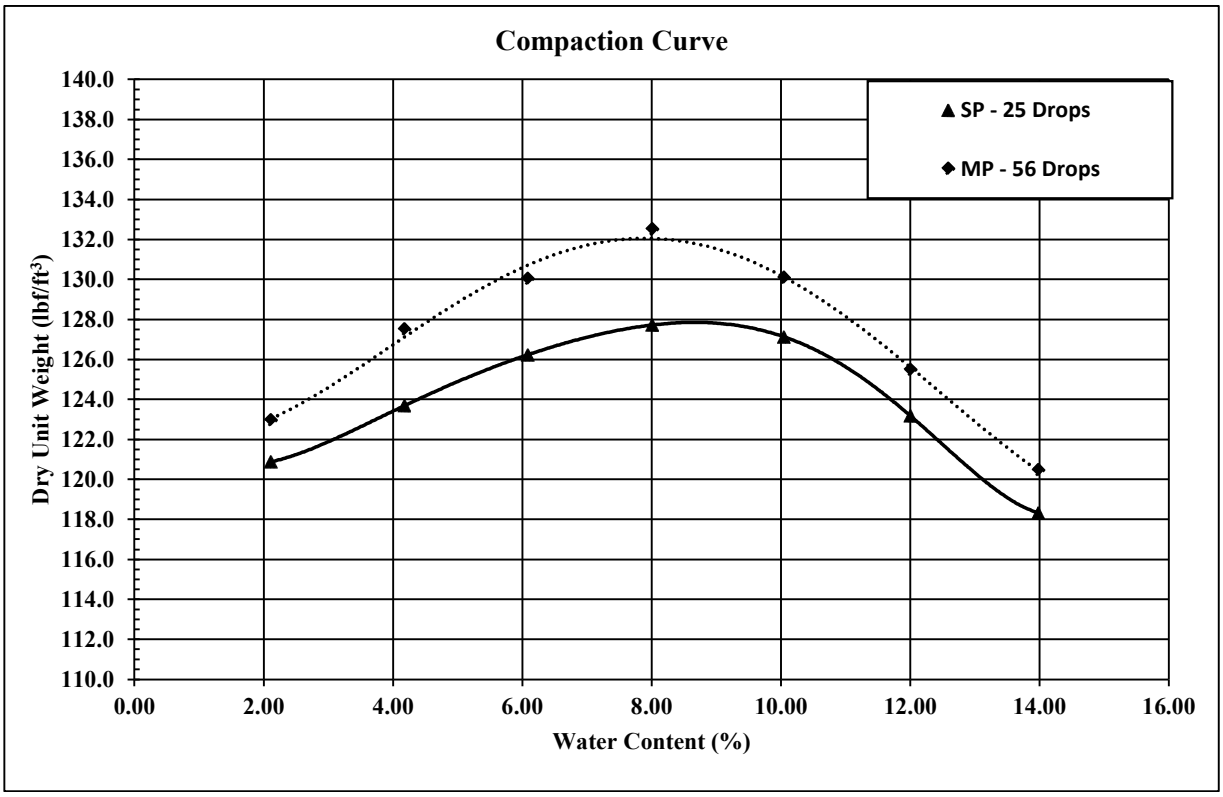

Figure 1: Laboratory compaction curves for Standard (SP) and Modified (MP) Proctor test.

Geotechnical engineers use compaction curves and water content calculations to determine the optimal moisture content (OMC) and maximum dry density (γ_{d}) of soils, assuring stability and performance. These characteristics are generated using conventional and customized proctor tests. To compute dry unit weight (γd) from total unit weight (γ) and water content (w), use the following equation:

$$\gamma_d = \frac{\gamma}{1 + w}$$

$$\gamma = \frac{W}{V}$$

where γ is the bulk unit weight in pounds per cubic foot (pcf), W is the total weight of soil (wet) in pounds (lb) occupying certain volume, and V is the total volume in cubic feet (ft^3). The water content is calculated using the oven-dry technique, which measures the weight of water lost during drying relative to the dry weight of the soil.

$$w = \frac{W_w}{W_s} \times 100$$

Where W_w is the weight of water in pounds, and W_s is the dry weight of soil in pounds. The compaction curve is plotted by compacting the soil at different moisture levels and determining the appropriate dry unit weights, resulting in a distinctive curve with a peak at the OMC.

The energy provided during compaction has a considerable impact on the compaction curve. The standard Proctor test (ASTM D698) involves compacting soil with a 5.5 lb hammer dropped from a height of 12 in, resulting in 12,375 ft-lb/ft^3 of energy. In comparison, the modified Proctor test (ASTM D1557) employs a 10 lb hammer delivered from an 18-inch height, giving 55,860 ft-lb/ft^3 of energy [20], [21], [22]. The higher energy in the modified Proctor test often results in a lower

OMC and a higher maximum dry density than the Standard Proctor test, indicating the denser soil structure possible with greater compactive effort. The compaction energy per unit volume used for the Standard proctor and Modified proctor test in Principles of Geotechnical Engineering 9th Edition by Braja M. Das and Khaled Sobhan:

$$E = \frac{\begin{pmatrix} Number\ of \\ blows \\ Per\ layer \end{pmatrix}\begin{pmatrix} Number \\ of \\ layers \end{pmatrix}\begin{pmatrix} Weight \\ of \\ Hammer \end{pmatrix}\begin{pmatrix} Height\ of \\ drop\ of \\ Hammer \end{pmatrix}}{Volume\ of\ mold}$$

The contrast between these tests is critical in geotechnical engineering practice, because the decision is determined by the soil's projected loads and performance requirements in individual projects. Engineers may use these equations and the effects of compaction energy to properly build soil structures that fulfill performance objectives. Traditional procedures, although effective, are sometimes time-consuming and labor-intensive.

In addition to laboratory studies, many non-destructive in situ procedures have been developed to more effectively measure soil compaction in the field. These include the Nuclear Density Gauge (NDG), the Sand Cone (SC) test, and the Electrical Density Gauge (EDG). The NDG, for example, is used to find out the

density and moisture content of soils after compaction is done. This tool measures quickly, accurately, and without disturbing the compacted soil that is being measured, so it is essential for quality control. Gamma radiation is used to measure density, and neutron scattering is used to measure moisture content. The NDG works on the principles of nuclear radiation. ASTM D6938, the Standard Test Method for In-Place Density and Water Content of Soil and Soil-Aggregate by Nuclear Methods (Shallow Depth), outline how the gauge works and how it should be used. By explaining the calibration process, the right way to place the test equipment, and the safety rules for working with nuclear materials, this method makes sure that the results are consistent. The NDG usually has a radioactive source (Cesium-137 for measuring density and Americium-241 mixed with Beryllium for measuring moisture), radiation detectors (like Geiger-Mueller tubes or scintillation detectors), a probe assembly that holds the sources and detectors, a control unit for showing and saving data, and a reference standard block for setting the machine up [23], [24], [25].

The NDG works by using a nuclear source to send out gamma rays that combine with the test material. A monitor measures how much these rays are weakened, which is directly linked to how dense the object is. The gauge sends out fast neutrons that are slowed down by hydrogen atoms in water to measure the

amount of water present. The slower neutrons are measured by this device to get an idea of how much water there is. Because of these features, the NDG is very useful for field uses like road building, stabilizing embankments, and compacting foundations, where getting the right material density is very important. Since NDG employs gamma rays to assess soil density fast and with low interruption, it has the disadvantage of radiation exposure, necessitating rigorous handling and regulatory requirements [24].

The Sand Cone test is a popular technique to determine the in-situ density of compacted soils. The process entails digging a small hole in the compacted soil, quantifying its volume using calibrated Ottawa sand, and determining the density of the extracted soil [17], [26]. The fundamental equations for the Sand Cone test are:

1. Bulk density (ρ_b) = Mass of excavated soil / Volume of excavation
2. Dry density (ρ_d) = Bulk density / (1 + moisture content)

The Sand Cone test, while straightforward and cost-effective, had several drawbacks. It is laborious, time-consuming, and less economical than contemporary procedures [26], [27]. The precision of the test may be influenced by variables such the dimensions and configuration of the test hole, the nature of the

sand used, and the compaction of sand particles during the filling procedure [26].

Research indicates that the Sand Cone test may provide superior compaction results relative to other approaches. Kaderabek and Ferris (1979) indicated that the Sand Cone technique achieved a 5% greater compaction compared to the nuclear test method [28]. This disparity underscores the need for possible biases when analyzing test data. The Sand Cone test, although simple and inexpensive, has substantial labor and material issues, such as the requirement for particular, non-reusable sand and difficulty in high humidity settings [29][17].

The EDG provides an alternative by detecting the soil's dielectric characteristics to calculate dry unit weight and moisture content without the requirement for soil excavation or radiation exposure. This approach, however, requires accurate calibration to maintain accuracy, and reading disparities when compared to other methods show the need for continuous development in calibration procedures [30]. While these non-destructive technologies provide useful information, they often fail to provide real-time, complete evaluations of compaction quality over wide regions.

Recognizing these limitations, researchers investigated more sophisticated systems

such as Continuous Compaction Control (CCC), Roller-Integrated Compaction Monitoring (RICM), and Intelligent Compaction (IC). These technologies allow real-time monitoring and a more dynamic knowledge of the compaction process across whole surfaces, improving the overall quality and lifetime of pavement structures [10], [27], [31], [32], [33].

In conclusion, although classic approaches such as the Proctor tests and different in situ procedures have established the framework for soil compaction evaluation, continual innovations are required to overcome their limits. The use of continuous, real-time monitoring systems has the potential to dramatically increase the accuracy and efficiency of soil compaction processes, resulting in better-engineered structures and more durable pavements.

2.2 Electrical Resistivity in Geotechnical Engineering

In geotechnical engineering, electrical resistivity techniques have become a vital tool because they provide a rapid, flexible, and non-destructive means of measuring soil characteristics including dry unit weight and water content. At first, subsurface investigations were the main use for electrical resistivity surveys, which assisted in locating objects such as water tables, bedrock, and boulders [34], [35]. When these surveys first began, geophysicists were needed to manage the intricate

processes of data collection, processing, and interpretation. The resulting images brought to light difficult ground conditions [34], [35].

Adebiyi et al. developed empirical models of subsoil parameters in conjunction of ER. The Wenner Array method was used to test the electrical resistivity of the soil and look at its properties on farmland. With an electrode distance of 1.3 m, measurements were taken from 0 to 50 cm depth, and soil samples were looked at to find out how much moisture, what is the size of the particles, the amount of organic matter (OM), the pH, and how well they conducted electricity (EC). A regression study showed that electrical resistance and soil qualities are strongly related. Figure 2 shows the connection between electrical resistivity and moisture level, showing the strong link found in the work by Adebiyi et al.

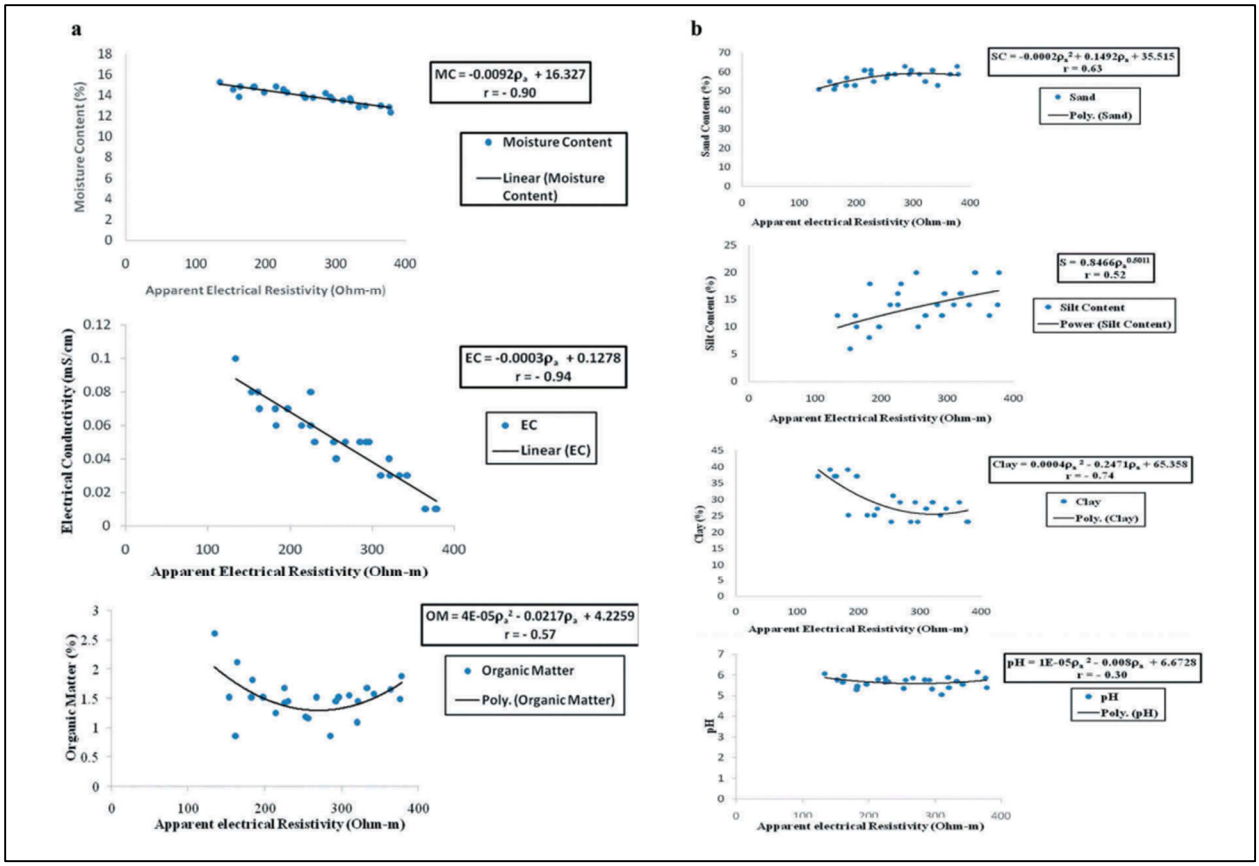

Table 6. Simple correlation coefficient between ER and soil properties.

Soil properties	Apparent electrical resistivity (r)
MC	−0.90[a]
EC	−0.94[a]
OM	0.57[b]
% Sand	0.63[b]
% Silt	n.s
% Clay	0.74[a]
pH	n.s

[a]Correlation is significant at $P < 0.01$ level
[b]Correlation is significant at $P < 0.05$ level
n.s: non-significant.

$$\% \text{ Sand} = -0.0002\rho a^2 + 0.1492\rho a + 35.515 \quad (7)$$

$$\% \text{ Silt} = 0.8466\rho a^{0.5011} \quad (8)$$

$$\% \text{ Clay} = 0.0004\rho a^2 - 0.2471\rho a + 65.358 \quad (9)$$

$$\text{pH} = 1\text{E} - 05\rho a^2 - 0.008\rho a + 6.6728 \quad (10)$$

Figure 2: Cross plots between soil properties and apparent electrical resistivity measurement in Adebiyi et al. (2020)

The uses of electrical resistivity have greatly increased as technology has developed. It is now commonly utilized for non-destructive and economical evaluation of the physical and chemical characteristics of soil in addition to subsurface research. This method is now especially useful for landslide research, shallow subsurface investigations, and even long-term continuous monitoring of changes in soil moisture [36], [37]. Electrical resistivity, for instance, is used in landslide studies to determine the landslide type, identify failure zones, and identify areas of excess moisture, all of which provide vital information for risk mitigation [36].

The capacity of electrical resistivity to clearly shows a correlation between resistivity and soil water content is one of its main advantages. This link has made it possible to establish clear relationships between hydraulic parameters and resistivity data, and some studies have found that they can accurately estimate volumetric water content [38], [39]. Further proving the usefulness of resistivity methods in soil analysis, they have also been applied to examine other significant soil characteristics such as density, degree of saturation, and hydraulic [38], [39].

However, electrical resistivity is still not widely used to evaluate the geotechnical characteristics of soil masses, despite its increasing popularity and potential [19],

[40], [41]. Resistivity surveys are useful for locating subsurface structures, but they are frequently not completely integrated with geotechnical factors such as shear strength and water potential. It can be difficult to create general correlations that apply to various soil types because of the complex relationship between resistivity and soil properties, which is influenced by elements like grain size, specific surface area, pore water conductivity, and degree of saturation. Furthermore, resistivity-based predictions might differ in accuracy; some studies have shown notable inaccuracies in the water content calculations [42], [43].

Datsios et al. (2017) studied how the electrical resistivity (ρ) of soil changes with the amount of water in it (w) using deionized water and NaCl solutions. As the water content rises, resistivity goes down because there are more hydrated ions available and the transmission lines through the pore water are better connected. It was found that percolation limits are around 10% w≈10% for NSS1 and AGS soils and around 20% w≈20% for NSS2 soils. Below these levels, continuous pore water paths form, which greatly lowers resistance. Larger grain sizes have higher resistance because they have fewer ions and more twisting. Adding NaCl solutions further decreased resistance (by 35–75%) compared to deionized water because salty solutions have more ions that carry electricity. Figure 3 displays the connection between the resistivity of soil and the amount of water in it for various grain sizes. It

shows how grain size and the continuation of pore water affect resistivity.

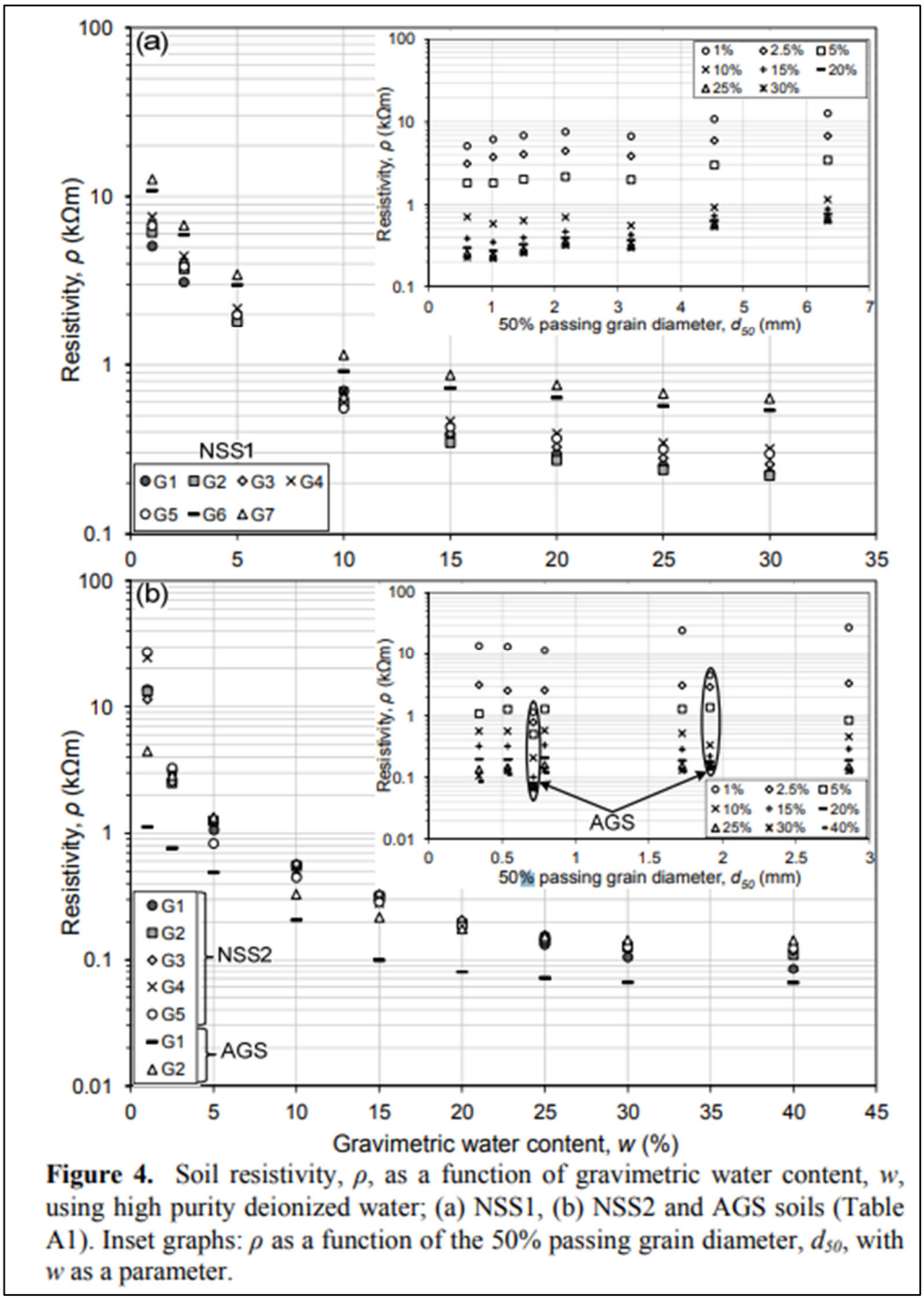

Figure 4. Soil resistivity, ρ, as a function of gravimetric water content, w, using high purity deionized water; (a) NSS1, (b) NSS2 and AGS soils (Table A1). Inset graphs: ρ as a function of the 50% passing grain diameter, d_{50}, with w as a parameter.

Figure 3: Soil resistivity, ρ, as a function of gravimetric water conten and grain size

However, recent studies have demonstrated that electrical resistivity values are

strongly influenced by soil mechanical characteristics, including moisture content, density, and composition. This implies that resistivity techniques can improve traditional geotechnical studies by offering a deeper understanding of soil behavior, in addition to mapping subsurface characteristics [43], [44], [45]. Electrical resistivity's transformation from a specialist geophysical instrument to a more general use in geotechnical engineering highlights its increasing significance. An essential tool in the field, electrical resistivity is set to become more and more important in evaluating and comprehending soil qualities by bridging the gap between geophysical measurements and soil mechanics.

In conclusion, electrical resistivity techniques have a lot of potential for measuring non-destructive soil properties, but their effective use necessitates careful evaluation of particular soil properties and possible error sources. To improve their usefulness in geotechnical engineering, more study is required to hone these methods and create more trustworthy correlations that can be used with a larger variety of soil types and circumstances.

2.3 The Wenner Four-Electrode Method

For the purpose of determining the electrical resistivity of soils and other subsurface materials, the Wenner Four-Electrode Method is a technique that is

frequently utilized in the fields of geotechnical sciences and environmental engineering. Developed by Frank Wenner in 1915, (Wenner, 1915) [46], this method is widely used because of its ease of use and efficiency in determining the conditions of the subsurface.

Electrodes are arranged in a straight line on the ground surface using the Wenner method. These electrodes are equally spaced apart from one another. A voltage difference is measured between the two innermost electrodes that are immediately adjacent to one another, which are referred to as the potential electrodes, while an electrical current is passed through the two electrodes that are located on the outside of the probes arrangement, as shown in Figure 4. After that, the resistance of the subsurface is determined by utilizing the formula that is presented below.

$$\rho = \frac{4a\pi R}{1 + (\frac{2a}{\sqrt{a^2 + 4h^2}} - \frac{a}{\sqrt{a^2 + h^2}})}$$

However, if h is small relative to a, then the equation can be reduced to:

$$\rho \approx 2\pi a \frac{V}{I}$$

where:

- $\boldsymbol{\rho}$ is the resistivity of the material,
- $\boldsymbol{a}$ is the spacing between the electrodes,

- $\boldsymbol{R}$ is the ratio of voltage to current in Ohms $\boldsymbol{R} = \frac{\boldsymbol{V}}{\boldsymbol{I}}$
- $\boldsymbol{V}$ is the measured voltage difference,
- $\boldsymbol{I}$ is the current injected into the ground,
- $\boldsymbol{h}$ is the depth of electrode in the ground in meters.

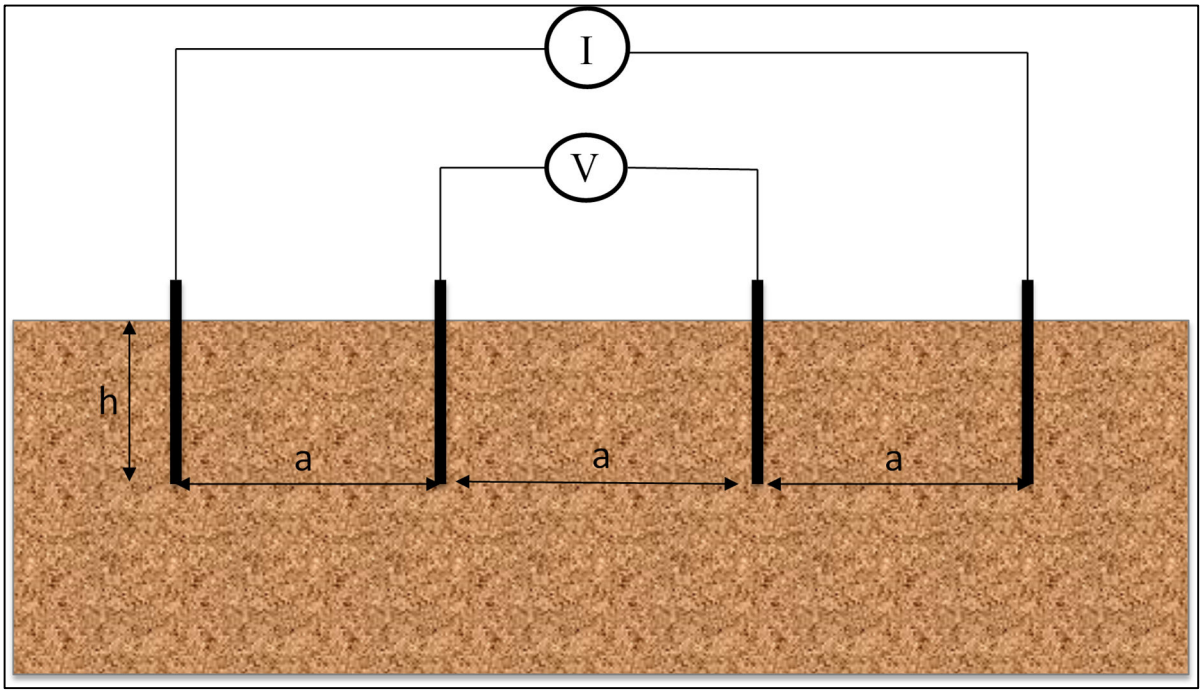

Figure 4: Wenner Four-Electrode Method Arrangement

Among the many benefits of this technique is the fact that it allows for the direct measurement of the subsurface material's average resistivity over the volume between the electrodes. By varying the electrode spacing, the method can probe different depths, allowing for the creation of a resistivity profile of the subsurface [8], [34], [47], [48], [49], [50].

The dependability and adaptability of the Wenner Four-Electrode Method have been proven in several geotechnical and environmental studies. One area where it has found extensive usage is groundwater research, namely for mapping aquifers and detecting salt intrusions. Geotechnical engineers have used the technique to determine whether embankments and earthen dams are stable by looking for areas of low resistivity, which could mean that the soil is too wet or too dense [5], [6], [9], [51], [52].

Soil compaction studies also make good use of the Wenner method to track how soil resistivity varies as compaction progresses. Because it permits continuous monitoring of soil parameters including moisture content and dry unit weight during compaction, this application is very pertinent to the current research. For instance, the Wenner approach is useful for evaluating the quality of compaction in real-time because research has demonstrated that resistivity decreases as soil compaction increases [38], [53]

A lot of recent work has also gone into making the Wenner method more precise and useful in a wider range of soil types and climates. The difficulties of interpreting resistivity data in heterogeneous soils were brought to light in a study by Zhou et al. (2001) that investigated the Wenner method in various soil textures. Using the

Wenner approach in complicated geological contexts requires careful calibration and interpretation, as highlighted by the study [42].

The simplicity, efficacy, and applicability of the Wenner Four-Electrode Method have ensured its continued use as a fundamental tool in geotechnical and environmental engineering. Groundwater exploration, soil compaction monitoring, and environmental pollution identification are just a few of the many uses for its capacity to provide precise subsurface resistivity profiles. In complicated or varied subsurface settings, however, its efficacy is dependent on precise calibration. This method's usability and relevance in modern geotechnical techniques are being further enhanced by continual improvement.

2.4 Dynamic On-Road Measurement Techniques

The application of electrical resistivity techniques in geotechnical engineering has experienced substantial growth, especially in relation to soil compaction and subsurface investigations. Electrical resistivity approaches, such as the Wenner four-electrode method, have historically been used for static studies, typically needing fixed setups. Recent developments have investigated the possibility of combining these techniques with mobile equipment to get uninterrupted, up-to-date information during soil compaction operations.

Significant progress has been made with the invention of Continuous Resistivity Profiling (CRP) devices, which replicate the Wenner four-electrode arrangement. These devices are installed on mobile platforms, such as tractors, boats, or roller compactors, to monitor dynamic soil resistivity while the machinery is in motion. The study by Thompson et al. [54] provides a detailed account of a CRP system that is especially tailored for geophysical profiling of ocean subsurface [54].

The continuous resistivity profiling technology acquires resistivity data in real-time while moving through the soil, providing vital information on soil qualities making is a crucial methodology for efficient soil compaction monitoring. The system's capacity to consistently monitor resistivity while in motion signifies a notable advancement in the integration of geophysical technologies with geotechnical operations.

Another method that has been reviewed by Zhang et al. involves combining intelligent compaction techniques with electrical resistivity data. This approach integrates the advantages of real-time compaction data with resistivity measurements to evaluate the soil compaction quality in a dynamic manner. While the practical use of these systems on roller compactors is currently restricted, the

idea is gaining popularity as a possible option for improving the precision and effectiveness of soil compaction monitoring [54], [55].

Although there have been significant developments, it seems that there is a lack of comprehensive documentation in the literature on a completely developed system that is especially designed to directly detect electrical resistivity on a roller compactor during the compaction process. Although the concepts of CRP and intelligent compaction [54], [55] provide a possible direction, more research and development are necessary to establish a reliable system that combines resistivity monitoring with soil compaction machines and can be used in the field. The difficulties involved in this integration encompass the task of sustaining a constant connection between the electrode and the soil, as well as guaranteeing precise resistivity measurements despite the ever-changing nature of the compaction process.

2.5 Gaps in Existing Research

The current database of research in geotechnical engineering has made substantial progress in devising systems to monitor soil compaction and its related parameters, such as dry unit weight and moisture content, through the use of electrical resistivity (ER) technologies. The Wenner four-electrode method and

Continuous Resistivity Profiling (CRP) are conventional techniques that have effectively been used to evaluate subsurface conditions and soil qualities in both static and dynamic situations. Nevertheless, there is still a significant deficiency in the current ability to monitor soil compaction in real-time, particularly in establishing a connection between the curve of compaction efforts and the number of passes needed to get the specified soil strength.

Existing research has been concentrated on static measurements or continuous profiling, which provides broad understanding of subsurface conditions. However, these technologies frequently lack the accuracy and immediate reactivity required for improving the compaction process in the field. The existing literature lacks enough coverage of a dynamic, real-time system that may offer instant feedback on the quality of compaction by considering the number of roller passes in conjunction with soil resistivity readings.

Our research fills this need by introducing a new kind of walk-behind resistivity meter that can track electrical resistivity in real-time as compaction takes place. You may directly correlate the compaction effort with the resulting soil strength with this gadget, which tracks the changes in resistivity with each pass of the compactor. Our main goal is to find a strong correlation between these factors so that we can

monitor compaction efforts in real-time with ER.

This novel method fills a need in the literature by expanding the use of electrical resistivity beyond the scope of static measurements and conventional subsurface studies. Its ultimate goal is to make soil compaction operations more precise and efficient by giving engineers a practical tool they can use in real-time.

Chapter 3: Material

3.1 Overview of Laboratory Tested Materials

Classifying the soil helps determine its engineering behavior and suitability for compaction, thus, the Unified Soil Classification System (USCS) in conjunction with the Atterberg limits and grain size distribution was used (ASTM D2487, 2017).

Soil samples were collected from two different sources to be processed for analysis. The two samples consisted of poorly graded sand, and fat clay. The grain size distribution of the soils was determined through sieve analysis and hydrometer analysis as required. In addition, the Atterberg limits were determined to classify the soils in accordance with the Unified Soil Classification System (USCS). Standard and Modified Proctor tests (Figure 5) were performed on both soils to establish their compaction curves.

Figure 5: Compacted Sandy Soil in Standard Proctor ASTM Mold

3.2 Soil Classification of Selected Materials

The soil samples utilized in this investigation were characterized using standard geotechnical techniques. The particle size distribution (PSD) of the clay is shown in Figure 6. The composition of the soil was found to consist of over 85% silt and clay, less than 3% gravel, and less than 12% sand. These findings lead to the soil's

classification as fine-grained. The soil's characteristics were further characterized by Atterberg limits tests, which showed a Plastic Limit (PL) of 17%, a Liquid Limit (LL) of 52%, and a Plasticity Index (PI) of 35%. The soil is classified as high-plasticity clay (CH) in accordance with the Unified Soil Classification System (USCS) based on the plasticity chart. According to these results, clay samples have a high degree of plasticity, which is essential to their compaction and ER behavior.

The classification of the sand sample used in this experiment was determined through a rigorous geotechnical evaluation. The particle size distribution (PSD) data revealed that the soil is made up of more than 95% sand, less than 3% gravel, and less than 2% silt and clay. This composition demonstrates its largely granular nature, with little fines presence in the sample as shown in Figure 7.

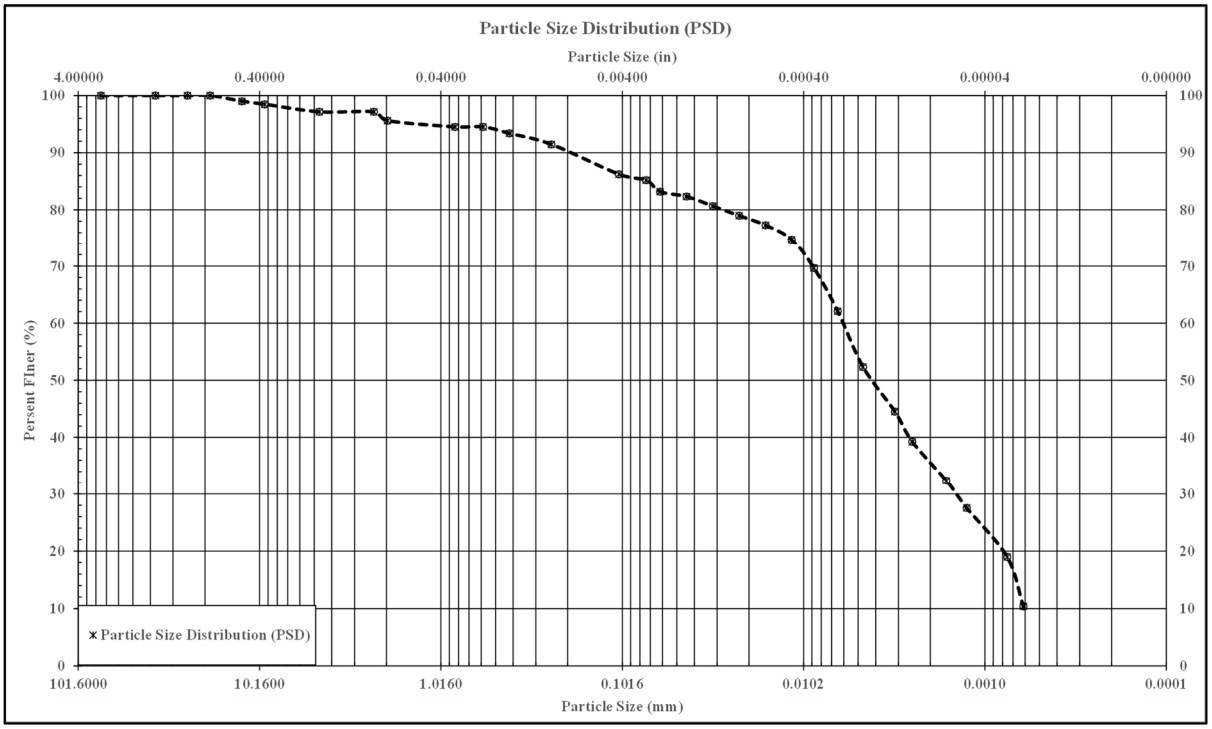

Figure 6: Particle Size Distribution of Fat Clay Soil

The PSD curve revealed key particle size factors, such as D_{10} = 0.21 mm, D_{30}=0.45 mm, and D_{60}= 0.58 mm. The coefficients of uniformity (C_u = 2.83) and curvature (C_c = 1.68) were calculated, confirming the sample's poor grading and uniformity. According to the Unified Soil Classification System (USCS), the soil is classified as Poorly Graded Sand. Plasticity tests revealed that the soil is non-plastic (NP), which is compatible with the lack of fine particles. These values reflect the soil's primarily sandy texture, as shown in Figure 7 and Figure 8, which influences its compaction and electrical resistivity performance.

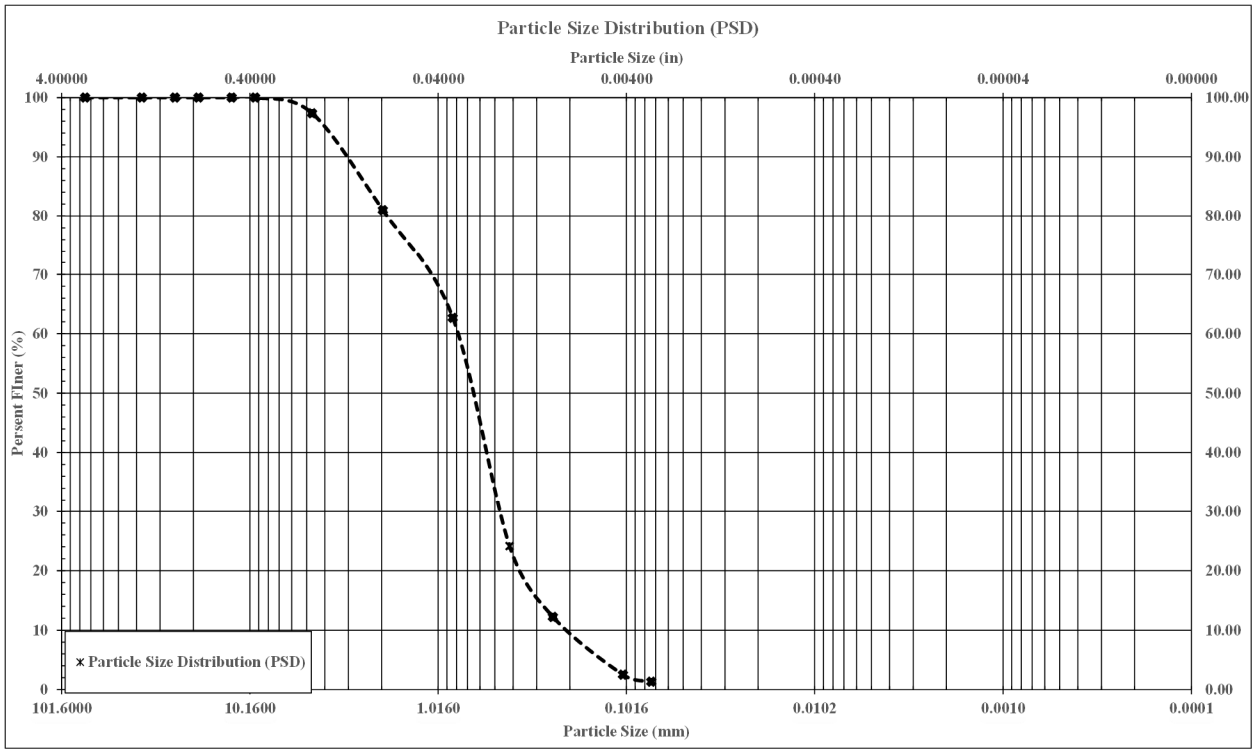

Figure 7: Particle Size Distribution of Poorly Graded Sand Soil

Figure 8: Poorly Graded Sand Particle Size Distribution

3.3 Compaction Curves of Selected Materials

The compaction tests using ASTM standards are crucial for assessing soil density and moisture relationships that are vital for quality control in construction projects. These tests include the Standard Proctor test (ASTM D698) and the Modified Proctor Test (ASTM D1557), each conducted using cylindrical molds with specific dimensions. The Standard Proctor (SP) test typically uses a 4-inch diameter mold (volume = 1/30 ft^3), while the Modified Proctor (MP) test may use a 6-inch diameter mold (volume = 1/13.3 ft^3). Four configurations—S-25, S-56, M-25, and M-56—are used to identify soil properties under different energy levels. The S-25 configuration (Standard Proctor with 3 layers, 25 blows per layer, and a standard 5.5 lb hammer with 12-inch in height) produces a compaction energy of 12,375 ft-lb/ft^3 using a 4-inch mold. The S-56 configuration (Standard Proctor with 3 layers, 56 blows per layer, and a standard 5.5 lb hammer with 12-inch in height) applies a higher energy of 27,720 ft-lb/ft^3, also using a 4-inch mold.

The Modified Proctor Test employs a heavier 10-lb hammer dropped from 18 inches, using a 6-inch mold for higher energy compaction. The M-25 configuration (Modified Proctor with 5 layers, 25 blows per layer, and a modified 10 lb hammer with 18-inch in height) provides 24,938 ft-lb/ft^3 of energy. The M-56 configuration (Modified Proctor with 5 layers, 56 blows per layer, and a modified 10 lb hammer

with 18-inch in height) delivers the highest compaction energy of 55,860 ft-lb/ft³. These energy levels affect the achievable maximum dry density and corresponding optimum moisture content of the soil. Table 2 shows the difference in compaction effort for the four compaction configurations.

Table 2: Comparison of Compaction Efforts Across Four Configurations

	# of blows/layer	# of layers	Weight of Hammer (lb)	Height of drop of Hammer (ft)	Volume of the Mold (ft^3)	Energy (ft-lb/ft^3)	Relative Energy to the Standard
S-25	25	3	5.5	1	0.03294	12,375	E
S-56	56	3	5.5	1	0.03294	27,720	2.25 E
M-25	25	5	10	1.5	0.06701	24,937	2.00 E
M-56	56	5	10	1.5	0.06701	55,860	4.50 E

In this section the compaction properties of the two soils were also investigated using a plastic mold. The plastic mold has the same volume as the ASTM Standard mold. The main reason for selecting a plastic mold is to be able to use the Wenner Four- Electrode method while replicating the compaction conditions of the Standard Proctor test. The result of soil compaction tests using the standard and plastic molds are comparable and aligned with research assumptions.

The compaction curves were developed for two soil types: fat clay, and poorly graded sand. Standard Proctor (SP) and Modified Proctor (MP) tests were used to assess the optimal moisture content (OMC) and maximum dry density (MDD) for

each soil type. The fat clay had OMC and MDD values of 14% and 114.5 lb/ft^3 under SP with 25 hammer drops in three-layer configuration, and 9% OMC and 137 lb/ft^3 MDD under MP with 56 hammer drops with five-layer configuration. Similarly, the poorly graded sand had OMC and MDD values of 8.5% and 120.5 lb/ft^3 for SP, and 8.0% and 132.5 lb/ft^3 for MP, respectively. The compaction curves in Figures 9 and Figure 10 demonstrate the effects of increasing compactive effort, with MP testing consistently achieving higher MDD and lower OMC as compared to SP and MP tests.

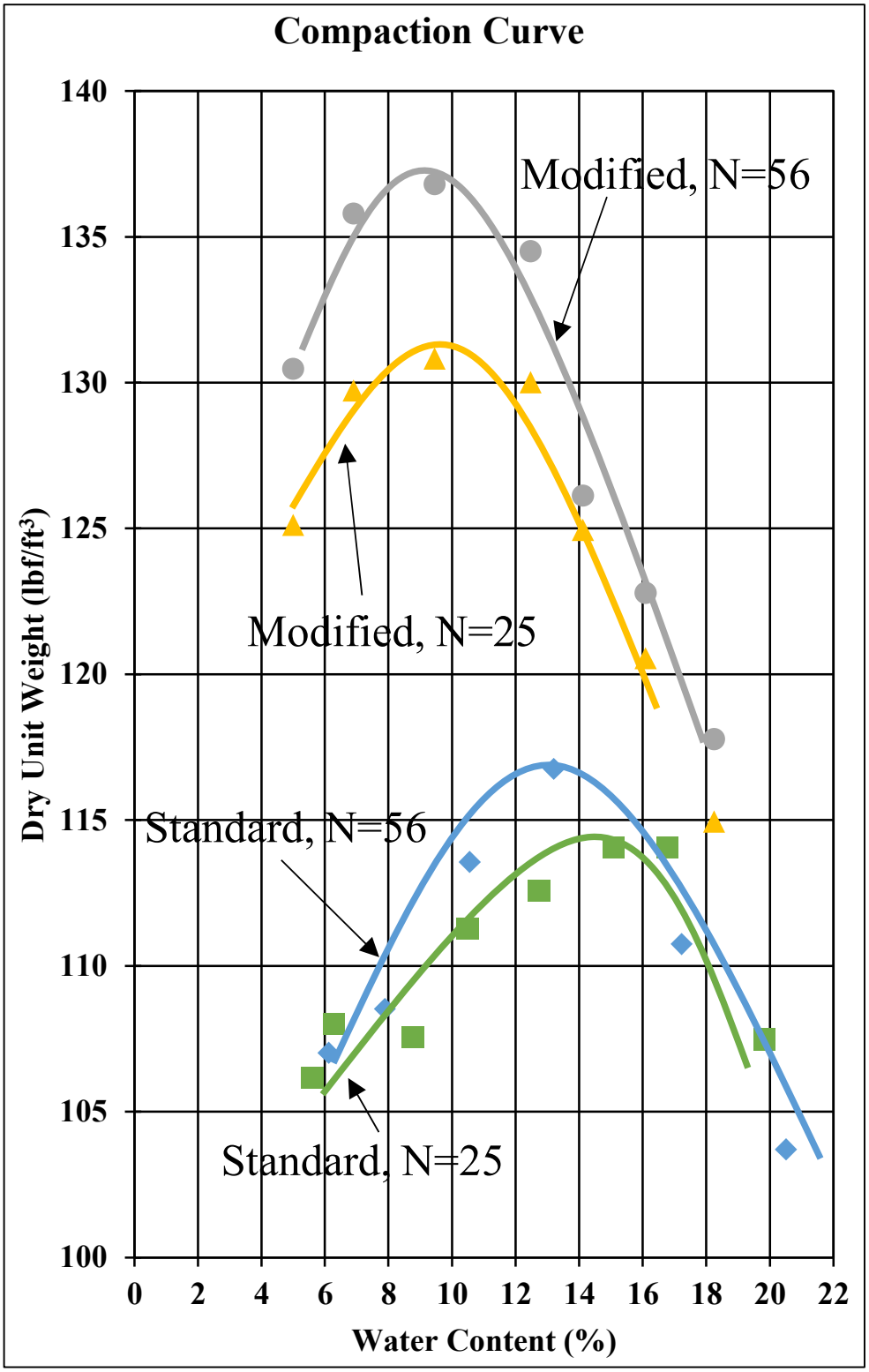

Figure 9: SP and MP Compaction Curves for Fat Clay Samples

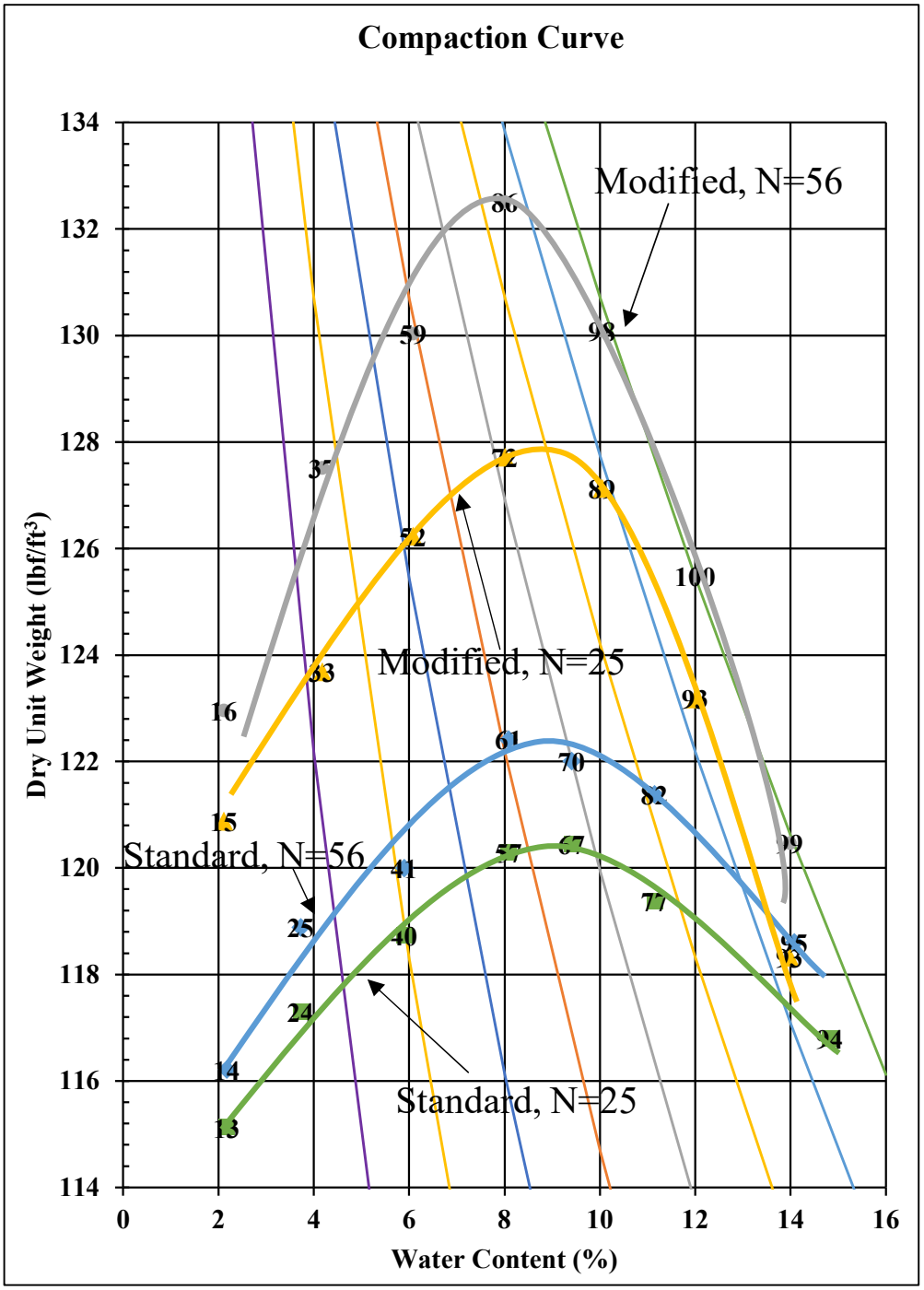

Figure 10: SP and MP Compaction Curves for Poorly Graded Sand

Chapter 4: Electrical Resistivity Testing with Proctor Molds

4.1 Modification of Plastic and ASTM Molds

This study examines the viability of employing electrical resistivity as a non-destructive technique for monitoring and predicting soil compaction characteristics, including dry unit weight and moisture content. The experimental approach consisted of repeated trials and adjustments to laboratory compaction molds, the development of a walk-behind resistivity meter, and the utilization of laboratory soil strip tests in a rigid container to simulate field conditions. The main goal is to create an association between the level of compaction, resistivity reading, and the soil properties at the site.

In order to achieve this objective, several critical modifications to the standard and modified compaction molds were implemented. First, the compaction curves were established under controlled conditions using the ASTM standard and modified compaction molds (Figure 9 and Figure 10). The compaction curves were replicated using plastic molds to circumvent the conductive nature of the ASTM steel molds, which could potentially interfere with soil resistivity measurements. This ensured that the results were comparable. As a result, resistivity measurements could be linked to varying compaction efforts without interference from the mold material.

To facilitate electrical resistivity measurements during the compaction process, plastic molds were the primary emphasis of the first development phase. This was done in order to facilitate electrical resistivity measurements throughout the process of compaction. To measure resistance, these molds were modified by drilling four 1/8" holes on opposite sides of the mold at varied spacings with a clear depth of ½ inch into the compacted soil. These holes are depicted in Figures 11a and 11b. The center-to -center distance between the probes were varied from 1 to 1.25 inches.

A digital multimeter (Instek GDM-8341) was utilized to measure the electrical resistivity of compacted soil in plastic, standard Proctor, and modified Proctor molds. These measurements were used to analyze the relationship between soil electrical resistivity and compaction effort.

In addition, the ASTM Standard and Modified Proctor (steel) molds were epoxy coated and modified to incorporate Wenner electrical probes at 1.25 inches clear distance, which allowed for the measurement of resistivity during compaction insuring no electrical transmission taking place except within the soil itself. This arrangement enabled the observation of resistivity values with compaction parameters, including moisture content and dry unit weight from both plastic

molds and ASTM molds.

a) Four holes on each side for the plastic mold

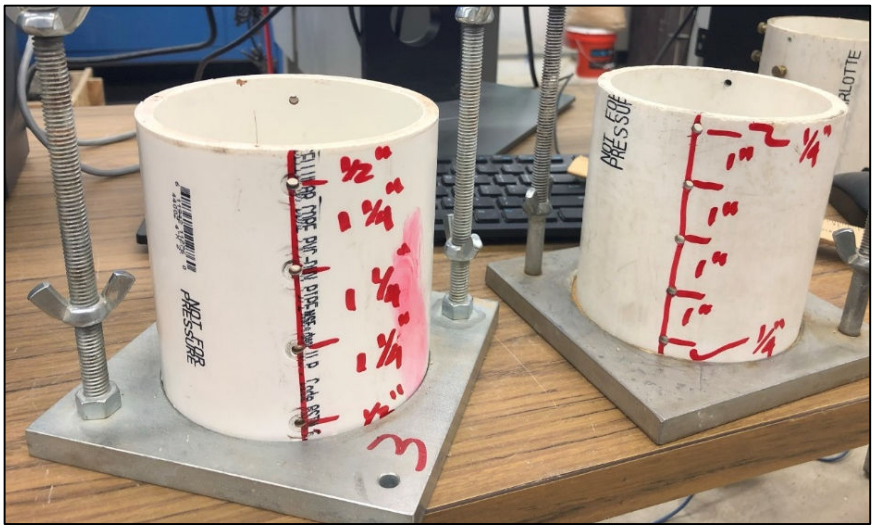

b) Four holes with different spacing arrangement

Figure 11: Plastic Mold for ER Measurements

The modifications of ASTM mold involved drilling four ½ inch holes on each side of the mold, with plastic rods (filler) fitted into the holes to prevent any electrical transmission through the steel mold and the steel Wenner probes as shown in Figure 12. The entire mold, including the base plate, was then coated with an epoxy layer to prevent any unintended transmission of electricity through the steel mold and into the soil. After the epoxy coating was applied, 1/8-inch holes were drilled through the plastic filler to allow access for the Wenner probes to the soil for ER measurements. This process was refined through multiple iterations and corrections to ensure the setup met acceptable laboratory standards for accurate and reliable electrical resistivity measurements.

a) Epoxy-coated Proctor mold with four holes on each side with plastic filler

b) Four holes drilled through the plastic filler

Figure 12: Modifications to the ASTM Mold for ER Measurements

4.2 Electrical Resistivity of Selected Materials using Plastic and ASTM Compaction Molds

After determining the compaction properties of the two soils, a plastic mold under Standard Proctor (25 drops) conditions were used to measure electrical resistivity (ER) during compaction. Figures 13 and 14 show the relationships for fat clay and poorly graded sand, respectively. In Figure 13a and Figure 14a, ER decreases as moisture content increases. In Figure 13b and Figure 14b, ER decreases with increasing water content, while dry unit weight rises to the maximum dry density (MDD) and then drops beyond the optimum moisture content (OMC).

The modified ASTM mold was adjusted to improve the accuracy and application of ER to adhere to Wenner Four-Electrode method. The mold was coated with epoxy to prevent moisture escape and outfitted with plastic (filler) rods to secure the electrodes. Figure 15 and Figure 16 present ER data collected using the modified ASTM mold. It is important to note that Figures 13 through 16 show some variations in ER trends; however, the overall trends remain consistent across different soil types and compaction attempts. This consistency demonstrates the experimental setup's applicability and confirms the modified ASTM mold as a reliable tool for ER testing.

Using plastic mold for soil compaction testing poses some issues, especially when

subjected to repeated hammering. Unlike the ASTM mold that can withstand repeated hammering due to its material, the plastic mold prone to breaking and stretching near the prefabricated holes regions where tension is more concentrated. The intrinsic material limits of plastic, which lack the strength and endurance of steel molds, are the cause of these fissures.

This study aimed to investigate the relationships between electrical resistivity (ER) and dry unit weight, as well as between ER and moisture content (MC). Although no conclusive resistivity or maximum dry unit weight values were determined, Figure 13 through Figure 16 shows similar patterns and trends. Critical insights are provided by the observed patterns, though, which show that ER sharply decreases, and dry unit weight increases as MC rises to optimal moisture content (OMC) ±2%. The ER curve flattens, and the dry unit weight decreases beyond the OMC, which is explained by the liquefaction-like effect of the high-water content. This behavior highlights the complex relationship between soil density and moisture, highlighting the necessity of long-lasting molds to guarantee accurate and consistent measurements.

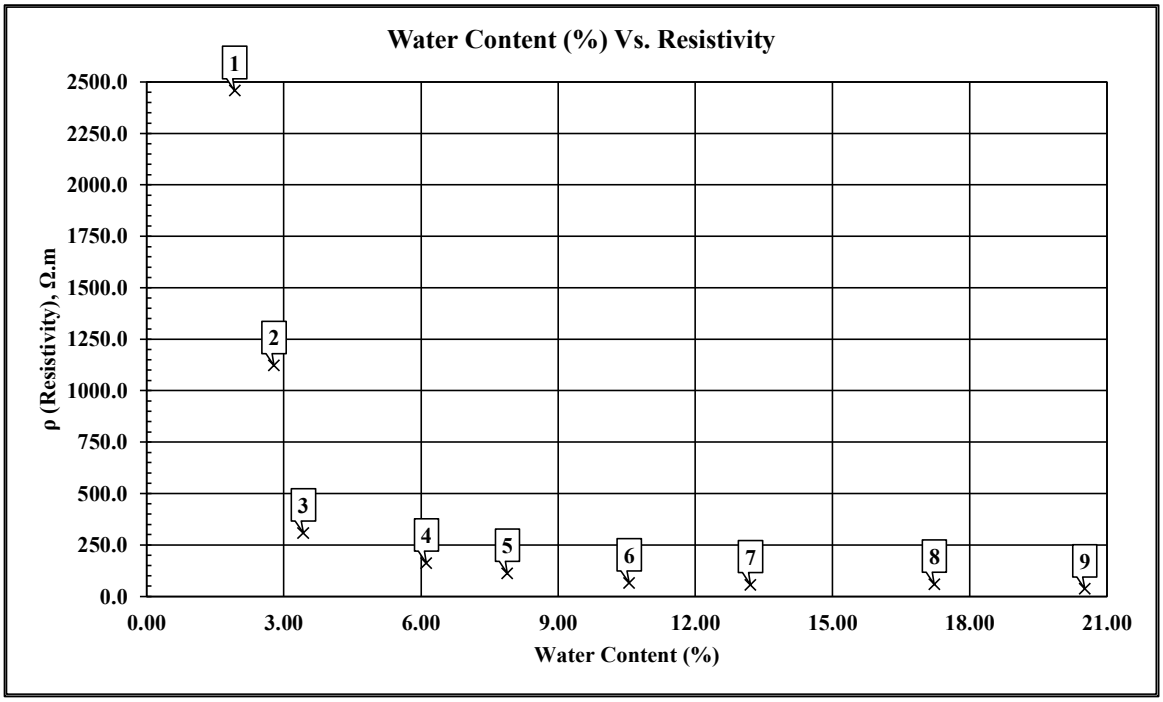

a) Water content vs. ER for Fat Clay (Plastic Mold, 25 Drops)

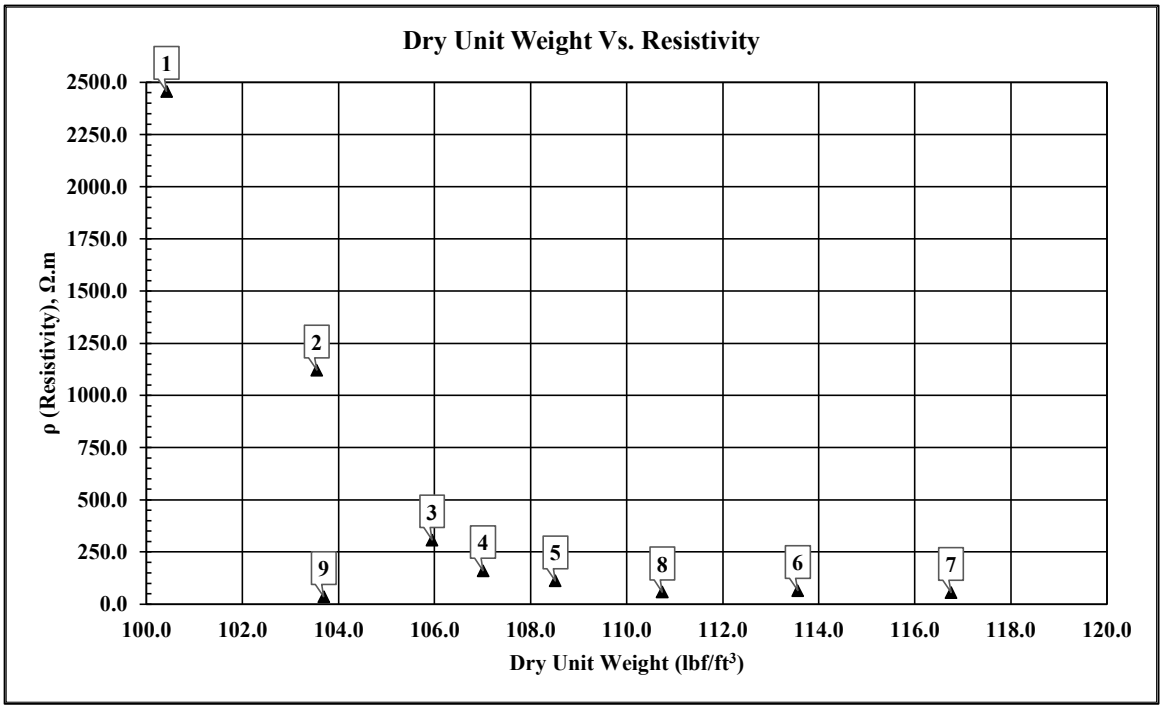

b) Dry Unit Weight vs. ER for Fat Clay (Plastic Mold, 25 Drops)

Figure 13: Moisture and Dry Unit Weight vs. ER for Fat Clay (Plastic Mold)

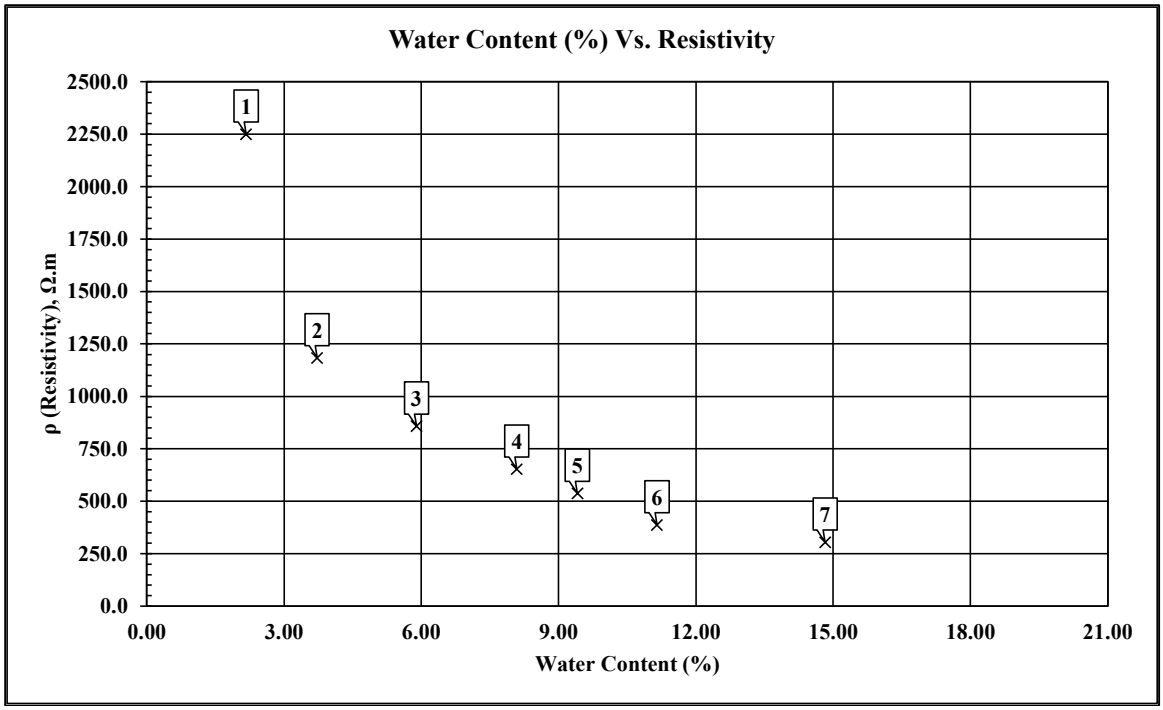

a) Water content vs. ER for Sand (Plastic Mold, 25 Drops)

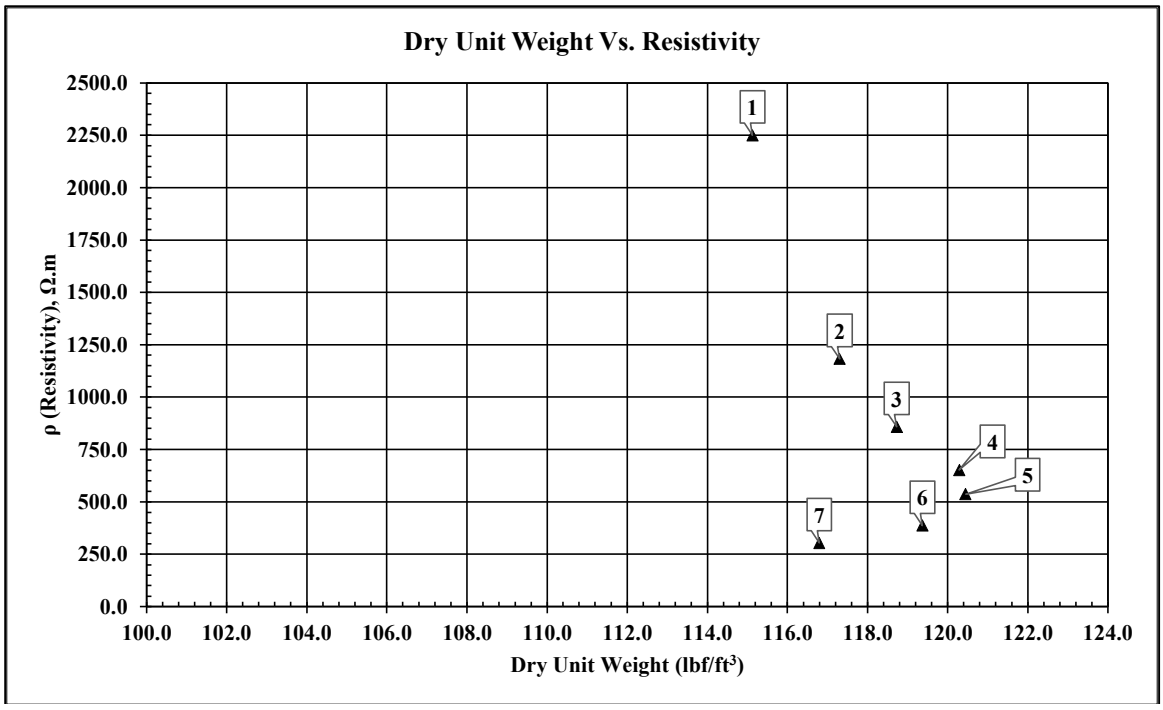

b) Dry Unit Weight vs. ER for Sand (Plastic Mold, 25 Drops)

Figure 14: Moisture and Dry Unit Weight vs. ER for Sand (Plastic Mold)

Overall, the study shows that, while soil type and compaction effort effect MDD, OMC, and ER, the experimental methodology is still reliable. The combination of plastic and modified ASTM molds with SP and MP compaction processes allows consistent ER readings with low variability, providing useful insights into the link between soil compaction and electrical resistivity.

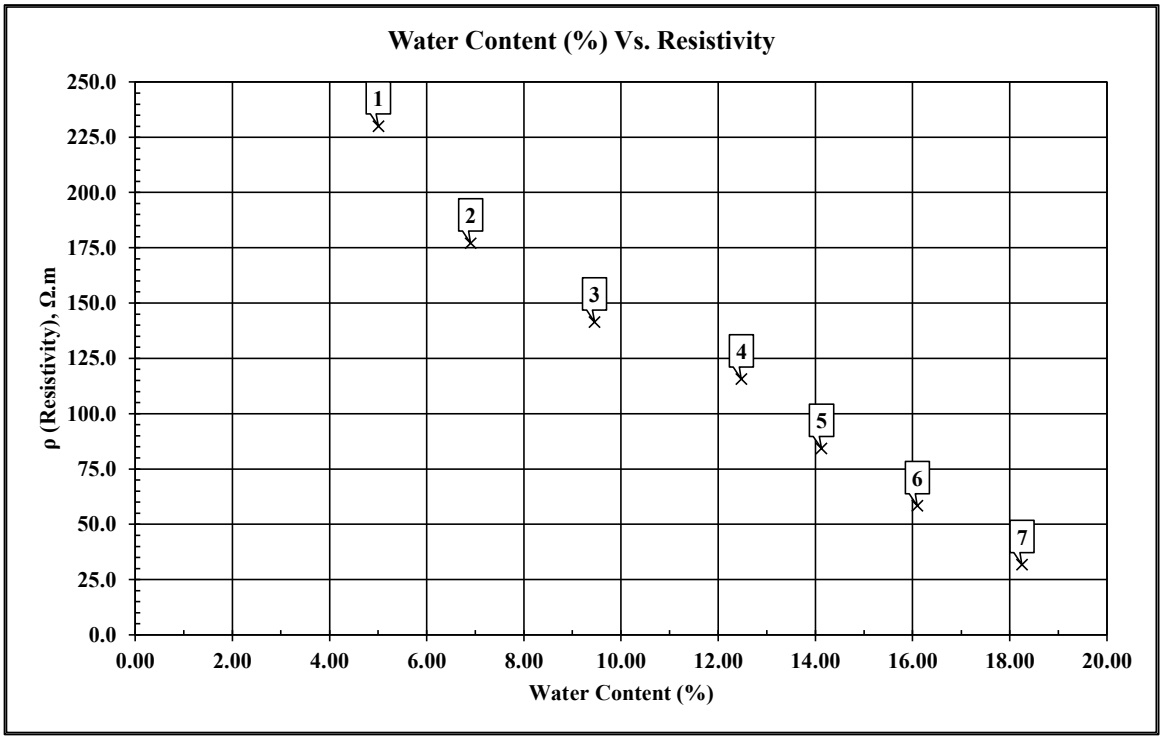

a) Water content vs. ER for Fat Clay (SP Mold, 25 Drops)

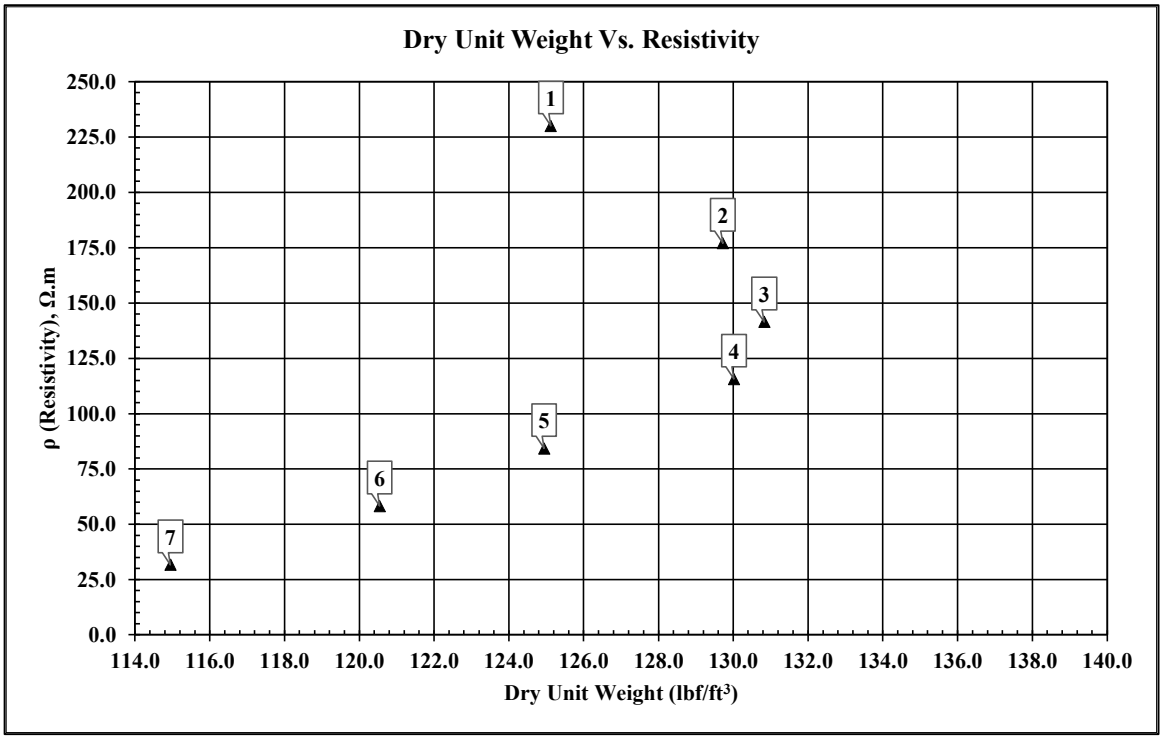

b) Dry Unit Weight vs. ER for Fat Caly (SP Mold, 25 Drops)

Figure 15: Moisture and Dry Unit Weight vs. ER for Fat Clay (SP Mold)

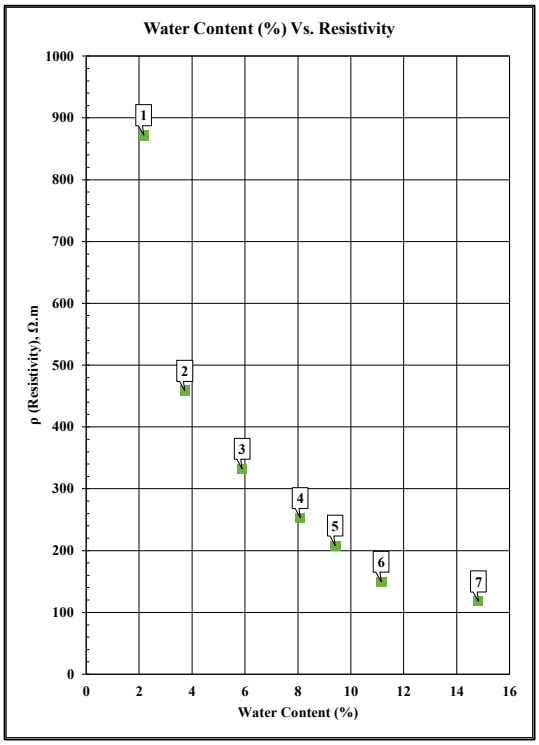

a) Water content vs. ER for Sand (SP Mold, 25 Drops)

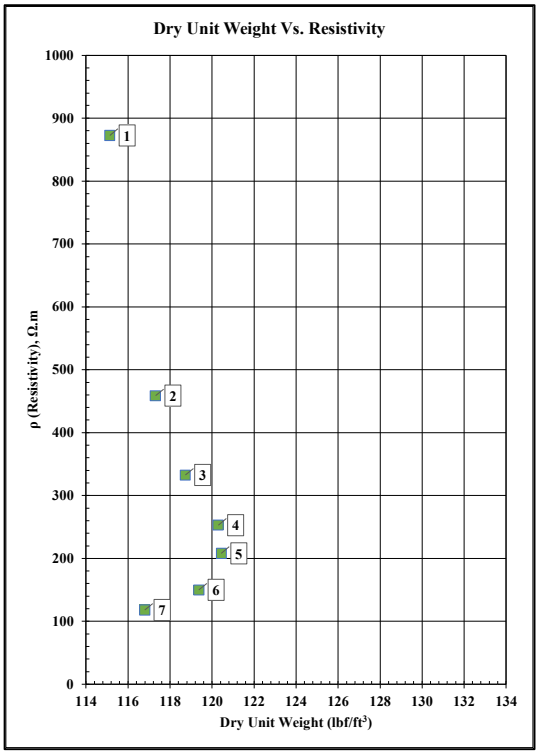

b) Dry Unit Weight vs. ER for Sand (SP Mold, 25 Drops)

Figure 16: Moisture and Dry Unit Weight vs. ER for Sand (SP Mold)

4.3 Electrical Resistivity versus Soil Properties in Laboratory Compaction Tests

Electrical resistivity tests have been shown to be an effective method for determining soil parameters, particularly moisture content and unit weight. Numbers of studies have found that electrical resistivity is inversely related to moisture content, with resistivity decreasing as moisture content increases [56], [57], [58]. This phenomenon is principally caused by water within soil pores acting as a conductor for electrical currents, facilitating charge transport and thereby lowering resistivity. As moisture content rises, the connection of water films improves, increasing the soil's electrical conductivity.

The link between electrical resistivity and soil characteristics, however, is not always clear. Moisture content has a continuous and significant inverse link with resistivity, although the relationship with unit weight is less clear as shown in the previous figures. Siddiqui and Osman (2012) found fewer connections between resistivity and unit weight, implying that soil compactness influences resistivity less than moisture [58]. Furthermore, the research found that resistivity in sandy soils is more dependent on water content. These data indicate that, while resistivity is a valid predictor of moisture content, its use to forecast unit weight or other physical attributes necessitates additional considerations.

Electrical resistivity is a potential, non-invasive method for determining critical soil parameters, particularly moisture content. However, its relationship to unit weight and other qualities appears to be modified by variables such as soil type, compaction level, and pore water characteristics. To improve the prediction capacities of resistivity measurements, more research is needed to create models that incorporate these variables and account for their complexities. Such developments may result in more accurate and comprehensive soil property estimation utilizing electrical resistivity [59], [60], [61].

4.4 Effects of Moisture Content and Soil Type on Resistivity Measurements

The study of the relationship between moisture content, dry density, and electrical resistivity in fat clay and poorly graded sand reveals unique behaviors that reflect the physical and structural variations between the soil types.

Figures 17-to-20 show the observed ER trends in fat clay and poorly graded sand using the ASTM molds. The connection between resistivity and moisture content for fat clay (Figure 17) demonstrates that resistivity decreases dramatically as water content increases. This is typical of fine-grained soils such as clay, where the large surface area and ability to retain water considerably improve electrical conductivity. Resistivity is high on the dry side of the optimal moisture content (OMC) due to the absence of continuous water sheets (OMC for fat clay is 14%). However, as the moisture content approaches the OMC, resistivity drops dramatically due to enhanced pore water connection. The link between resistivity and dry density (Figure 18) provides additional evidence for these conclusions. At low water content, high air voids increase soil resistivity, and as compaction increases, voids are reduced, lowering resistivity. Beyond OMC point, resistivity drops slowly, as moisture content takes precedence over dry density due to near-saturated conditions.

Figure 19 shows the behavior of poorly graded sand. Unlike clay, sand's particle packing properties [12] create a clearer resistivity-moisture relationship, with higher resistivity at low water content due to air voids. Beyond OMC, resistivity decreases but stabilizes faster as compaction and pore water dispersion become less significant. Figure 20 shows that the resistivity-dry density relationship differs between sand and clay. In sand, resistivity decreases gradually with dry density due to limited reduction of voids during compaction, making moisture content the dominant factor.

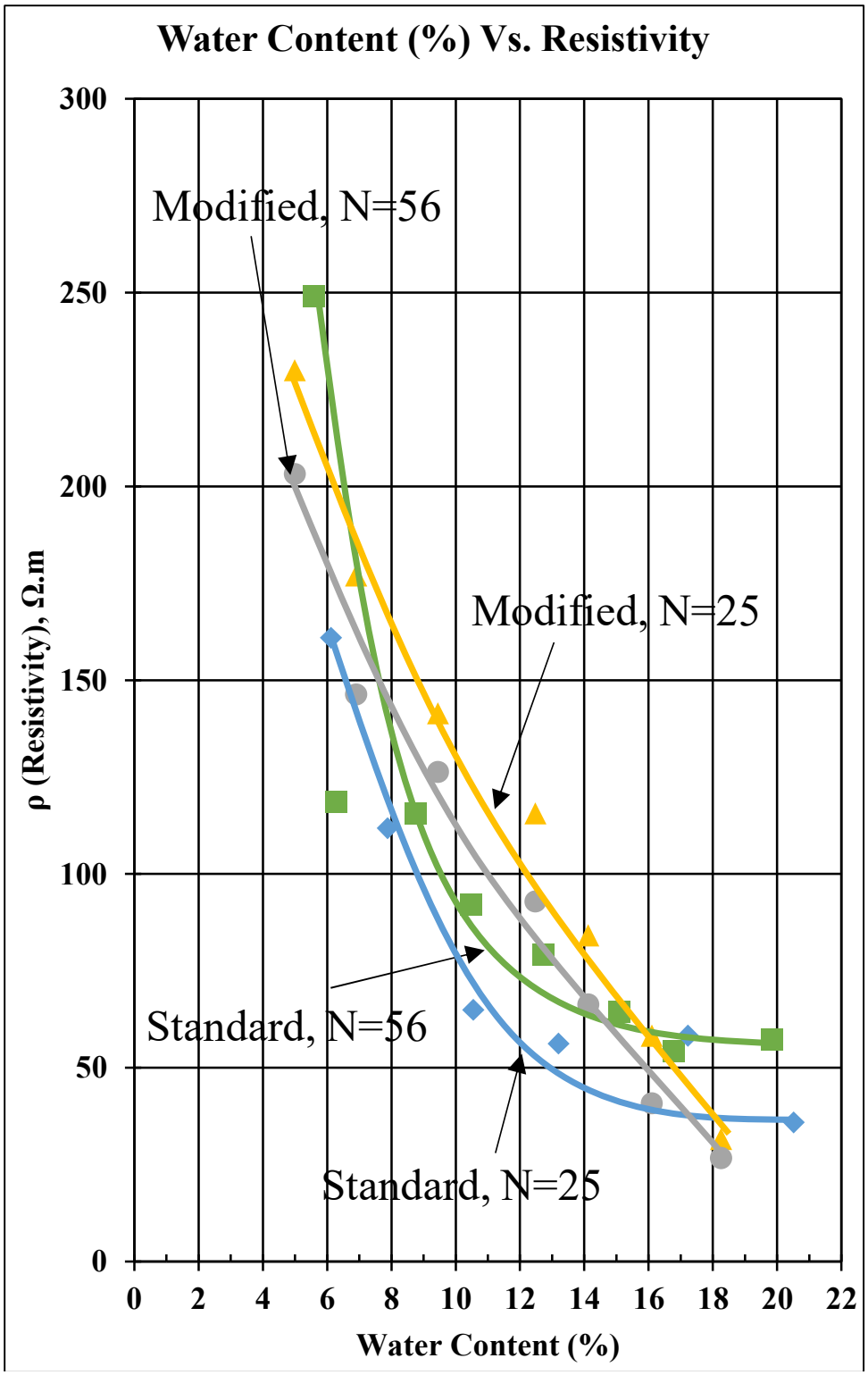

Figure 17: Moisture Content Vs. ER for Modfified SP and MP for fat clay

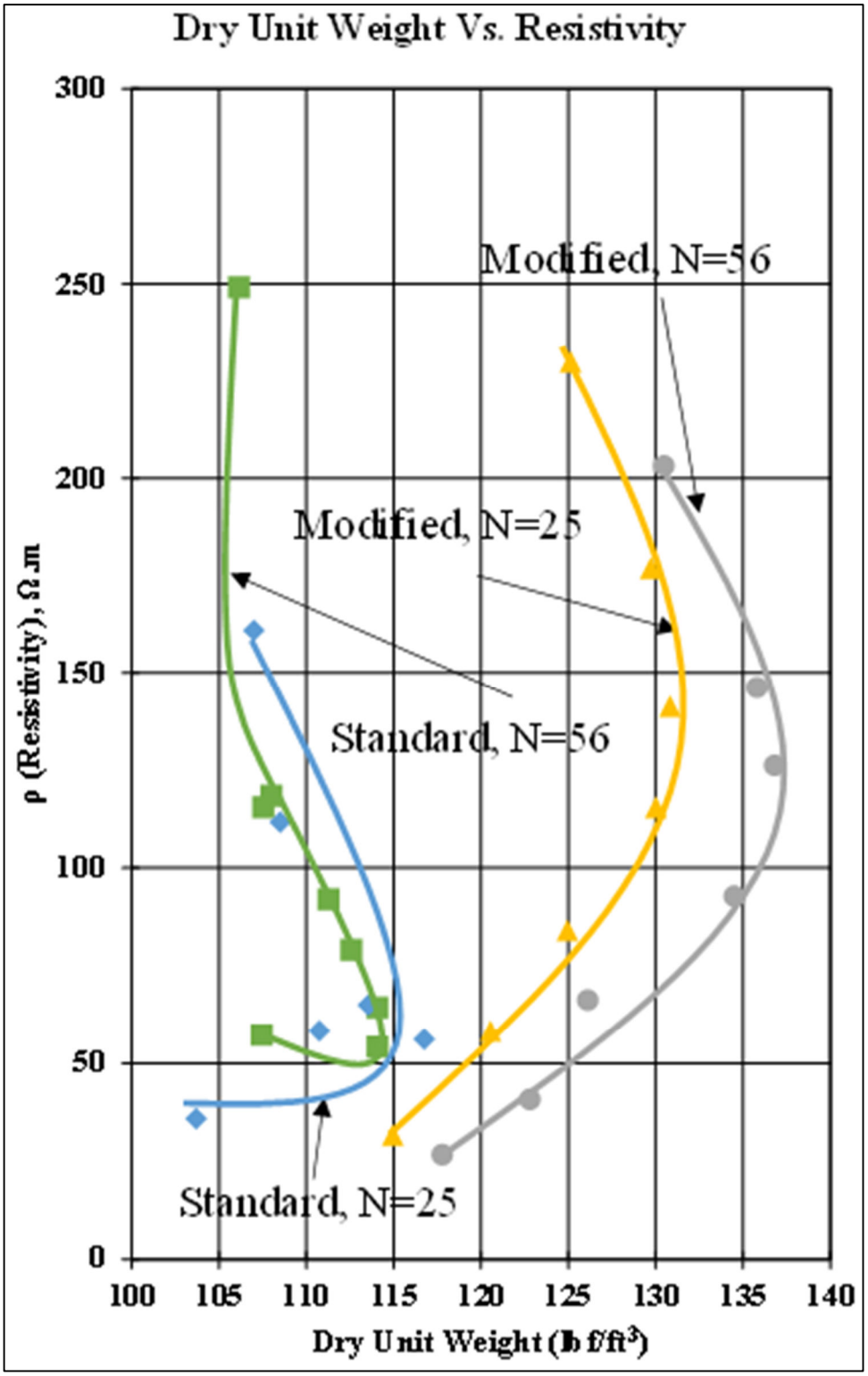

Figure 18: Dry unit Weight Vs. ER for Modified SP and MP for fat clay

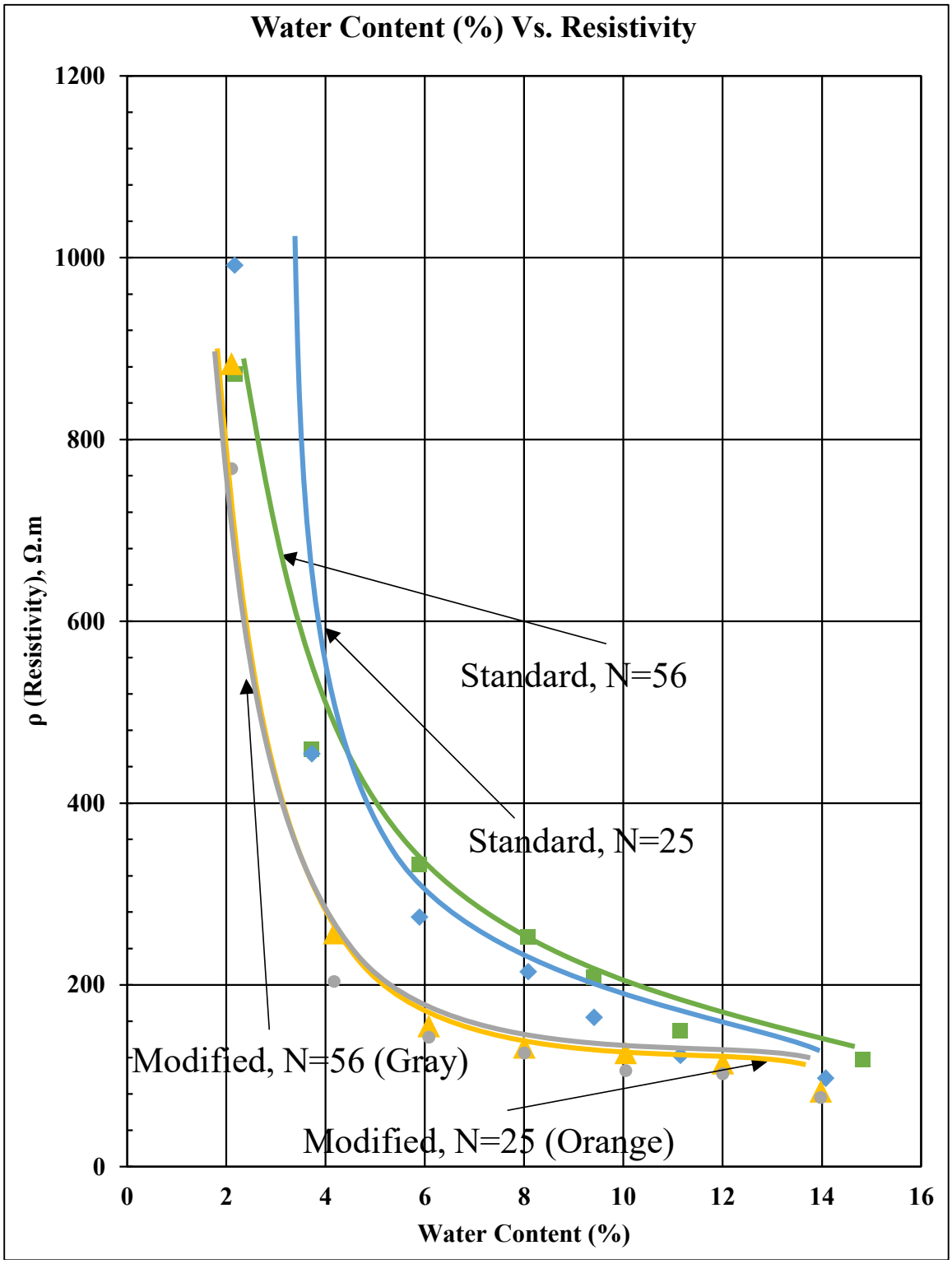

Figure 19: Moisture Content Vs. ER for Modified SP and MP for Poorly Graded Sand

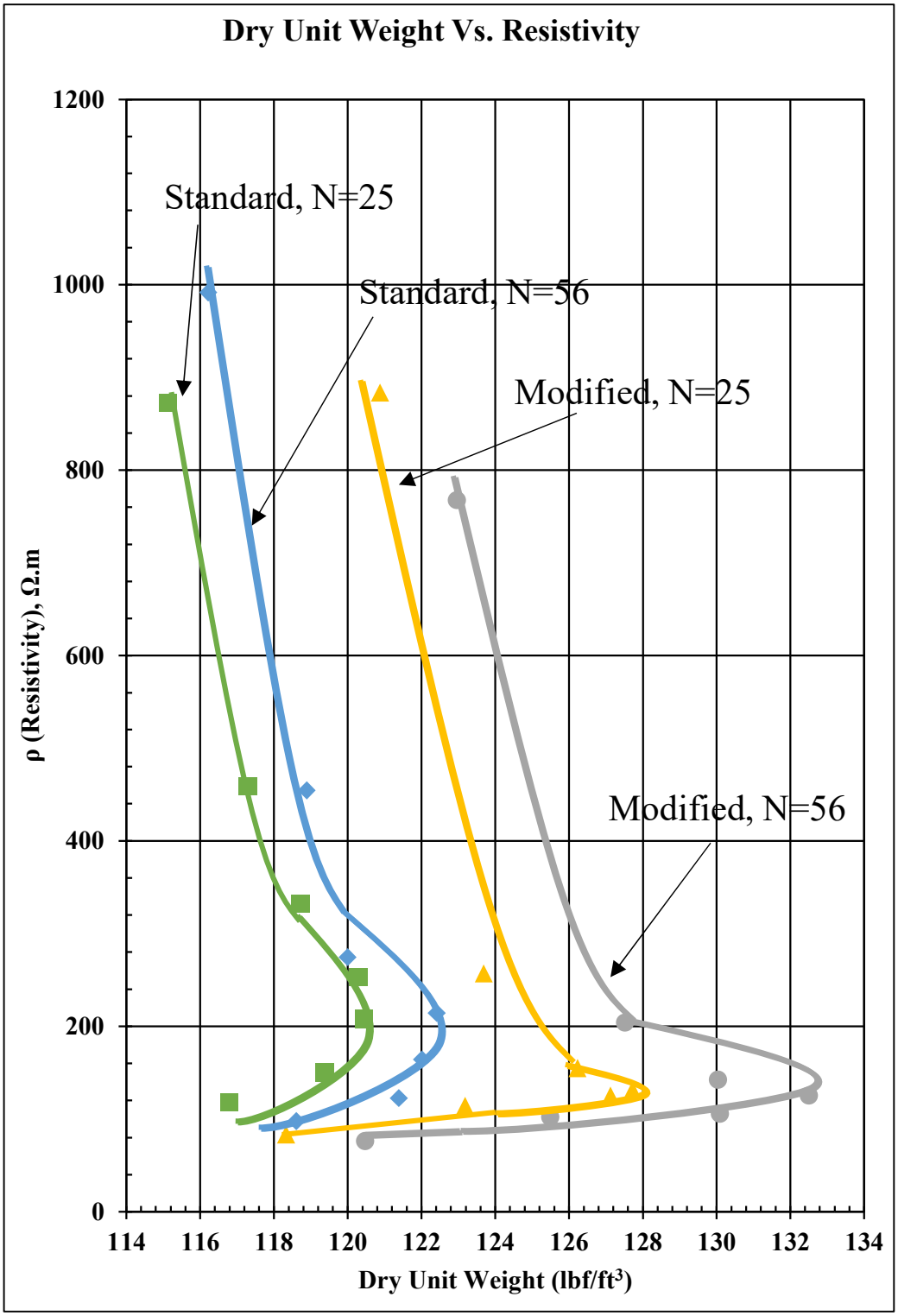

Figure 20: Dry unit Weight Vs. ER for Modfified SP and MP for Poorly Graded Sand

4.5 Interpretation of Laboratory Findings

Moisture content is key to electrical resistivity in soils. Low moisture increases resistivity due to air voids, while higher moisture forms water films, boosting conductivity and lowering resistivity. Fat clay with high plasticity slows this decline compared to sand, which has larger pores and lower water retention.

In conclusion, moisture content has a greater influence on electrical resistivity than dry density, particularly in coarse-grained soil. Coarse-grained soils, such as sand, stabilize faster with less drastic resistivity changes beyond OMC. These findings underscore the importance of considering soil type and compaction in geotechnical resistivity analysis

Chapter 5: Preliminary Design of Walk-behind Electrical Resistivity Meter

5.1 Preliminary Design of Walk-behind Electrical Resistivity Meter

After establishing the laboratory relationship of electric resistivity (ER) and compaction properties via standard and modified proctor tests, multiple iterations were necessary to develop and engineer the walk-behind resistivity meter in order to reach a reasonable degree of confidence in measuring ER in simulated field conditions. The customized rough version of the walk-behind electrical resistivity meter (ERM) is shown in Figures 21a and 21b. The ERM was used to measure the electrical resistivity of soil in the laboratory soil strip tests (Figure 22a and 22b) in real time after one, three, and six passes of a walk-behind electric compaction machine (Figure 22).

As shown in Figures 21 and 22, the plastic cylindrical drum in the ERM is equipped with four evenly spaced stainless steel disk inclusions. The purpose of the steel disks is to serve as Wenner four electrodes, facilitating in-motion measurements of electrical resistance of the soil during compaction.

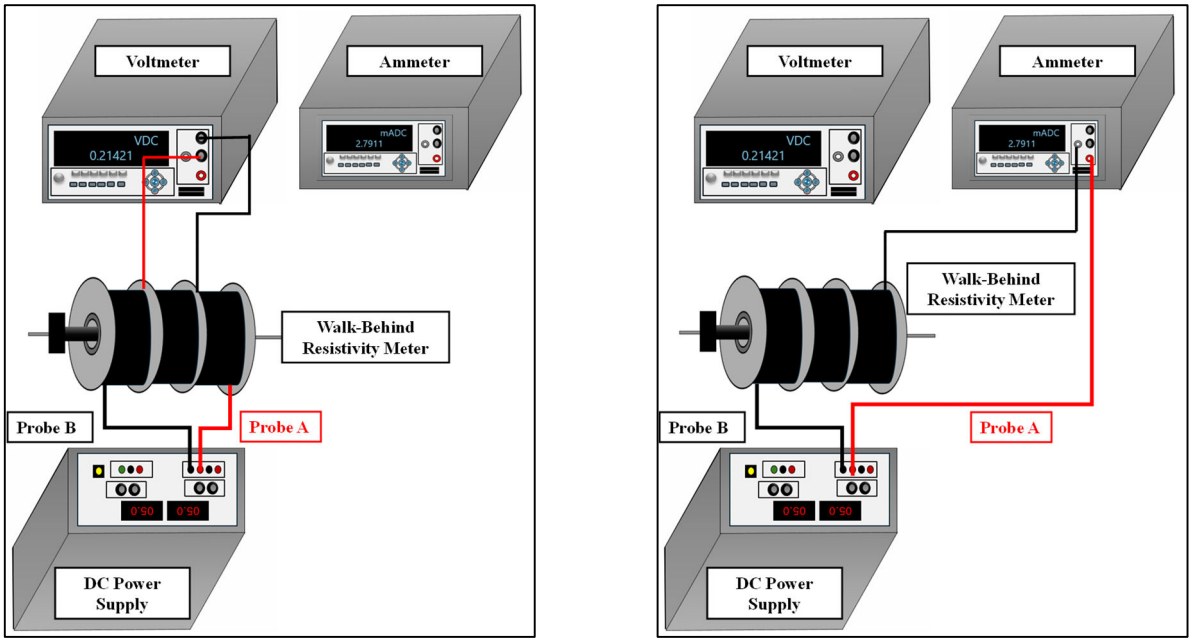

Figure 21: The Walk-Behind Electrical Resistivity Meter

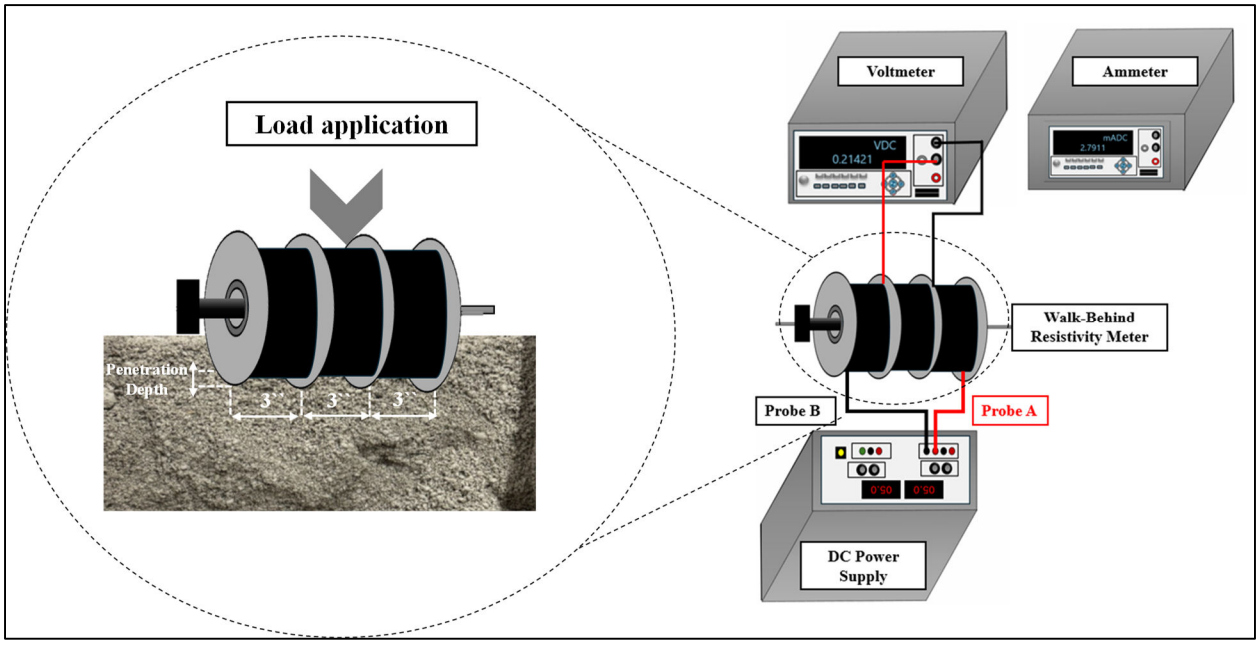

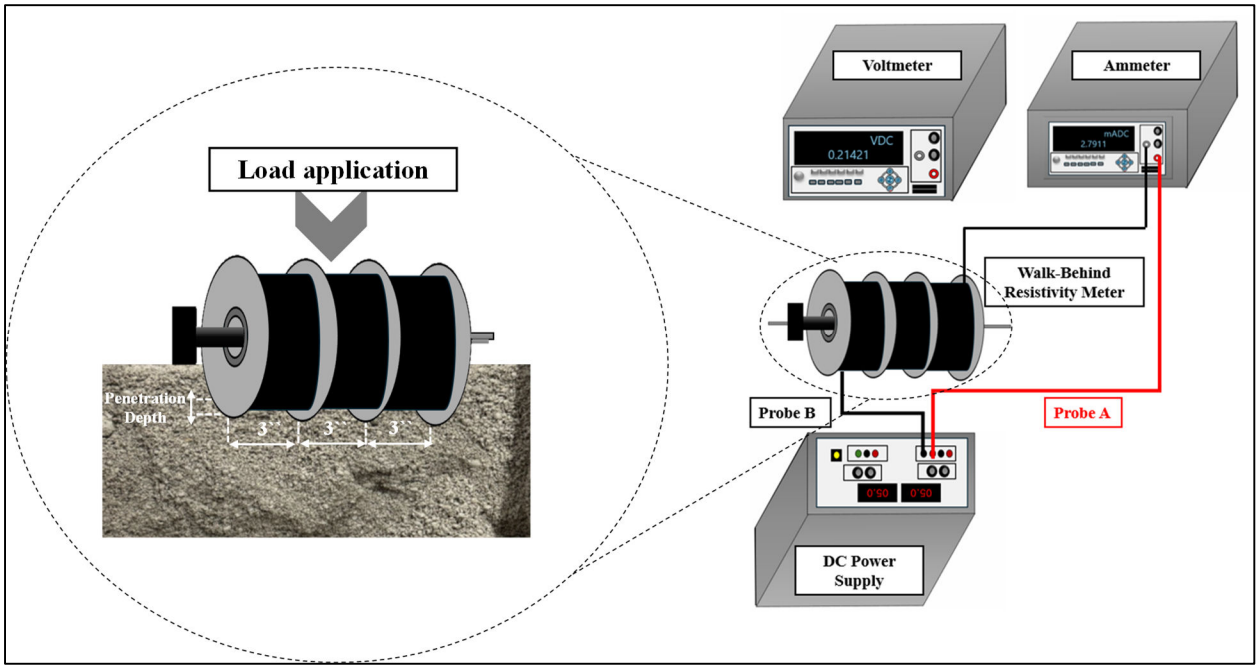

b)

Figure 22: The Walk-Behind Electrical Resistivity Meter for Soil Strip Tests on Sand

Calibration was essential to determine the ideal depth for saw cuts to ensure accurate resistivity propagation consistent with the Wenner Four-Electrode Method. Testing protocols were also developed to apply the necessary pressure for effective soil penetration by the drum. These steps were vital to ensure the walk-behind resistivity meter accurately replicated laboratory compaction-resistivity measurements and produced reliable results.

5.2 Preliminary Design of Soil Strip Container

A soil container, Figure 23, was used for testing the performance of the walk-behind electrical resistivity meter. The soil container was sized to accommodate two 6-

inch-thick layers of soil, and with enough width and length to accommodate the compaction procedure using the walk-behind compaction machine (Figure 25). The inner dimensions of the container are 14 inches in width, 96 inches in length, and 14 inches in depth, as shown in Figure 23a. The container was strengthened on all sides with lateral supports affixed to the laboratory floor to avoid any lateral movement of the soil during compaction, thereby avoiding uncertainties when calculating soil volume and the corresponding in situ density.

a) View of the Testing Container Development

b) View of the Testing Container with Lateral Reinforcement

Figure 23: Soil Testing Container

To prevent the loss of soil moisture through the walls of the wood container and to the concrete floor, and to reduce electrical current dissipation through the boundaries, the inside of the container was shielded with a thin plexiglass layer. The plexiglass was firmly affixed to the container walls and the concrete floor, as shown in Figures 24a and 24b. These implementations were necessary to ensure reliable measurements for both compaction and electrical resistivity. The poorly graded sand tested earlier was deemed appropriate for this set of tests because of its availability and ease of compaction as opposed to fat clay.

a) Top View of Container with Plexiglass Lining

b) Interior View of Container with Plexiglass Lining

Figure 24: Plexiglass-Lined Testing Container for Controlled Compaction and ER Testing

A walk-behind electrical plate compactor, Evolution H320-E, was used to compact the sandy soil at different numbers of passes (Figure 25). Data was taken in real-time after one, three, and six passes of the compactor. Next, the walk-behind resistivity meter, which was operated manually, was used to measure electrical resistivity at different locations as shown in Figure 26a. Subsequently, the moisture content of the soil and its dry density were measured. The soil density was measured using the sand cone test method (ASTM D1556).

To simulate field conditions, both one- and two-compacted layer systems were used. For each system, compaction was performed in sequences of one, three, and six passes per layer as shown in Figures 26a and 26b. This approach ensured the findings were representative of typical field applications involving multilayer systems.

Figure 25: Electrical plate compactor, Evolution H320-E

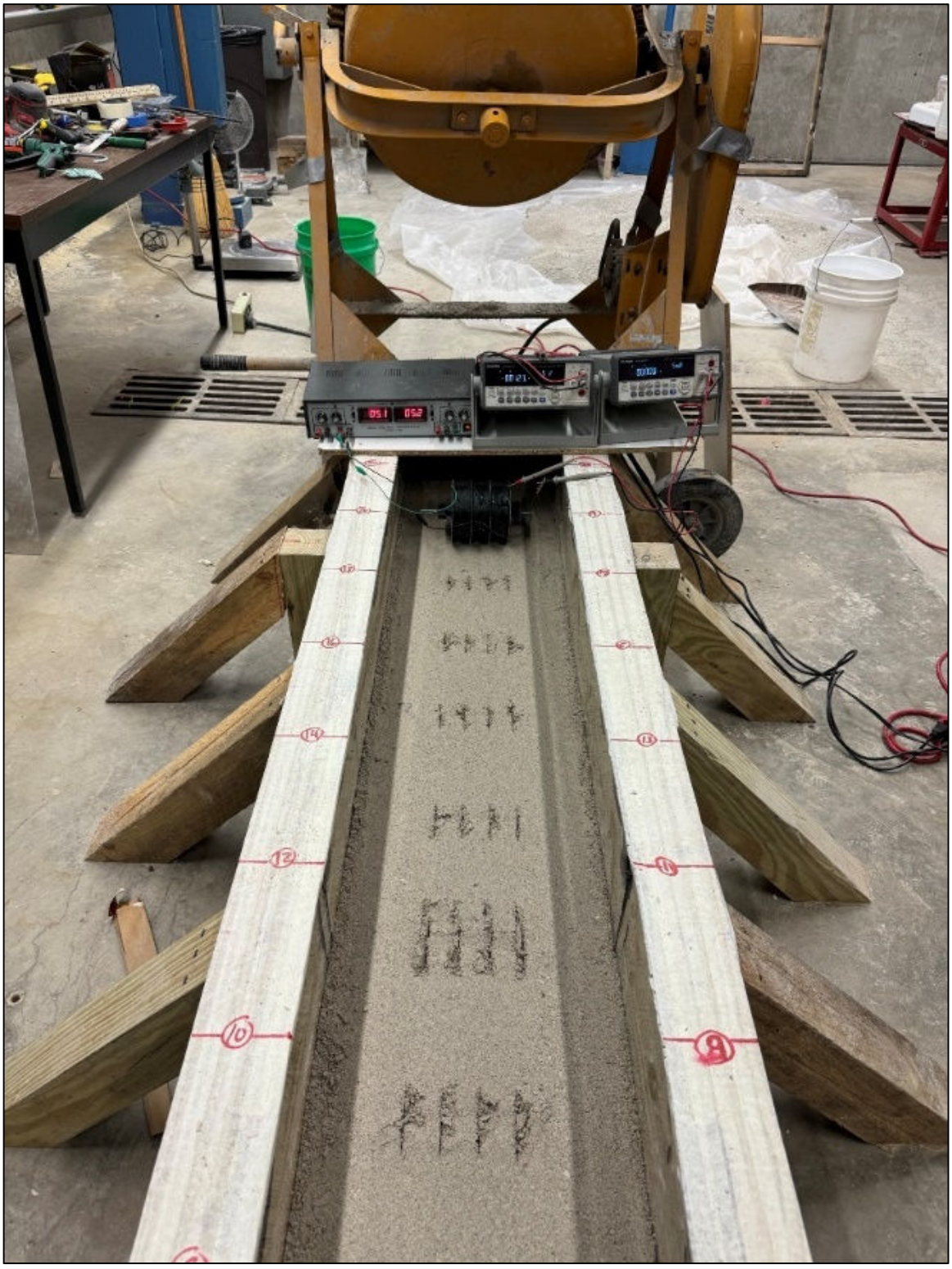

a) Single-Layer Sand Compaction System for ER Testing

b) Two-Layer Sand Compaction System for ER Testing

Figure 26: Comparison of Single- and Two-Layer Compaction Systems

Chapter 6: Laboratory Soil Strip Tests

6.1 Overview

After evaluating two soil types, poorly graded sand was selected for testing due to its favorable compaction characteristics. It was possible to generate accurate trends in electrical resistivity measurements and compaction characteristics due to the granular structure of this type of soil. After performing new Standard Proctor (SP) and Modified Proctor (MP) tests on the selected soil, the optimum moisture content (OMC) was determined and used for the soil strip compaction study.

Preliminary soil strip tests were performed to determine an appropriate compaction speed, using a walk-behind compactor (Figure 25), revealing that 7 to 10 feet per minute was optimal for the study. This incremental approach was developed with the intention of capturing the changes in soil electrical resistivity that occurred at various compactive efforts. Following each series of passes, the electrical resistivity of the sand was measured using the newly devised walk-behind electrical resistivity meter (ERM), which has been calibrated specifically for this experiment. The average ER results from the soil strip study of each pass measurement were compared to the laboratory-scale reading at OMC. To ensure accuracy and minimize the impact of time-dependent changes (losses) in moisture distribution, the resistivity measurements were carried out immediately after the

compaction process.

To compare soil strip test results with laboratory compaction effort (Table 2), electrical resistivity values and measured densities were plotted after 1, 3, and 6 passes against the SP and MP laboratory graphs. These passes simulated S-25, S-56/M-25, and M-56 curves, representing increasing compactive effort and dry density (Table 3). In other words, a lower density corresponding to one pass (S-25), moderate density to three passes (S-56/M-25), and higher density to six passes (M-56). SP compaction, with lower effort, produced lower dry densities and higher moisture contents, resulting in higher resistivity values. MP compaction, with greater effort, achieved higher dry densities and lower resistivity. Comparing SP and MP resistivity curves provided insights into the relationship between compactive effort, soil conductivity, and resistivity trends.

Table 3: SP and MP Compaction and their ER Values

	ω (%)	γ_d (lb/ft^3)	ρ (Resistivity) Ω.m	Saturation (%)
Standard Proctor N=25	2.67	125.2	335	20
	4.74	129.1	161	41
	7.48	132.1	97	71
	9.36	128.6	62	80
Standard Proctor N=56	2.39	128.8	294	20
	4.70	133.0	149	46
	6.93	135.2	94	74
	9.31	129.8	58	82
Modified Proctor N=25	2.09	130.7	310	19
	4.94	135.6	153	53
	7.36	138.7	86	89
	8.97	134.5	60	93
Modified Proctor N=56	2.31	135.9	290	25
	4.76	139.6	145	60
	7.10	141.2	84	95
	8.76	136.0	55	96

To provide additional assertion that the experimental findings are accurate, spot tests of the moisture content and moist unit weight were carried out at three different locations using sand cone method in accordance with A STM D1556. The sand cone test was used to determine the density of the compacted sand after the sixth pass. Also, when conducting these spot tests, the oven-dry method was utilized to properly quantify the amount of moisture that was present in the sand after it had been compacted. Electrical resistivity data reliability was examined by comparing spot-tested moisture content and density with resistivity measurements. As shown in Figure 29, there was a distinct pattern of diminishing resistivity with increased compaction (effort) passes. As the compaction effort

increased, there was a decrease in the air voids and an improvement in the connectivity of water films within the sand matrix. The measured resistivity trends were consistent throughout the soil strip study.

The resistivity data for one, three, and six compaction passes highlighted the progressive impact of compactive effort on soil properties. Similar to laboratory findings, after one pass, high resistivity values reflected significant air voids and low density. By the third pass, resistivity decreased substantially due to increased density and reduced void ratio. After six passes, resistivity stabilized, indicating diminishing effects of additional compaction on soil density and conductivity (Figure 27).

To highlight the sensitivity of electrical resistivity to compaction effort and dry density in poorly graded sand, routine testing was conducted as previously described. By combining resistivity data with compaction parameters like OMC and dry unit weight, the study provided insights into soil behavior under various field conditions, such as multilayer compaction and loss of moisture. The walk-behind electrical resistivity meter proved to be effective in measuring granular soils' electrical resistivity and its corresponding compaction levels. This research established a robust framework for assessing the relationship between soil

compaction and electrical resistivity by integrating soil strip testing with traditional spot testing methods.

6.2 Laboratory Soil Strip Tests Results

This research employed soil strip testing to analyze trends in electrical resistivity (ER), dry unit weight, and compaction effort under controlled conditions. Testing began with uncompacted soil layers: 8 inches for Test 1 and Test 2, and 6 inches for Test 3 and Test 4. ER measurements were taken longitudinally at 8-inch intervals, yielding 12 values per pass. The mean ER was calculated for consistency. Results for Tests 1–4 are presented in Figures 27–30 as blue, red, green, and orange lines, respectively.

Tests 1 and 2 involved a single soil layer measuring 8 inches in uncompacted thickness. ER was measured after one, three, and six compactor passes, alongside volumetric unit weight (=the entire soil layer weight/the compacted layer volume), sand cone, and moisture content tests. Tests 3 and 4 used a two-layer system with 6-inch uncompacted soil layers. Test 3 was performed on the first layer at slightly higher OMC due to moisture loss during preparation. Test 4 was conducted on the second layer.

New laboratory compaction curves were developed for poorly graded sand to determine OMC and MDD values consistent with the larger borrowed soil sample. Standard Proctor (SP) and Modified Proctor (MP) tests were conducted to establish these parameters. Under SP with 25 hammer drops in a three-layer configuration, the sand had an OMC of 7.5% and an MDD of 132 lb/ft³, while MP with 56 hammer drops in a five-layer configuration yielded an OMC of 6.75% and an MDD of 141 lb/ft³. These values are critical for linking compaction parameters to the number of passes and ER values, providing a baseline for soil strip testing. Figure 27 illustrates compaction curves in green, blue, red, and black, representing SP and MP conditions.

Baseline ER values and curves were also established. For SP three-layer conditions, ER dropped from 335 Ω.m to 62 Ω.m, while MP five-layer conditions experienced a drop from 290 Ω.m to 55 Ω.m, as shown in Table 3. Average water content vs. ER (Figure 28) and saturation vs. ER (Figure 30) curves were developed. The dry unit weight and ER curves for SP and MP tests showed consistent behavior with earlier poorly graded sand testing. MDD and ER curves for the larger soil sample are presented in Figure 29.

After establishing these curves, soil strip tests were performed. In Test 1, the dry unit weight rose from 111 lb/ft³ after one pass to 120 lb/ft³ after six passes,

demonstrating the influence of uncompacted layer thickness (lift) on the resulting compaction. The associated ER values dropped from 155 Ω.m to 138 Ω.m. Test 2, which featured improved mixing of the soil at optimal moisture content (OMC) and repeated measurements, indicated a higher increase in dry unit weight, from 118 lb/ft³ to 131 lb/ft³, but ER values fell from 134 Ω.m to 120 Ω.m. The findings indicated a distinct negative correlation between electrical resistivity and soil density with increasing compaction effort.

The testing technique was refined by reducing the uncompacted layer thickness (lift) to 6 inches, followed by the execution of further experiments (Test 3 and Test 4), represented in green and orange lines (Figures 27-30), respectively. In Test 3, the first soil layer of the two-layer system was compacted, resulting in a drop in ER values from 134 Ω.m after one pass to 118 Ω.m after six passes in a linear progression. In Test 4, the second layer of two-layer system was compacted, resulting in a decrease in the ER values from 114 Ω.m to 87 Ω.m as compaction advanced. In Test 3, the density of the first layer increased from 117 lb/ft³ to 125 lb/ft³, and in Test 4, the second layer's density rose from 122 lb/ft³ to 136 lb/ft³ over six passes. The findings underscored the effect of decreasing the uncompacted thickness and stacking on density and ER trends, shedding light on the role of soil thickness in compaction efficiency. Table 4 presents the soil strip testing summary

for the four test results.

Simultaneously with the field experiments, laboratory analyses were performed to establish benchmark correlations for the examined soil. The Standard Proctor (SP) and Modified Proctor (MP) tests were conducted to ascertain the optimum moisture content (OMC) and maximum dry unit weight using 25 and 56 hammer drops, respectively. These investigations established the basis for developing moisture content vs. ER curves and dry unit weight vs. ER curves for the tested soil. Furthermore, saturation vs. average electrical resistivity charts were created to illustrate the interplay of moisture, compaction, and electrical resistivity.

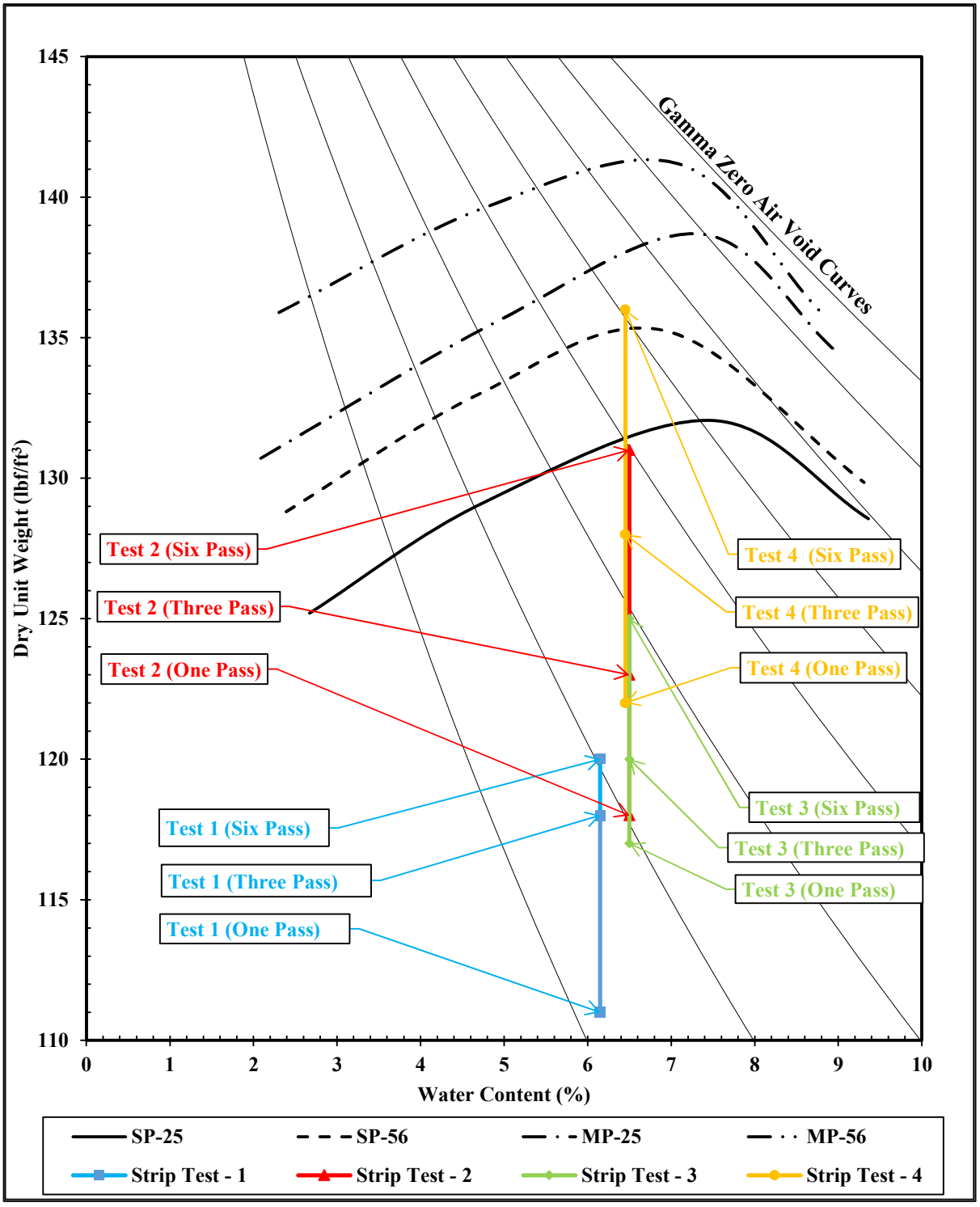

Figure 27: Moisture content vs Dry unit weight Modfified SP and MP for poorly graded sand and soil strip tests.

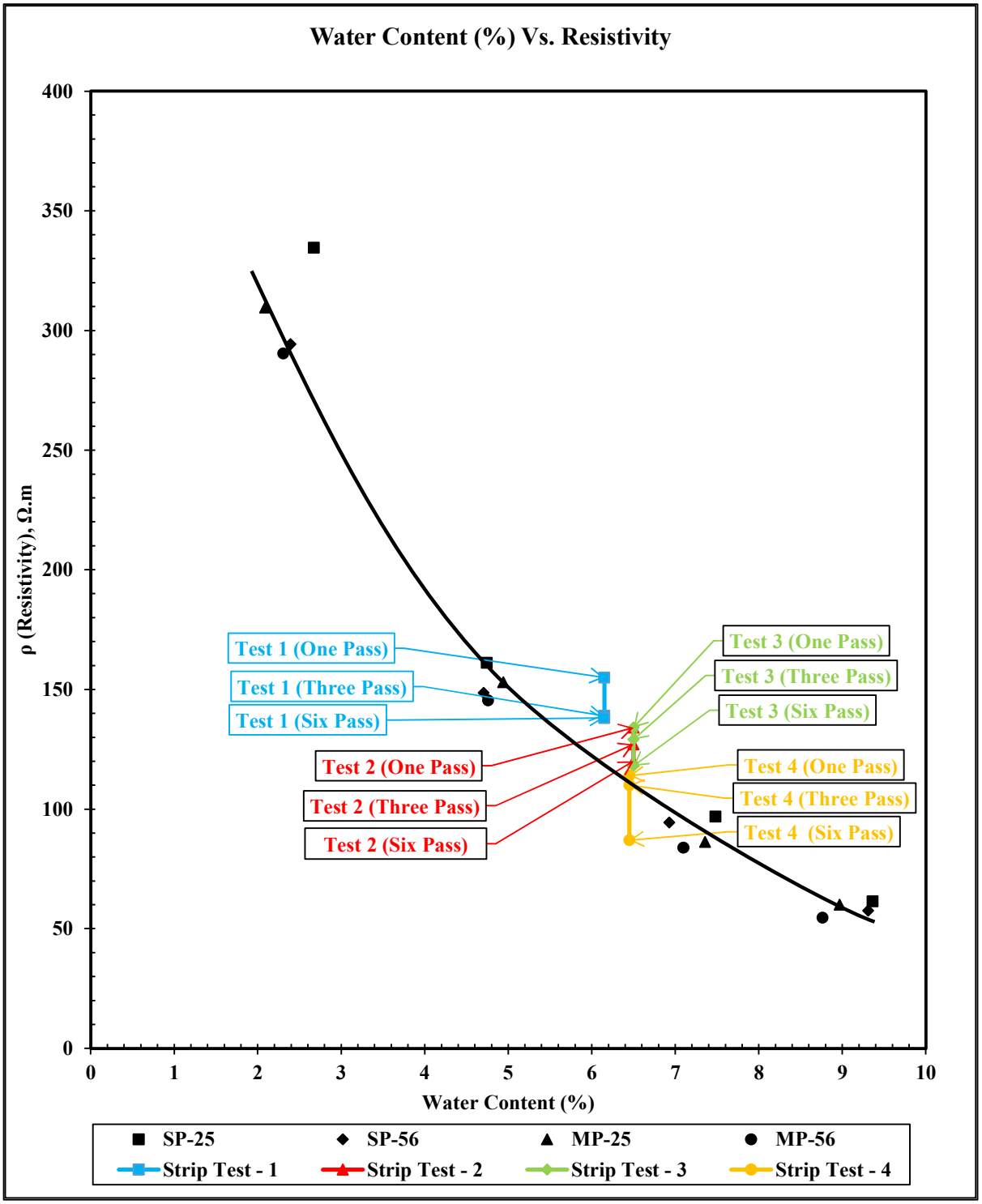

Figure 28: Moisture content vs ER SP and MP for poorly graded sand and soil strip test

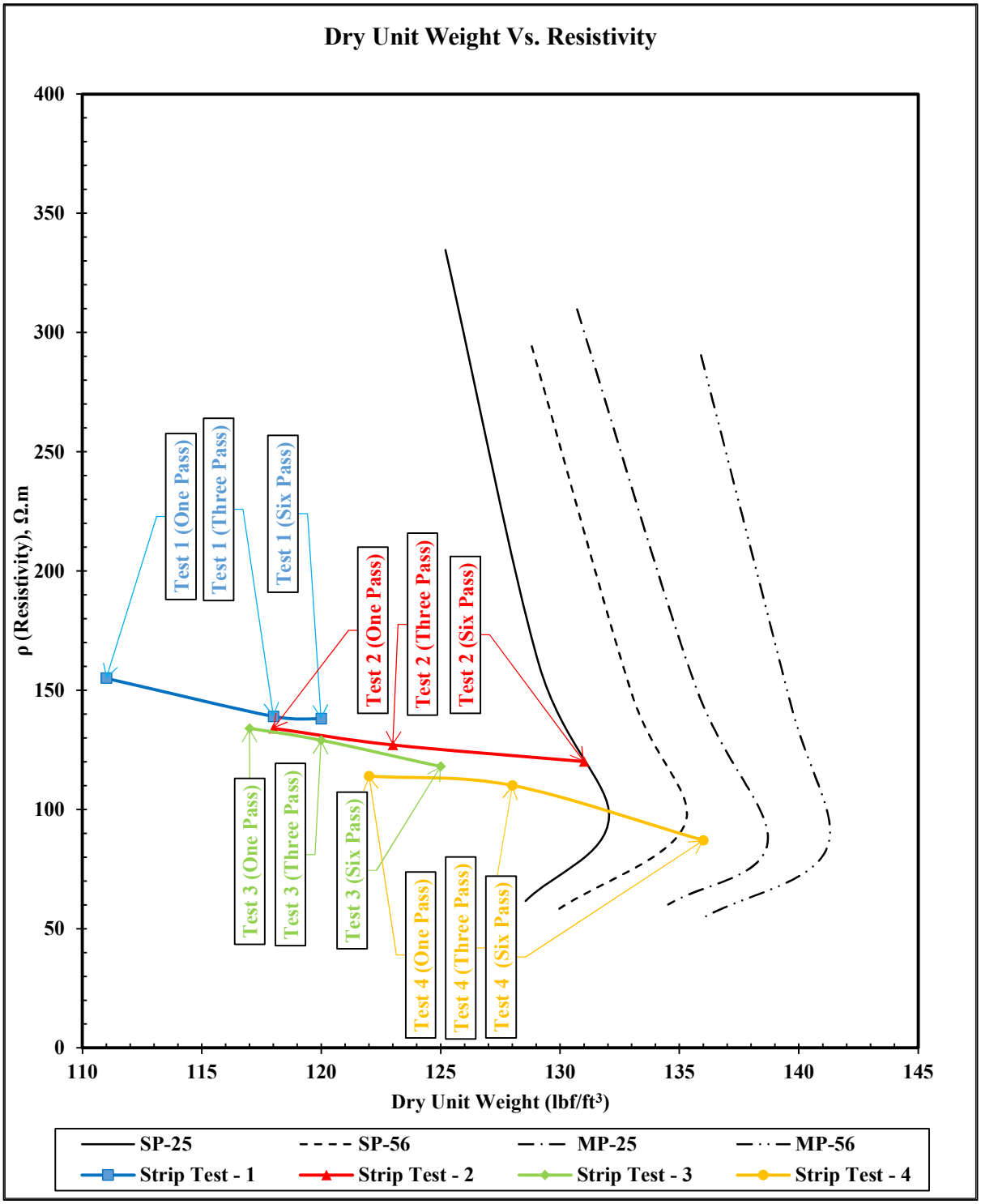

Figure 29: Dry unit weight vs ER SP and MP for poorly graded sand and soil strip tests

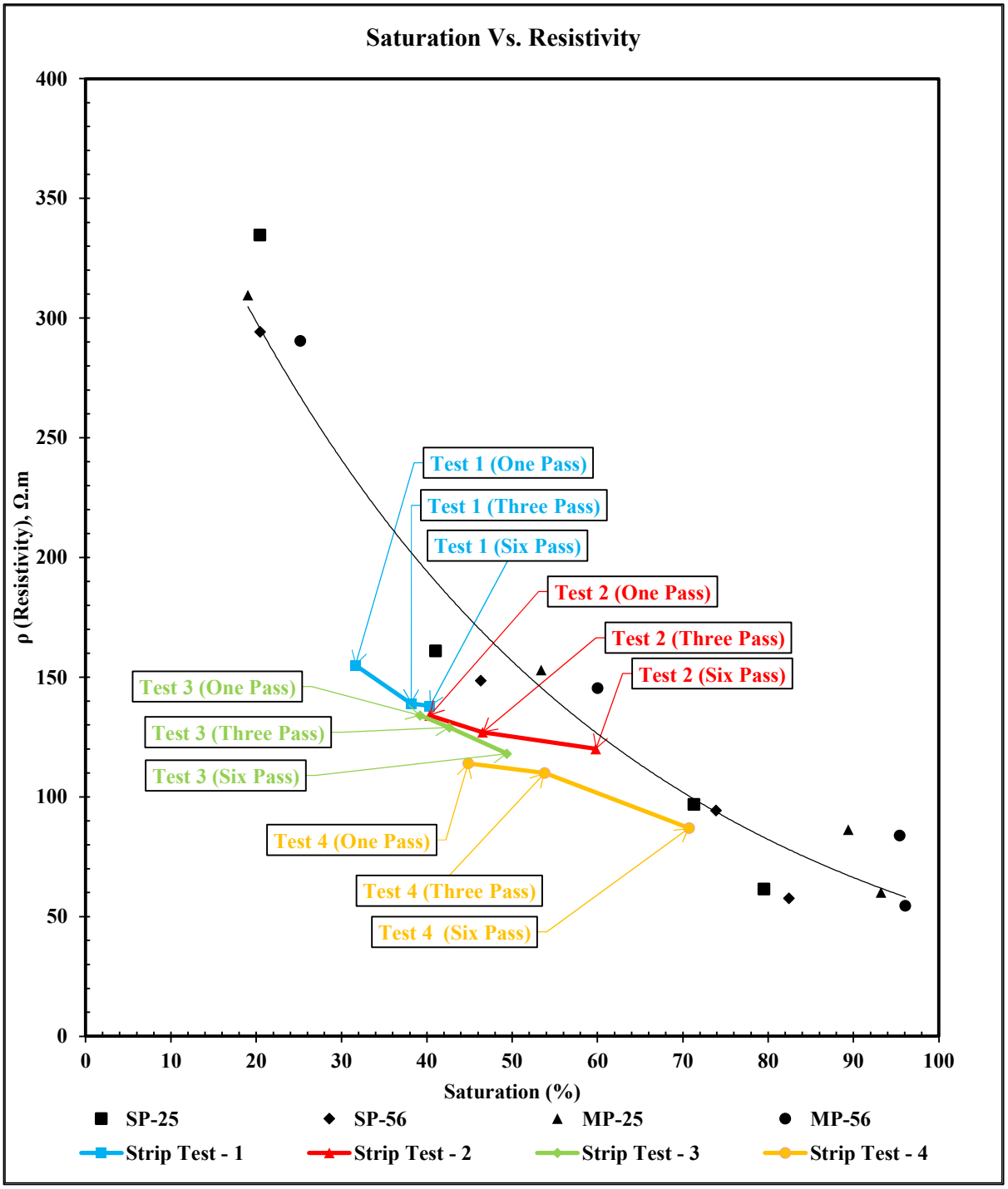

Figure 30: Percent of Saturation (%) vs ER Modfified SP and MP For Poorly Graded Sand and Soil Strip Tests.

The results of the four tests were plotted against the laboratory-derived curves to

assess the patterns seen during compaction. The findings indicated that as the number of passes rose, resistivity constantly dropped, according to trends from the laboratory results while keeping the moisture content around OMC. The results corroborated the notion that electrical resistivity may reliably indicate compaction progress and soil density in the field. Furthermore, three spot testing were carried out to confirm the dry unit weight and moisture content against measured soil strip testing ER value. The sand dry unit weight, measured using the Sand Cone (SC) test, were 127.9, 131.5, and 138.9 lb/ft^3 for SC-1, SC-2 and SC-4, respectively after the 6^{th} pass. Figure 31 and Figure 32 highlights black trend line indicating sand cone test results, which measured electrical resistivity (ER) values based on saturation (Figure 31), then plotting dry unit weight (Sand Cone Test) with measured ER (Laboratory), as shown in Figure 33. The moisture content remained close to the OMC (6.5%), confirmed via the oven-dry method. Tracking these values along the established laboratory curves in Figure 32 shows a decrease in predicted ER from 147 Ω.m to 86 Ω.m. This trend aligns with soil strip testing results, where ER decreased from 138 Ω.m to 87 Ω.m. While saturation could serve as an additional parameter to predict ER, it was not investigated in this study.

Table 4: SP and MP Compaction and ER Values for Soil Strip Testing

		γ_d (lb/ft^3)	ρ (Resistivity) Ω.m	ω (%)	S(%)	Relative Compaction (%)
test 1	One Pass	111	155	6.15	32	80.0
	Three Pass	118	139	6.15	38	85.1
	Six Pass	120	138	6.15	40	86.5
test 2	One Pass	118	134	6.5	40	85.1
	Three Pass	123	127	6.5	47	88.7
	Six Pass	131	120	6.5	60	94.4
test 3	One Pass	117	134	6.5	39	84.4
	Three Pass	120	129	6.5	43	86.5
	Six Pass	125	118	6.5	49	90.1
test 4	One Pass	122	114	6.45	45	88.0
	Three Pass	128	110	6.45	54	92.3
	Six Pass	136	87	6.45	71	98.1

This technique offers a comprehensive framework for field soil strip testing, facilitating the identification of patterns that inform the optimal number of passes necessary to get specified compaction levels. This method correlates ER values with moisture content and dry unit weight, providing a practical and effective way of improving compaction operations in real time. The incorporation of laboratory and field data highlights the relevance of electrical resistivity measurements in geotechnical engineering, facilitating the development of sophisticated soil compaction monitoring methods.

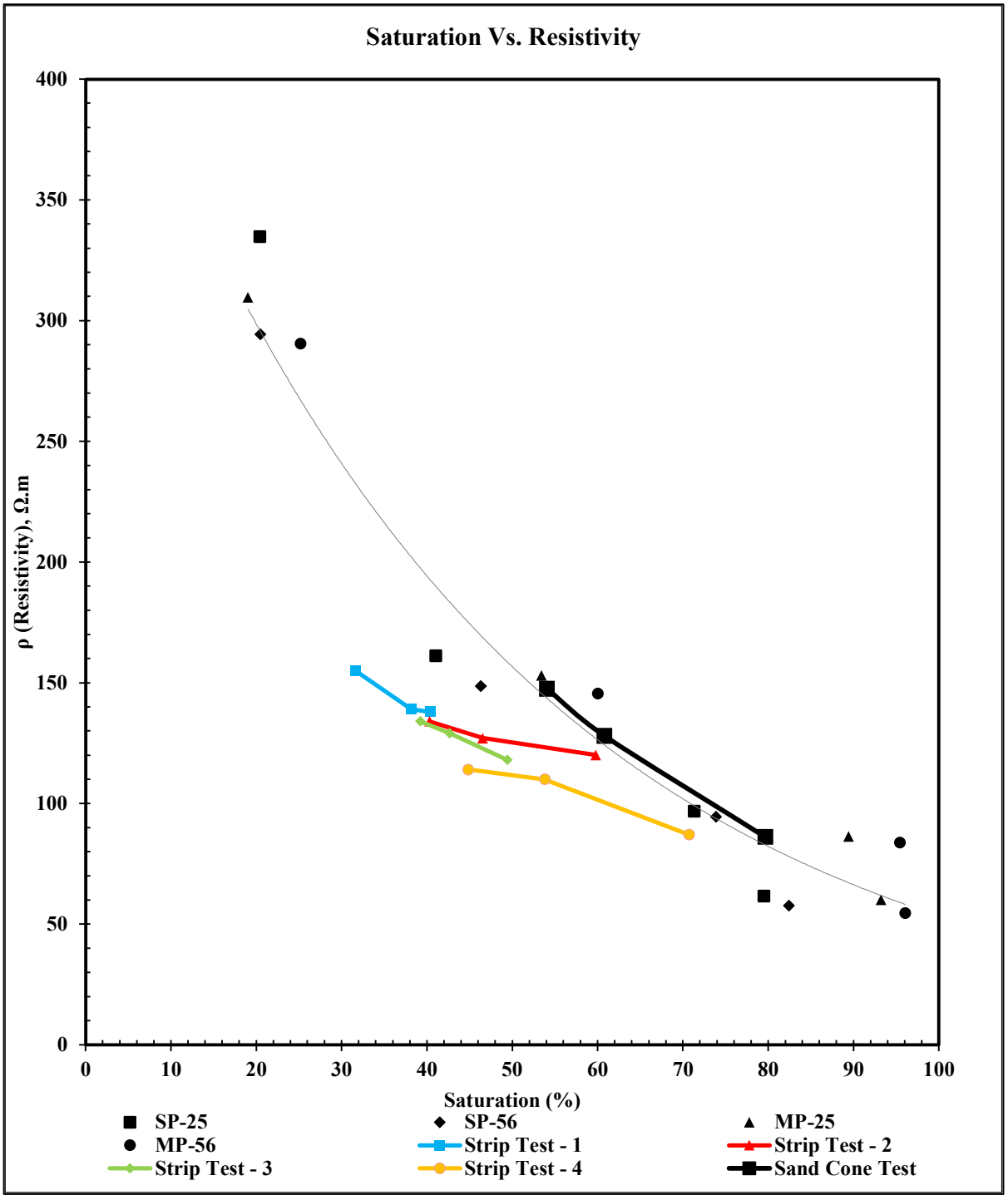

Figure 311: Sand Cone Test Saturation and Measured Electrical Resistivity Associated with Laboratory Results Trend

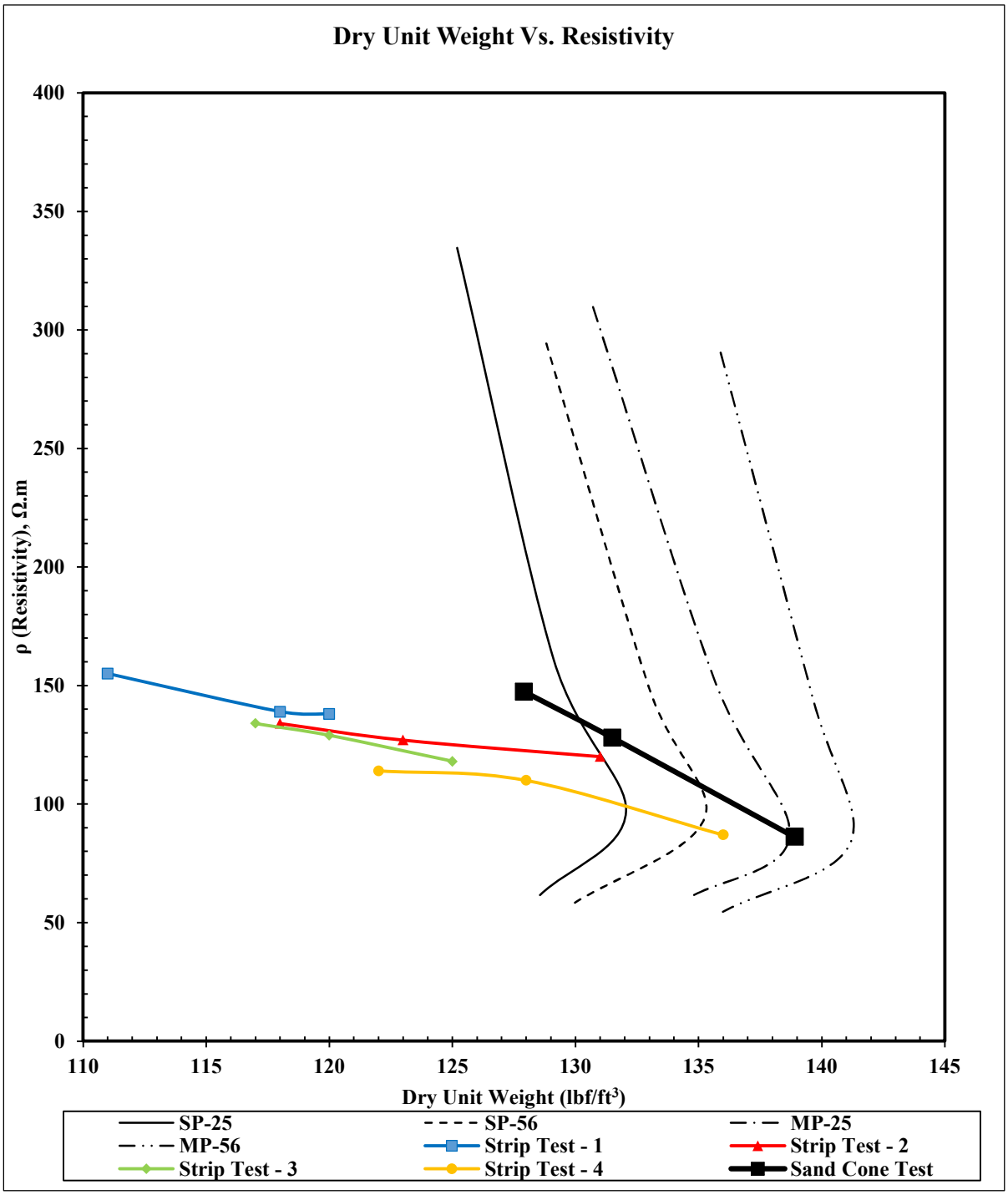

Figure 32: Sand Cone Test Dry Unit Weight and Measured Electrical Resistivity Associated with Laboratory Results Trend

6.3 Comparison Between Laboratory and Soil Strip Tests Results

For the purpose of verifying the approaches established in this research and guaranteeing that they are applicable in real geotechnical engineering, it is essential that the results obtained in the field and those obtained in the laboratory be in agreement with one another. For the purpose of establishing baseline connections between electrical resistivity (ER), moisture content, and dry unit weight, laboratory testing offered a controlled setting in which to conduct the investigations. In order to provide a standard for the interpretation of soil strip test data, these relationships, which were generated from the Standard Proctor (SP) and Modified Proctor (MP) compaction procedures, were used. These laboratory findings were compared to the results of the soil strip tests, which were carried out under a variety of compaction efforts and layer configurations, in order to evaluate the consistency and dependability of the results.

A series of curves were produced in the laboratory to capture the basic behavior of the soil that was examined. These curves included moisture content versus ER, dry unit weight versus ER, and saturation levels versus ER. According to the results of these studies, there is a direct connection between ER and both the moisture content and the dry unit weight. A drop in resistivity was seen as a result of an improvement in electrical connection across the soil, which occurred as the

moisture content rose. In a similar manner, the reduction in air voids and the greater continuity of water films brought an increase in electrical conductivity, which further decreased resistance. This occurred when the dry unit weight rose due to the process of compaction. According to these tendencies, a solid framework was established for the interpretation of field data.

The reliability of electrical resistivity as a proxy for soil compaction characteristics was confirmed by the fact that the results of soil strip testing were in close alignment with the curves that were obtained in the laboratory. For instance, the electrical resistivity (ER) continuously declined with increased compaction effort in the soil strip experiments, which is comparable with the trends found in the laboratory. When the dry unit weight increased from 111 lb/ft^3 to 120 lb/ft^3, the resistivity in Test 1 decreased from 155 Ω.m to 138 Ω.m. As the dry unit weight increased from 118 lb/ft^3 to 131 lb/ft^3, the ER decreased from 134 Ω.m to 120 Ω.m in Test 2, demonstrating a similar pattern. In particular, these tendencies were in good agreement with the observation that were established in the laboratory.

The similarity between the findings obtained from the soil strip tests and those obtained in the laboratory was further corroborated by the decrease of the uncompacted thickness in Tests 3 and 4. The ER values in Test 3 decreased linearly

from 134 Ω.m to 118 Ω.m during the course of six compaction passes when the soil layer thickness was decreased to 6 inches. At the same time, the dry unit weight rose from 117 lb/ft^3 to 125 lb/ft^3. The same thing happened in Test 4, when the ER values decreased from 114 Ω.m to 87 Ω.m as the dry unit weight increased from 122 lb/ft^3 to 136 lb/ft^3. The fact that these linear trends were in close alignment with the ER curves that were obtained in the laboratory is evidence that the resistivity changes that were seen in the soil strip tests were in agreement with those that were anticipated by the laboratory tests.

Tests of the spot moisture content and measurements of the volumetric unit weight provided further confirmation that the soil strip test data were accurately interpreted. Through the use of these auxiliary tests, it was verified that the soil strip resistivity measurements properly reflected the features of soil compaction. This provided further proof that the results of the laboratory were in agreement with the soil strip test data. A consistent pattern that provided support for the idea that electrical resistivity may consistently predict soil moisture content and dry unit weight has been realized. This was accomplished by superimposing the soil strip data on the laboratory-derived ER curves.

The combination of data from the laboratory and the soil strip tests indicated that

the patterns of electrical resistivity, which are determined by the amount of moisture present and the amount of effort put into compaction, are constant across a variety of types of testing situations. This alignment highlights the resilience of the approach that was established as well as its potential for applications in the real world. This research concludes that the use of electrical resistivity, embodied in the electrical resistivity meter developed throughout this research, is viable for monitoring and optimizing soil compaction in real-time field situations, although more laboratory and field soil strip tests on other types of soils are needed for further verification.

6.4 Practical Implications of Dynamic On-Road Measurements

The practicality of the established approach to offer non-destructive, efficient, and accurate measurements of soil compaction parameters is a significant factor that contributes to the feasibility and usefulness of the method in making use of electrical resistivity (ER) in real-world settings. The use of ER methods, in particular the Wenner Four-Electrode Method, provides a quick and scalable option for evaluating important soil parameters during the process of compaction. These soil parameters include moisture content and dry unit weight. In geotechnical engineering practice, where the importance of making timely decisions and making optimal use of resources cannot be overstated, this advancement presents a viable

solution to close the gaps that have been identified [62], [63].

The proposed approach establishes a trend between the electrical resistivity of soil and its moisture content and dry unit weight. The reliability of ER as a tool for monitoring compaction trends was confirmed by the soil strip testing, which showed a significant agreement with the data obtained in the laboratory. For example, the linear decrease in ER values that occurs with increase in compaction effort is a reflection of the predictable behavior of the soil, which enables practitioners to dynamically (real time) determine the desired soil compaction has been achieved. This "adaptive compaction" solution is needed for large-scale infrastructure projects because of differences in soil conditions throughout a site [64].

The integration of the proposed walk-behind resistivity meter with field compaction equipment may be the first step towards adaptive compaction (see Figure 22). As a result, engineers are able to continually monitor the progress of the compaction process and make modifications as required, which ultimately results in an improvement in both the quality and efficiency of the compression process. Furthermore, the method's reliance on recognized correlations between electrical resistivity, moisture content, and dry unit weight allows for a reduction in the

requirement for extensive sampling and laboratory testing, hence reducing interruption to the site and expediting project timeframes [63], [65].

The capability of the procedure to be adapted to a variety of soil types and circumstances is another thing that demonstrates its effectiveness. The robustness of the approach was proven as indicated above, but only for one type of soil (poorly graded sand). The performed tests revealed the system's ability to capture patterns that are compatible with geotechnical principles. In addition, the scalability of the technique, which includes field strip testing to determine ER-based compaction trends, provides a viable foundation for the deployment of the methodology on a larger scale. The developed technique offers an option for monitoring soil compaction that is both cost-effective and ecologically friendly. This is accomplished by lowering the reliance on conventional static testing methods.

Chapter 7: Suggested Field-Testing Procedure

7.1 Introduction to the Soil Strip Technique

The soil strip testing procedure involves performing resistivity measurements along a predetermined soil strip, using the proposed walk-behind electrical resistivity meter, and establishing an association between the compaction effort, expressed by the number of passes, and relevant soil parameters including moisture content, dry unit weight, and electrical resistivity. Conventional techniques for evaluating field soil compaction, such as the nuclear density device and the sand cone test, are based on sampling that is both time consuming and labor intensive, whereas the soil strip approach offers a dynamic framework that allows for decision-making in real time throughout the compaction process.

Although no formal mathematical models have been established, the trends presented in Chapter 6 clearly demonstrate a decline in electrical resistivity with increasing dry unit weight at optimum moisture content (OMC). These trends offer valuable insights into the relationship between electrical resistivity and compaction parameters.

While the soil strip approach often relies on generating predictive mathematical models from experimental data, this study highlights the potential to interpret

compaction behavior based on resistivity trends without the need for repetitive, labor-intensive testing like the Proctor test. Laboratory experiments conducted under Standard Proctor (SP) and Modified Proctor (MP) conditions, along with soil strip tests using a walk-behind resistivity meter, provide evidence for these trends. For example, the relationship between electrical resistivity and moisture content follows an inverted trend—resistivity decreases as moisture content increases, and with higher compaction efforts, resistivity further decreases due to reduced air voids and enhanced connectivity of pore water films. Similarly, resistivity consistently decreases with increasing dry unit weight.

To align these findings with real-world applications, the observed trends were compared with soil strip testing results. For instance, a linear relationship was identified between electrical resistivity and the number of compaction passes for both single-layer and two-layer systems. Additionally, an exponential relationship was observed between resistivity and moisture content. These trends provide engineers with a practical tool to estimate optimal compaction parameters, such as the required number of passes, with a good degree of accuracy.

Through the incorporation of this soil strip testing methodology in the field with larger dimensions and different intervals, the technique can offer a useful means

for the purpose of monitoring and optimizing soil compaction passes in the field. Compaction trends may be predicted with the use of these trends, which guarantee that the intended soil qualities will be obtained in an effective and consistent manner. This method not only improves the accuracy of field compaction, but also reduces the amount of expensive laboratory testing that is required. As a result, it is a solution that is cost-effective for geotechnical engineering applications.

7.2 Implementation of the Soil Strip Technique in the Field.

In order to use the soil strip approach, results from both the lab and the field have to be combined to make a useful and effective way to check the factors of soil compaction using electrical resistivity. This method uses the relationships among ER, moisture content, and dry unit weight to give a real-time, non-invasive picture of how compaction is progressing. The soil strip method is intended to get the optimum compaction with the least number of passes.

To establish a field methodology for soil compaction testing, laboratory compaction tests using Standard Proctor (SP) and Modified Proctor (MP) methods are conducted to determine optimum moisture content (OMC) and maximum dry density (MDD) as baselines. Field soil strip tests employ the soil strip testing technique, where electrical resistivity is measured in real-time using a walk-behind

resistivity meter. Moisture content and dry density are evaluated using sand cone and oven-dry testing methods, while a compaction graph, plotting the number of passes against dry unit weight, is developed during field testing to monitor compaction progression. The spot density measurements and ER values along the soil strip are then correlated with laboratory-derived dry unit weight vs. ER trends. This allows for establishing a compaction effort vs. ER trend, the red curve in Figure 33, to guide field operations. This trend enables compactor operators to identify the number of passes needed to achieve the target resistivity and corresponding dry density, as illustrated in Figure 33.

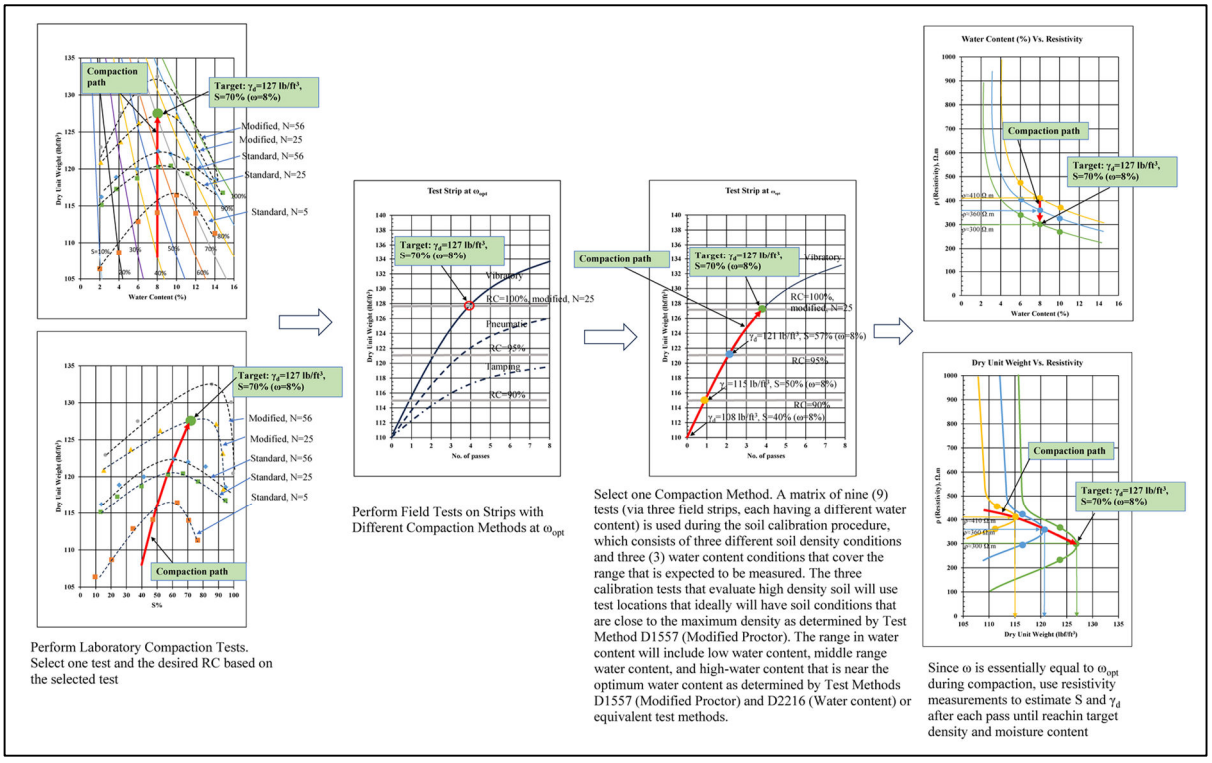

Figure 33: Suggested Field Calibration Procedure

The soil strip method involves compacting a strip of soil using a compaction machine (e.g., a roller compactor), with electrical resistivity measurements taken along the soil strip to establish a relationships among ER, the number of passes, and dry unit weight. ER values are averaged for each pass using a walk-behind or mounted resistivity meter, and spot sand cone tests are performed at several locations along the soil strip.

The method was laboratory tested with varying soil layer thicknesses, such as 8-inch and 6-inch layers, and multi-layer configurations to simulate field conditions. Laboratory soil strip ER readings were compared with ER measurements for SP and MP curves to track compaction trends and identify the point where additional passes yield diminishing results. This allows for real-time decision-making during soil compaction, optimizing passes to save time and resources while achieving the desired density.

In summary, the soil strip method integrates the results of laboratory and field tests to provide a flexible, cost-effective, and non-intrusive approach for monitoring and optimizing field soil compaction.

Chapter 8: Conclusions and Recommendations

8.1 Summary of Findings

This research developed a practical and reliable methodology for monitoring and optimizing soil compaction using electrical resistivity (ER) as a key indicator. Laboratory compaction tests established baseline relationships between soil properties and ER, which were validated through laboratory soil strip tests under controlled conditions. The study demonstrated that ER consistently decreases with increased compaction due to reductions in air voids and improved connectivity of water films within the soil matrix.

Laboratory soil strip testing integrated real-time ER measurements with compaction data, providing insights into the relationship between compaction effort, soil density and moisture content, and resistivity. The developed methodology successfully correlated the laboratory test data, enabling real-time monitoring and optimization of the compaction process. The soil strip testing approach proved adaptable across various soil configurations and conditions, offering a flexible and efficient framework for geotechnical applications. Overall, the study highlighted the utilization of ER as a non-invasive, cost-effective, and efficient alternative for monitoring compaction progress, providing a significant advancement in soil compaction practices.

8.2 Contributions to Knowledge

This study contributes to the area of geotechnical engineering. First, it expands the use of electrical resistivity as a real-time, non-invasive technique for determining soil compaction characteristics. The research presents a reliable approach for associating ER with moisture content, dry unit weight, and compaction effort by combining laboratory data with field testing. Second, the soil strip method was developed to bring a dynamic approach to soil compaction monitoring, allowing engineers to optimize compaction operations effectively, albeit further laboratory and field testing is needed. The research also shows that ER measurements are adaptable across various soil types and thickness configurations, broadening the applicability of this technology to a wide range of geotechnical applications. Finally, the study lays the groundwork for utilizing ER trends to enhance sustainability by avoiding needless compaction passes, which saves energy and materials.

8.3 Practical Recommendations

This study's conclusions have several practical ramifications for geotechnical undertakings. First, the soil strip approach is recommended for field compaction monitoring since it provides for continuous, real-time evaluation of soil density and moisture content, reducing the need for labor-intensive and time-consuming field-testing techniques. A proposed walk-behind resistivity meter is used for dynamic

data gathering along test strips, with resistivity trends utilized to calculate the appropriate number of compaction passes. Second, using laboratory-established ER curves in field operations creates a credible foundation for forecasting compaction results. Contractors and engineers could explore utilizing ER data to dynamically alter compaction tactics, especially for large-scale earthworks or changeable soil conditions. Furthermore, training programs should be designed to acquaint field operators with the technique, guaranteeing proper application and interpretation of ER data.

8.4 Limitations and Future Research

Although the research met its aims, certain limitations were discovered. The study mainly focused on poorly graded sand, well-graded sand with gravel, and clay, which may not accurately represent the behavior of highly organic soils or soils with severe variability. Laboratory and soil strip testing were carried out under controlled settings, but further study is required to assess the methodology's efficacy under field conditions. Furthermore, the produced models are particular to the studied soil types and testing conditions; future research should apply the concept to other soil types.

Future studies should look at the use of new technologies like machine learning

and artificial intelligence to improve the prediction capacities of ER models. These approaches could improve correlations between ER and soil parameters by accounting for complicated factors like pore fluid conductivity and mineralogical composition. Furthermore, the development of more advanced field equipment, such as resistivity-enabled roller compactors, can potentially increase the methodology's scalable nature.

Finally, this study demonstrates the transformational potential of electrical resistivity in geotechnical engineering, providing a realistic, economical, and sustainable solution to soil compaction monitoring and optimization. By resolving the highlighted constraints and following the recommended future research areas, the technique may be enhanced and extensively adopted, propelling the field forward to more inventive and successful methods.

Chapter 9: References

[1] J. Kodikara, T. Islam, and A. Sounthararajah, 'Review of soil compaction: History and recent developments', *Transportation Geotechnics*, vol. 17, pp. 24–34, Dec. 2018, doi: 10.1016/j.trgeo.2018.09.006.

[2] J. Kodikara, T. Islam, and A. Sounthararajah, 'Review of soil compaction: History and recent developments', *Transportation Geotechnics*, pp. 24–34, 2018, doi: 10.1016/j.trgeo.2018.09.006.

[3] M. N. Rakhmawati, S. Sutrisno, Y. Sudiyanto, and W. Hidayat, 'Identification of Iron Ore Deposit in Sub-Surface using Resistivity and Induced Polarization Methods at Sarakaman, Sebuku Island, South Kalimantan', *Al-Fiziya: Journal of Materials Science, Geophysics, Instrumentation and Theoretical Physics*, vol. 5, no. 2, pp. 77–86, Jun. 2023, doi: 10.15408/fiziya.v5i2.25648.

[4] B. Sharma and A. Deka, 'Static Compaction Test and Determination of Equivalent Static Pressure', in *Geotechnical Characterisation and Geoenvironmental Engineering*, vol. 16, V. K. Stalin and M. Muttharam, Eds., Singapore: Springer Singapore, 2019, pp. 3–10. doi: 10.1007/978-981-13-0899-4_1.

[5] A. Sadiq Yasun and J. N. Al Abbasi, 'A Proposed Approach for Evaluating Soils Optimum Moisture Content Arithmetically and Use Statistical Functions for Checking Method', *International Journal of Engineering & Technology*, vol. 7, no. 4.20, pp. 287–292, Nov. 2018, doi: 10.14419/ijet.v7i4.20.25941.

[6] A. Heitor, B. Indraratna, and C. Rujikiatkamjorn, 'Characterising compacted soil using shear wave velocity and matric suction', *Australian Geomechanics Journal*, vol. 47, pp. 79–86, Dec. 2012.

[7] S. Alzabeebee, S. A. Mohamad, and R. Kh. S. Al-Hamd, 'Surrogate models to predict maximum dry unit weight, optimum moisture content and California bearing ratio form grain size distribution curve', *Road Materials and Pavement Design*, vol. 23, no. 12, pp. 2733–2750, Dec. 2022, doi: 10.1080/14680629.2021.1995471.

[8] A. Samouëlian, I. Cousin, A. Tabbagh, A. Bruand, and G. Richard, 'Electrical resistivity survey in soil science: a review', *Soil Tillage Res*, vol. 83, no. 2, pp. 173–193, Sep. 2005, doi: 10.1016/j.still.2004.10.004.

[9] A. T. S. Azhar, Z. A. M. Hazreek, M. Aziman, D. S. Haimi, and Z. M. Hafiz, 'Acidic Barren Slope Profiling using Electrical Resistivity Imaging (ERI) at Ayer Hitam area Johor, Malaysia', *J Phys Conf Ser*, vol. 710, p. 12008, Apr. 2016, doi: 10.1088/1742-6596/710/1/012008.

[10] Y. Chen, Z. Wei, M. Irfan, J. Xu, and Y. Yang, 'Laboratory investigation of the relationship between electrical resistivity and geotechnical properties of phosphate tailings', *Measurement*, vol. 126, pp. 289–298, Oct. 2018, doi: 10.1016/j.measurement.2018.05.095.

[11] A. Hassan and G. Nadhum, 'Geotechnical-Electrical Evaluation of Soil Compaction Parameters, South of Baqubah City', *Iraqi Geological Journal*, vol. 56, no. 1D, pp. 144–155, Apr. 2023, doi: 10.46717/igj.56.1D.12ms-2023-4-21.

[12] S. M. T. Islam, Z. Chik, Mohd. M. Mustafa, and H. Sanusi, 'Model with artificial neural network to predict the relationship between the soil resistivity and dry density of compacted soil', *Journal of Intelligent & Fuzzy Systems*, vol. 25, no. 2, pp. 351–357, 2013, doi: 10.3233/IFS-2012-0641.

[13] H. Bhuyan, A. Scheuermann, D. Bodin, and R. Becker, 'Soil moisture and density monitoring methodology using TDR measurements', *International Journal of Pavement Engineering*, vol. 21, no. 10, pp. 1263–1274, Aug. 2020, doi: 10.1080/10298436.2018.1537491.

[14] S. Shimobe and G. Spagnoli, 'Relationship between dielectric constant of soils with clay content and dry unit weight', *Environmental Geotechnics*, vol. 8, no. 2, pp. 134–147, Apr. 2021, doi: 10.1680/jenge.18.00098.

[15] Q. Sun, C. Lyu, and W. Zhang, 'The relationship between thermal conductivity and electrical resistivity of silty clay soil in the temperature range − 20 C to 10 C', *Heat and Mass Transfer*, vol. 56, no. 6, pp. 2007–2013, Jun. 2020, doi: 10.1007/s00231-020-02813-0.

[16] M. Zhou, J. Wang, L. Cai, Y. Fan, and Z. Zheng, 'Laboratory Investigations on Factors Affecting Soil Electrical Resistivity and the Measurement', *IEEE Trans Ind Appl*, vol. 51, no. 6, pp. 5358–5365, Nov. 2015, doi: 10.1109/TIA.2015.2465931.

[17] S. S. Park, P. D. Ogunjinmi, H. I. Lee, S. W. Woo, and D. E. Lee, 'Effect of Wetting Conditions on the in Situ Density of Soil Using the Sand-Cone Method', *Applied Sciences (Switzerland)*, vol. 11, no. 2, pp. 1–10, 2021, doi: 10.3390/app11020718.

[18] G. S. Faé, F. Montes, E. Bazilevskaya, R. M. Añó, and A. R. Kemanian, 'Making Soil Particle Size Analysis by Laser Diffraction Compatible with Standard Soil Texture Determination Methods', *Soil Science Society of America Journal*, vol. 83, no. 4, pp. 1244–1252, Jul. 2019, doi: 10.2136/sssaj2018.10.0385.

[19] V. Gingine, A. S. Dias, and R. Cardoso, 'Compaction Control of Clayey Soils Using Electrical Resistivity Charts', *Procedia Eng*, vol. 143, pp. 803–810, 2016, doi: 10.1016/j.proeng.2016.06.130.

[20] 'ASTM D1557, "Standard Test Methods for Laboratory Compaction Characteristics of Soil Using Modified Effort," ASTM International, 2017'.

[21] 'ASTM D698, "Standard Test Methods for Laboratory Compaction Characteristics of Soil Using Standard Effort," ASTM International, 2017'.

[22] 'ASTM D2216, "Standard Test Methods for Laboratory Determination of Water (Moisture) Content of Soil and Rock," ASTM International, 2017'.

[23] W. J. Baker and C. L. Meehan, 'A Comparison of In-Place Unit Weight and Moisture Content Measurements Made Using Nuclear Based Methods and the Drive Cylinder Method', in *IFCEE 2018*, Orlando, Florida: American Society of Civil Engineers, Jun. 2018, pp. 1–11. doi: 10.1061/9780784481585.001.

[24] W. J. Baker III and C. L. Meehan, 'A Comparison of In-Place Unit Weight and Moisture Content Measurements Using Nuclear-Based Methods and the Drive Cylinder Method', *Unknown Journal*, 2018.

[25] W. J. B. Iii, S. M. Asce, C. L. Meehan, and F. Asce, ‘A Comparison of In-Place Unit Weight and Moisture Content Measurements Made Using Nuclear Based Methods and the Drive Cylinder Method’.

[26] S.-S. Park, P. D. Ogunjinmi, H.-I. Lee, S.-W. Woo, and D.-E. Lee, ‘Effect of Wetting Conditions on the In Situ Density of Soil Using the Sand-Cone Method’, *Applied Sciences*, vol. 11, no. 2, p. 718, Jan. 2021, doi: 10.3390/app11020718.

[27] Z. Xu, H. Khabbaz, B. Fatahi, and D. Wu, ‘Real-time determination of sandy soil stiffness during vibratory compaction incorporating machine learning method for intelligent compaction’, *Journal of Rock Mechanics and Geotechnical Engineering*, vol. 14, no. 5, pp. 1609–1625, Oct. 2022, doi: 10.1016/j.jrmge.2022.07.004.

[28] T. Kaderabek and W. Ferris, ‘Comparisons of Field Density Test Results’, *Geotechnical Testing Journal*, vol. 2, no. 4, pp. 206–210, Dec. 1979, doi: 10.1520/GTJ10459J.

[29] R. B. Freeman, C. A. Gartrell, L. D. Wakeley, E. S. Berney, and J. R. Kelley, ‘Steel-shot method for measuring the density of soils’, *Canadian Geotechnical Journal*, vol. 47, no. 11, pp. 1299–1304, Nov. 2010, doi: 10.1139/T10-034.

[30] A. Lekea, D. Kalumba, and F. Chebet, ‘Application of an Electrical Density Gauge for Measuring In Situ Density and Moisture Content’, in *Geo-China 2016*, Shandong, China: American Society of Civil Engineers, Jul. 2016, pp. 43–50. doi: 10.1061/9780784480083.006.

[31] Z. Xu, H. Khabbaz, B. Fatahi, and D. Wu, ‘Real-time determination of sandy soil stiffness during vibratory compaction incorporating machine learning method for intelligent compaction’, *Journal of Rock Mechanics and Geotechnical Engineering*, vol. 14, no. 5, pp. 1609–1625, Oct. 2022, doi: 10.1016/j.jrmge.2022.07.004.

[32] Z. Xu, H. Khabbaz, B. Fatahi, and D. Wu, ‘Real-time determination of sandy soil stiffness during vibratory compaction incorporating machine learning method for intelligent compaction’, *Journal of Rock Mechanics and Geotechnical Engineering*, vol. 14, no. 5, pp. 1609–1625, Oct. 2022, doi: 10.1016/j.jrmge.2022.07.004.

[33] Y. Chen, Z. Wei, M. Irfan, J. Xu, and Y. Yang, ‘Laboratory investigation of the relationship between electrical resistivity and geotechnical properties of phosphate tailings’, *Measurement*, vol. 126, pp. 289–298, Oct. 2018, doi: 10.1016/j.measurement.2018.05.095.

[34] A. Samouëlian, I. Cousin, A. Tabbagh, A. Bruand, and G. Richard, ‘Electrical resistivity survey in soil science: a review’, *Soil Tillage Res*, vol. 83, no. 2, pp. 173–193, Sep. 2005, doi: 10.1016/j.still.2004.10.004.

[35] A. D. Adebiyi, K. A. N. Adiat, and A. B. Eluwole, ‘Development of empirical models for analysis of subsoil agricultural parameters from resistivity measurement in a basement complex terrain’, *NRIAG Journal of Astronomy and Geophysics*, vol. 9, no. 1, pp. 260–271, Jan. 2020, doi: 10.1080/20909977.2020.1732571.

[36] R. Kalinski and W. Kelly, ‘Estimating Water Content of Soils from Electrical Resistivity’, *Geotechnical Testing Journal*, vol. 16, no. 3, pp. 323–329, Sep. 1993, doi: 10.1520/GTJ10053J.

[37] J. A. Muñoz-Castelblanco, J. M. Pereira, P. Delage, and Y. J. Cui, 'The Influence of Changes in Water Content on the Electrical Resistivity of a Natural Unsaturated Loess', *Geotechnical Testing Journal*, vol. 35, no. 1, pp. 11–17, Jan. 2012, doi: 10.1520/GTJ103587.

[38] R. J. Kalinski and W. E. Kelly, 'Electrical-Resistivity Measurements For Evaluating Compacted-Soil Liners', *Journal of Geotechnical Engineering*, vol. 120, no. 2, pp. 451–457, Feb. 1994, doi: 10.1061/(ASCE)0733-9410(1994)120:2(451).

[39] H. Bhuyan, A. Scheuermann, D. Bodin, and R. Becker, 'Soil moisture and density monitoring methodology using TDR measurements', *International Journal of Pavement Engineering*, vol. 21, no. 10, pp. 1263–1274, Aug. 2020, doi: 10.1080/10298436.2018.1537491.

[40] V. Gingine, A. S. Dias, and R. Cardoso, 'Compaction Control of Clayey Soils Using Electrical Resistivity Charts', *Procedia Eng*, vol. 143, pp. 803–810, 2016, doi: 10.1016/j.proeng.2016.06.130.

[41] V. Gingine, A. S. Dias, and R. Cardoso, 'Compaction Control of Clayey Soils Using Electrical Resistivity Charts', *Procedia Eng*, pp. 803–810, 2016, doi: 10.1016/j.proeng.2016.06.130.

[42] M. Zhou, J. Wang, L. Cai, Y. Fan, and Z. Zheng, 'Laboratory Investigations on Factors Affecting Soil Electrical Resistivity and the Measurement', *IEEE Trans Ind Appl*, vol. 51, no. 6, pp. 5358–5365, Nov. 2015, doi: 10.1109/TIA.2015.2465931.

[43] Z. G. Datsios, P. N. Mikropoulos, and I. Karakousis, 'Laboratory characterization and modeling of DC electrical resistivity of sandy soil with variable water resistivity and content', *IEEE Transactions on Dielectrics and Electrical Insulation*, vol. 24, no. 5, pp. 3063–3072, Oct. 2017, doi: 10.1109/TDEI.2017.006583.

[44] E. A. Atekwana, D. D. Werkema, and E. A. Atekwana, 'BIOGEOPHYSICS: THE EFFECTS OF MICROBIAL PROCESSES ON GEOPHYSICAL PROPERTIES OF THE SHALLOW SUBSURFACE', in *Applied Hydrogeophysics*, vol. 71, H. Vereecken, A. Binley, G. Cassiani, A. Revil, and K. Titov, Eds., Dordrecht: Springer Netherlands, 2006, pp. 161–193. doi: 10.1007/978-1-4020-4912-5_6.

[45] G. Kibria and M. S. Hossain, 'Investigation of Geotechnical Parameters Affecting Electrical Resistivity of Compacted Clays', *Journal of Geotechnical and Geoenvironmental Engineering*, vol. 138, no. 12, pp. 1520–1529, Dec. 2012, doi: 10.1061/(ASCE)GT.1943-5606.0000722.

[46] F. Wenner, 'A method for measuring earth resistivity', *J Franklin Inst*, vol. 180, no. 3, pp. 373–375, Sep. 1915, doi: 10.1016/S0016-0032(15)90298-3.

[47] A. Samouëlian, I. Cousin, A. Tabbagh, A. Bruand, and G. Richard, 'Electrical resistivity survey in soil science: a review', *Soil Tillage Res*, vol. 83, no. 2, pp. 173–193, Sep. 2005, doi: 10.1016/j.still.2004.10.004.

[48] A. Samouëlian, I. Cousin, A. Tabbagh, A. Bruand, and G. Richard, 'Electrical resistivity survey in soil science: a review', *Soil Tillage Res*, vol. 83, no. 2, pp. 173–193, Sep. 2005, doi: 10.1016/j.still.2004.10.004.

[49] A. Samouëlian, I. Cousin, A. Tabbagh, A. Bruand, and G. Richard, 'Electrical resistivity survey in soil science: a review', *Soil Tillage Res*, vol. 83, no. 2, pp. 173–193, Sep. 2005, doi: 10.1016/j.still.2004.10.004.

[50] A. Samouëlian, I. Cousin, A. Tabbagh, A. Bruand, and G. Richard, 'Electrical resistivity survey in soil science: a review', *Soil Tillage Res*, vol. 83, no. 2, pp. 173–193, Sep. 2005, doi: 10.1016/j.still.2004.10.004.

[51] A. Sadiq Yasun and J. N. Al Abbasi, 'A Proposed Approach for Evaluating Soils Optimum Moisture Content Arithmetically and Use Statistical Functions for Checking Method', *International Journal of Engineering & Technology*, vol. 7, no. 4.20, pp. 287–292, Nov. 2018, doi: 10.14419/ijet.v7i4.20.25941.

[52] A. T. S. Azhar, Z. A. M. Hazreek, M. Aziman, D. S. Haimi, and Z. M. Hafiz, 'Acidic Barren Slope Profiling using Electrical Resistivity Imaging (ERI) at Ayer Hitam area Johor, Malaysia', *J Phys Conf Ser*, vol. 710, p. 12008, Apr. 2016, doi: 10.1088/1742-6596/710/1/012008.

[53] R. J. Kalinski and W. E. Kelly, 'Electrical-Resistivity Measurements For Evaluating Compacted-Soil Liners', *Journal of Geotechnical Engineering*, vol. 120, no. 2, pp. 451–457, Feb. 1994, doi: 10.1061/(ASCE)0733-9410(1994)120:2(451).

[54] M. Thompson, B. Arntsen, and L. Amundsen, 'Full-azimuth imaging through consistent application of ocean-bottom seismic', in *SEG Technical Program Expanded Abstracts 2007*, Society of Exploration Geophysicists, Jan. 2007, pp. 936–940. doi: 10.1190/1.2792560.

[55] Q. Zhang, Z. An, Z. Huangfu, and Q. Li, 'A Review on Roller Compaction Quality Control and Assurance Methods for Earthwork in Five Application Scenarios', *Materials*, vol. 15, no. 7, p. 2610, Apr. 2022, doi: 10.3390/ma15072610.

[56] A. D. Adebiyi, K. A. N. Adiat, and A. B. Eluwole, 'Development of empirical models for analysis of subsoil agricultural parameters from resistivity measurement in a basement complex terrain', *NRIAG Journal of Astronomy and Geophysics*, vol. 9, no. 1, pp. 260–271, Jan. 2020, doi: 10.1080/20909977.2020.1732571.

[57] A. A. Bery and N. E. H. Ismail, 'Empirical Correlation Between Electrical Resistivity and Engineering Properties of Soils', *Soil Mechanics and Foundation Engineering*, vol. 54, no. 6, pp. 425–429, Jan. 2018, doi: 10.1007/s11204-018-9491-7.

[58] F. I. Siddiqui and S. B. A. B. S. Osman, 'Simple and multiple regression models for relationship between electrical resistivity and various soil properties for soil characterization', *Environ Earth Sci*, vol. 70, no. 1, pp. 259–267, Sep. 2013, doi: 10.1007/s12665-012-2122-0.

[59] H. Rostami and A. Osouli, 'Electrical Resistivity Changes in Wet and Dry Side of Optimum Moisture Content for Soils with Low to High Fines Content', in *Advances in Transportation Geotechnics IV*, vol. 165, E. Tutumluer, S. Nazarian, I. Al-Qadi, and I. I. A. Qamhia, Eds., Cham: Springer International Publishing, 2022, pp. 829–836. doi: 10.1007/978-3-030-77234-5_68.

[60] J. B. Kollat, P. M. Reed, and J. R. Kasprzyk, 'A new epsilon-dominance hierarchical Bayesian optimization algorithm for large multiobjective monitoring network design problems', *Adv Water Resour*, vol. 31, no. 5, pp. 828–845, May 2008, doi: 10.1016/j.advwatres.2008.01.017.

[61] I. J. Won, D. Keiswetter, and E. Novikova, 'Electromagnetic Induction Spectroscopy', *J Environ Eng Geophys*, vol. 3, no. 1, pp. 27–40, Mar. 1998, doi: 10.4133/JEEG3.1.27.

[62] R. J. Kalinski and W. E. Kelly, ‘Electrical-Resistivity Measurements For Evaluating Compacted-Soil Liners’, *Journal of Geotechnical Engineering*, vol. 120, no. 2, pp. 451–457, Feb. 1994, doi: 10.1061/(ASCE)0733-9410(1994)120:2(451).

[63] A. Samouëlian, I. Cousin, A. Tabbagh, A. Bruand, and G. Richard, ‘Electrical resistivity survey in soil science: a review’, *Soil Tillage Res*, vol. 83, no. 2, pp. 173–193, Sep. 2005, doi: 10.1016/j.still.2004.10.004.

[64] K. P. Bube and T. Nemeth, ‘Fast line searches for the robust solution of linear systems in the hybrid ℓ1/ℓ2 and Huber norms’, *GEOPHYSICS*, vol. 72, no. 2, pp. A13–A17, Mar. 2007, doi: 10.1190/1.2431639.

[65] A. Samouëlian, I. Cousin, A. Tabbagh, A. Bruand, and G. Richard, ‘Electrical resistivity survey in soil science: a review’, *Soil Tillage Res*, vol. 83, no. 2, pp. 173–193, Sep. 2005, doi: 10.1016/j.still.2004.10.004.

Chapter 10: Appendix

Plastic Mold Test (Compaction and ER Testing for 25 Drops) – Fat Clay

Test #	Weight (g)		Weight (g)			ω (%)	γ (kN/m³)	γd (kN/m³)	γ (lb/ft³)	γd (lb/ft³)	VDC			mADC			Resistance	ρ (Resistivity) Ω.m	ρ (Resistivity) Ω.ft
	(Mold)	(Mold + Moist Soil)	(Can)	(Can + Moist Soil)	(Can + Dry Soil)						VDC (Side 1)	VDC (Side 2)	VDC (AVG)	mADC (Side 1)	mADC (Side 2)	mADC (AVG)			
1	2451.05	4082.61	20.96	98.52	95.23	4.43	17.0	16.2	108.0	103.4	0.257	0.553	0.405	0.379	0.389	0.384	1055.1	665	2181
2	2451.05	4144.96	20.92	104.49	100.06	5.60	17.6	16.7	112.1	106.1	0.333	0.183	0.258	0.817	0.488	0.653	395.4	249	817
3	2451.05	4186.1	20.98	108.65	103.46	6.29	18.0	17.0	114.8	108.0	0.325	0.262	0.294	2.060	1.060	1.560	188.1	119	389
4	2451.05	4219.02	20.94	97.12	90.98	8.77	18.4	16.9	117.0	107.6	0.318	0.361	0.340	1.840	1.861	1.851	183.5	116	379
5	2451.05	4309.31	20.95	98.76	91.37	10.49	19.3	17.5	123.0	111.3	0.490	0.285	0.388	2.790	2.520	2.655	146.0	92	302
6	2451.05	4369.29	20.9	99.36	90.5	12.73	19.9	17.7	126.9	112.6	0.384	0.402	0.393	3.200	3.060	3.130	125.6	79	260
7	2451.05	4435.26	21.07	87.56	78.84	15.09	20.6	17.9	131.3	114.1	0.420	0.402	0.411	4.000	4.050	4.025	102.1	64	211
8	2451.05	4464.5	21.02	75.62	67.77	16.79	20.9	17.9	133.2	114.1	0.371	0.377	0.374	4.300	4.400	4.350	86.0	54	178
9	2451.05	4397.5	20.93	91.16	79.53	19.85	20.2	16.9	128.8	107.5	0.466	0.425	0.446	5.000	4.800	4.900	90.9	57	188

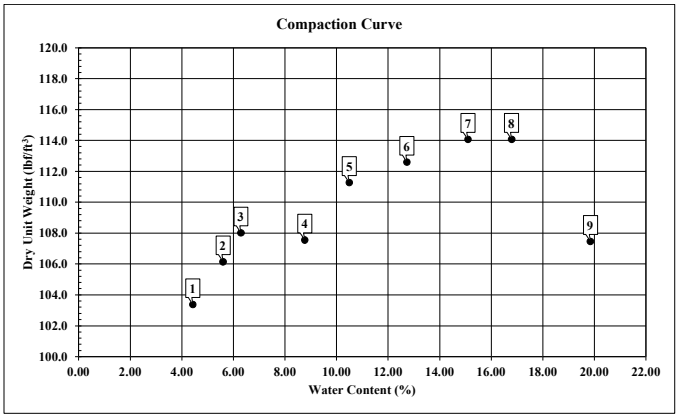

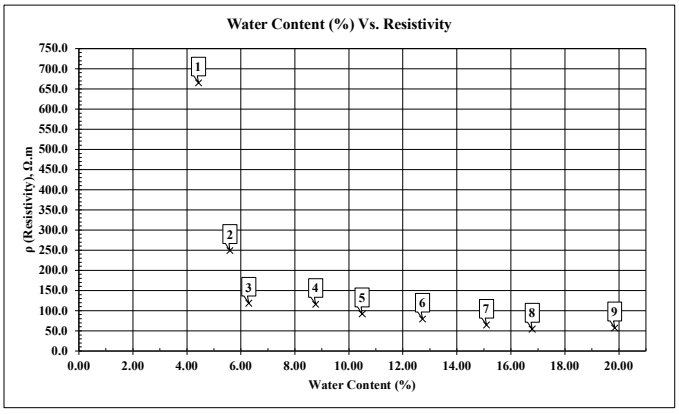

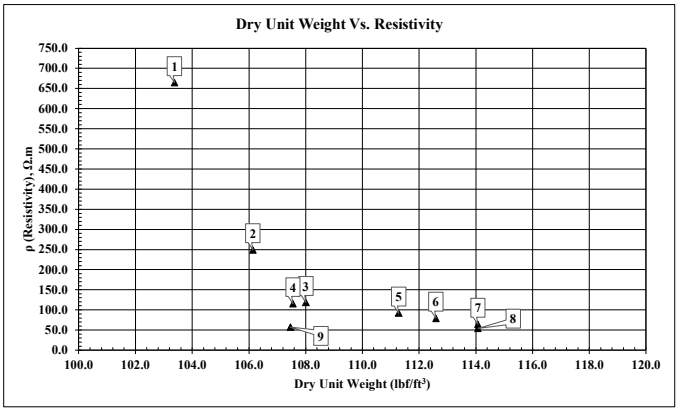

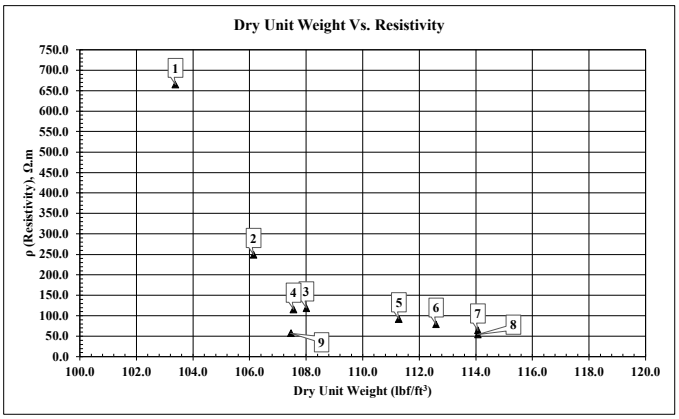

Plastic Mold Test (Compaction and ER Testing for 35 Drops) – Fat Clay

Test #	Weight (g)		Weight (g)			ω (%)	γ (kN/m³)	γd (kN/m³)	γ (lb/ft³)	γd (lb/ft³)	VDC			mADC			Resistance	ρ(Resistivity) Ω.m	ρ (Resistivity) Ω.ft
	(Mold)	(Mold + Moist Soil)	(Can)	(Can + Moist Soil)	(Can + Dry Soil)						VDC (Side 1)	VDC (Side 2)	VDC (AVG)	mADC (Side 1)	mADC (Side 2)	mADC (AVG)			
1	2425.99	4092.54	20.92	94.63	92.66	2.75	17.3	16.9	110.3	107.3	0.050	0.054	0.052	0.040	0.060	0.050	1040.0	655	2150
2	2425.99	4117.86	20.97	90.14	87.8	3.50	17.6	17.0	111.9	108.2	0.178	0.219	0.199	0.240	0.300	0.270	735.2	463	1520
3	2425.99	4156.61	20.94	91.93	88.76	4.67	18.0	17.2	114.5	109.4	0.204	0.240	0.222	0.630	0.530	0.580	382.8	241	791
4	2425.99	4201.55	20.9	90.69	86.45	6.47	18.5	17.3	117.5	110.3	0.278	0.241	0.260	1.540	1.240	1.390	186.7	118	386
5	2425.99	4242.22	21.01	84.31	79.2	8.78	18.9	17.4	120.2	110.5	0.295	0.316	0.306	2.200	2.650	2.425	126.0	79	260
6	2425.99	4355.19	20.97	88.29	81.51	11.20	20.1	18.0	127.7	114.8	0.367	0.343	0.355	3.750	3.480	3.615	98.2	62	203
7	2425.99	4442.1	21.02	90.54	81.64	14.68	21.0	18.3	133.4	116.3	0.334	0.333	0.334	4.130	4.010	4.070	81.9	52	169
8	2425.99	4460	21.01	97.65	86.5	17.03	21.1	18.1	134.6	115.0	0.401	0.404	0.403	5.680	5.610	5.645	71.3	45	147
9	2453.69	4390				21.00	20.1	16.6	128.1	105.9	0.404	0.442	0.423	7.300	7.000	7.150	59.2	35	115

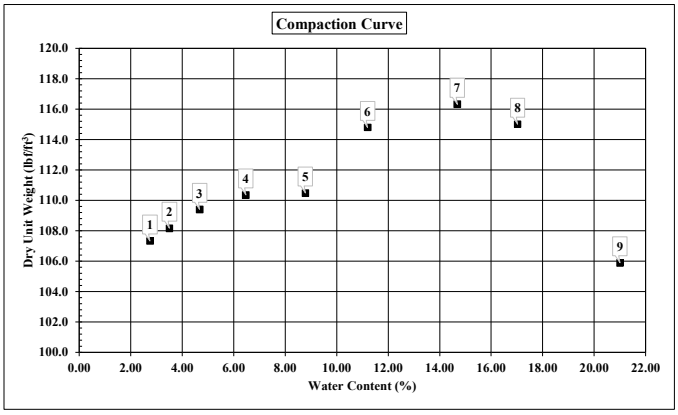

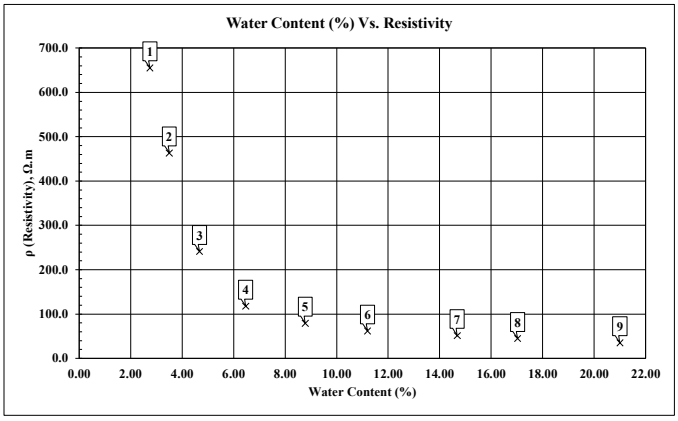

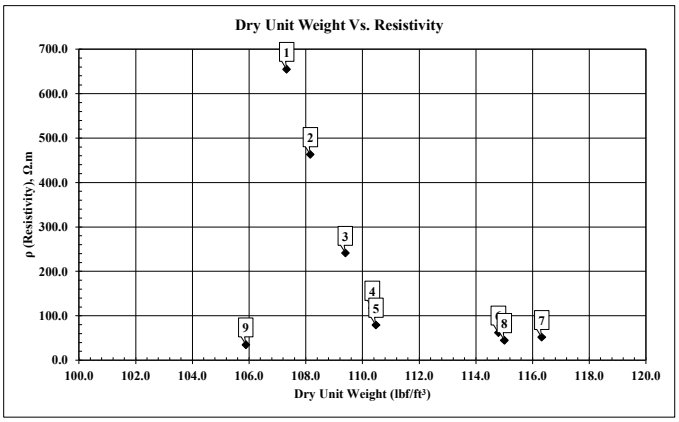

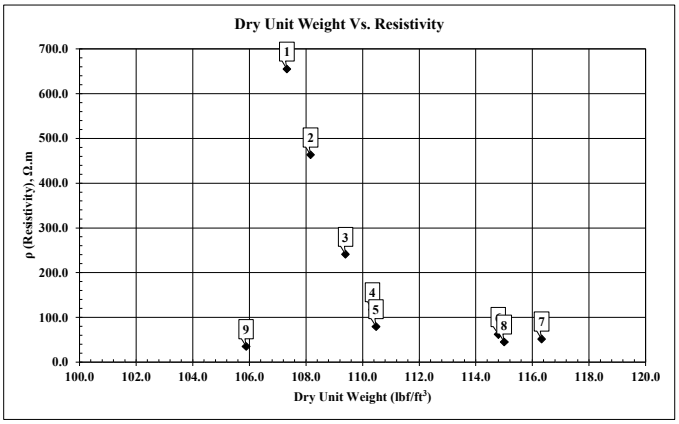

Plastic Mold Test (Compaction and ER Testing for 45 Drops) – Fat Clay

Test #	Weight (g)		Weight (g)			ω (%)	γ (kN/m³)	γ₄ (kN/m³)	γ (lb/ft³)	γ₄ (lb/ft³)	VDC			mADC			Resistance	ρ (Resistivity) Ω.m	ρ (Resistivity) Ω.ft
	(Mold)	(Mold + Moist Soil)	(Can)	(Can + Moist Soil)	(Can + Dry Soil)						VDC (Side 1)	VDC (Side 2)	VDC (AVG)	mADC (Side 1)	mADC (Side 2)	mADC (AVG)			
1	2453.69	4133.35	21.05	96.76	94.73	2.76	17.0	16.6	108.5	105.6	0.101	0.155	0.128	0.050	0.080	0.065	1969.2	1241	4071
2	2453.69	4152.97	21.01	93.76	91.17	3.69	17.2	16.6	109.8	105.9	0.215	0.215	0.215	0.360	0.360	0.360	597.2	376	1235
3	2453.69	4188.2	21.02	89.31	86.23	4.72	17.6	16.8	112.1	107.0	0.256	0.223	0.240	0.570	0.700	0.635	377.2	238	780
4	2453.69	4231.89	20.99	92	88.21	5.64	17.7	16.8	112.9	106.9	0.283	0.274	0.279	1.470	1.420	1.445	192.7	121	398
5	2453.69	4271.74	21	87.53	83.33	6.74	18.1	17.0	115.5	108.2	0.281	0.256	0.269	1.630	1.620	1.625	165.2	104	342
6	2453.69	4365.82	21.01	86.74	81.6	8.48	19.1	17.6	121.5	112.0	0.336	0.340	0.338	2.820	2.900	2.860	118.2	74	244
7	2453.69	4439.83	20.75	85.8	79.67	10.40	19.8	17.9	126.2	114.3	0.370	0.368	0.369	3.900	3.830	3.865	95.5	60	197
8	2453.69	4535.42	20.99	99.5	90.27	13.32	20.8	18.3	132.2	116.7	0.350	0.333	0.342	4.660	4.750	4.705	72.6	46	150
9	2453.69	4493.24	20.99	91.31	81.55	16.12	20.3	17.5	129.5	111.6	0.500	0.430	0.465	5.780	6.330	6.300	73.8	47	153
10	2453.69	4430				21.00	19.7	16.3	125.5	103.7	0.404	0.442	0.423	7.300	7.000	7.150	59.2	35	115

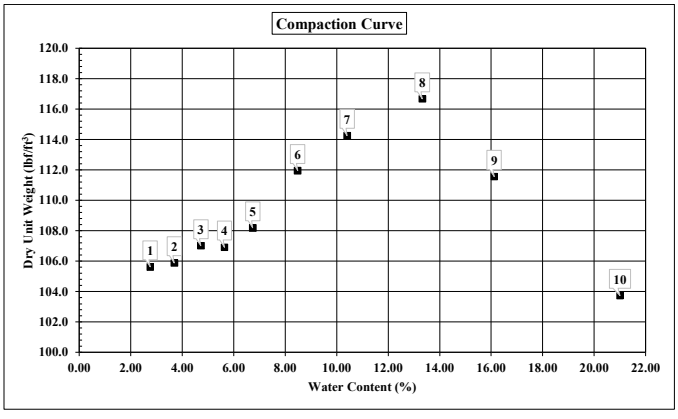

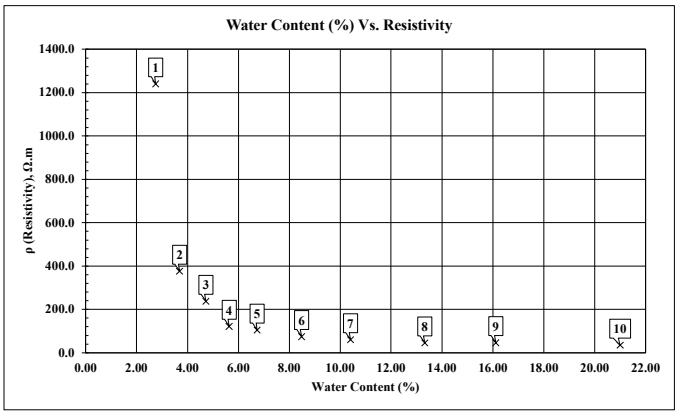

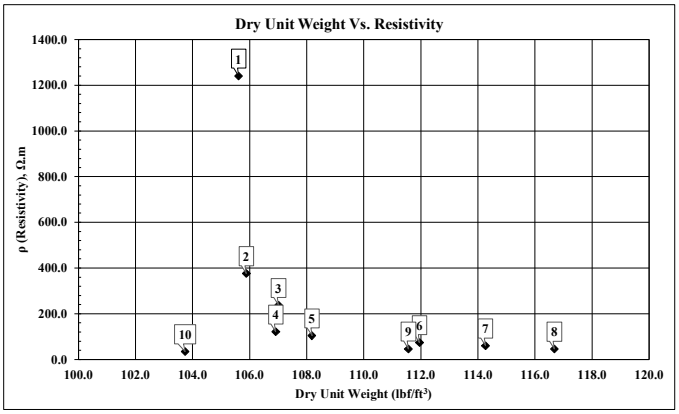

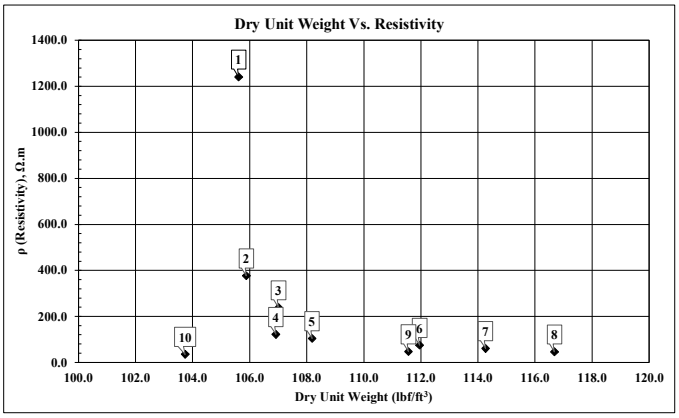

Plastic Mold Test (Compaction and ER Testing for 56 Drops) – Fat Clay

Test #	Weight (g)		Weight (g)			ω (%)	γ (kN/m³)	γd (kN/m³)	γ (lb/ft³)	γd (lb/ft³)	VDC			mADC			Resistance	ρ(Resistivity) Ω.m	ρ (Resistivity) Ω.ft
	(Mold)	(Mold + Moist Soil)	(Can)	(Can + Moist Soil)	(Can + Dry Soil)						VDC (Side 1)	VDC (Side 2)	VDC (AVG)	mADC (Side 1)	mADC (Side 2)	mADC (AVG)			
1	2451.39	4062.91	21.03	93.96	92.58	1.93	16.1	15.8	102.4	100.4	0.025	0.053	0.039	0.010	0.010	0.010	3900.0	2457	8062
2	2451.39	4127.06	21.01	103.3	101.07	2.79	16.7	16.3	106.4	103.5	0.111	0.067	0.089	0.030	0.070	0.050	1780.0	1121	3679
3	2451.39	4176.61	20.88	92.1	89.74	3.43	17.2	16.6	109.6	105.9	0.193	0.305	0.249	0.420	0.600	0.510	488.2	308	1009
4	2451.39	4239.24	21.08	96	91.68	6.12	17.8	16.8	113.6	107.0	0.260	0.228	0.244	0.990	0.920	0.955	255.5	161	528
5	2451.39	4294.67	20.98	91	85.88	7.89	18.4	17.0	117.1	108.5	0.231	0.287	0.259	1.250	1.670	1.460	177.4	112	367
6	2451.39	4428.01	20.94	97	89.74	10.55	19.7	17.8	125.5	113.6	0.422	0.276	0.349	4.320	2.450	3.385	103.1	65	213
7	2451.39	4532.33	20.97	94.69	86.09	13.21	20.8	18.3	132.2	116.8	0.297	0.303	0.300	3.550	3.180	3.365	89.2	56	184
8	2451.39	4495.29	21.01	86.88	77.2	17.23	20.4	17.4	129.8	110.7	0.354	0.412	0.383	4.160	4.120	4.140	92.5	58	191
9	2460.55	4428.02	21	80.86	70.67	20.52	19.6	16.3	125.0	103.7	0.394	0.404	0.399	7.300	6.700	7.000	57.0	36	118

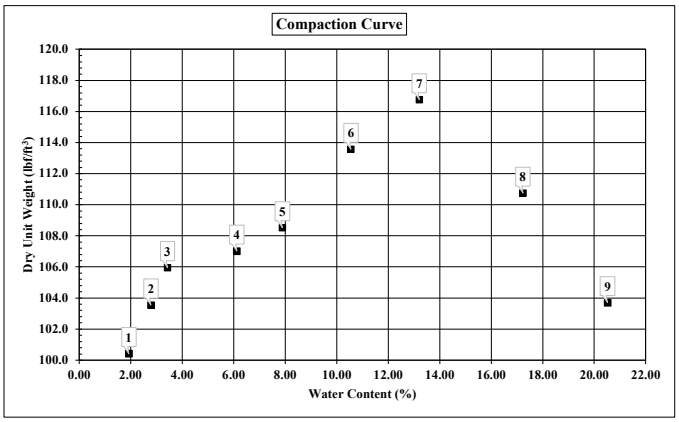
Compaction Curve
Dry Unit Weight (lbf/ft³)
Water Content (%)
120.0
118.0
116.0
114.0
112.0
110.0
108.0
106.0
104.0
102.0
100.0
0.00
2.00
4.00
6.00
8.00
10.00
12.00
14.00
16.00
18.00
20.00
22.00
1
2
3
4
5
6
7
8
9

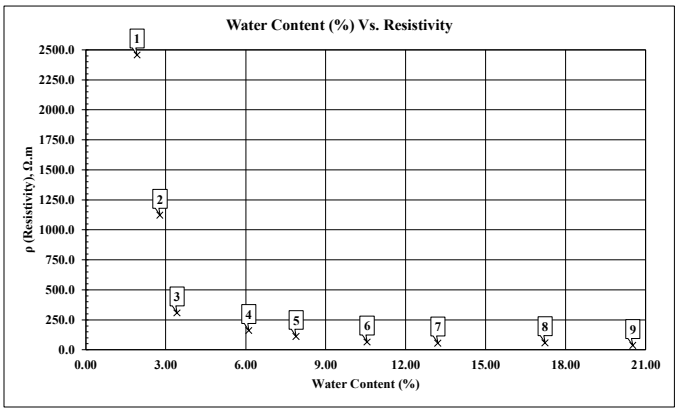
Water Content (%) Vs. Resistivity
ρ (Resistivity), Ω.m
Water Content (%)
2500.0
2250.0
2000.0
1750.0
1500.0
1250.0
1000.0
750.0
500.0
250.0
0.0
0.00
3.00
6.00
9.00
12.00
15.00
18.00
21.00
1
2
3
4
5
6
7
8
9

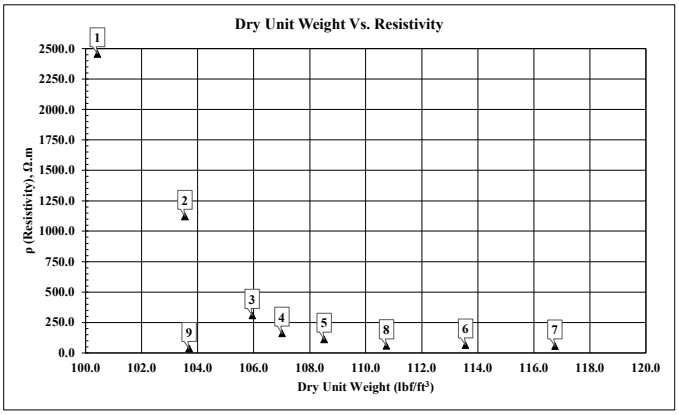
Dry Unit Weight Vs. Resistivity
ρ (Resistivity), Ω.m
Dry Unit Weight (lbf/ft³)
2500.0
2250.0
2000.0
1750.0
1500.0
1250.0
1000.0
750.0
500.0
250.0
0.0
100.0
102.0
104.0
106.0
108.0
110.0
112.0
114.0
116.0
118.0
120.0
1
2
3
4
5
6
7
8
9

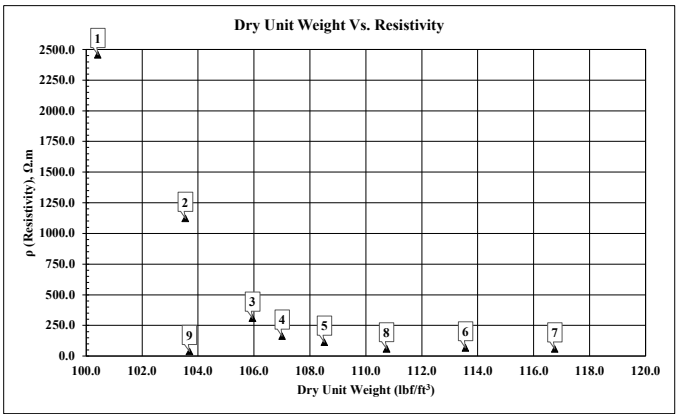

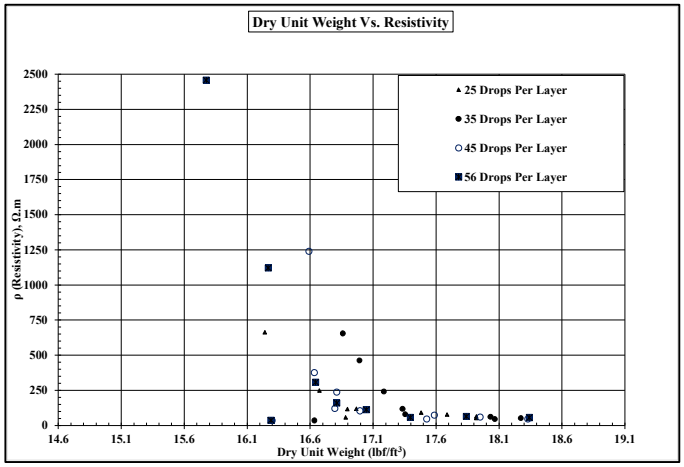

Plastic Mold Test (Compaction and ER Testing for 25 Drops) – Poorly Graded Sand

Test #	Weight (g)		Weight (g)			ω (%)	γ (kN/m³)	γd (kN/m³)	γ (lb/ft³)	γd (lb/ft³)	VDC			mADC			Resistance	ρ (Resistivity) Ω.m	ρ (Resistivity) Ω.ft
	(Mold)	(Mold + Moist Soil)	(Can)	(Can + Moist Soil)	(Can + Dry Soil)						VDC (Side 1)	VDC (Side 2)	VDC (AVG)	mADC (Side 1)	mADC (Side 2)	mADC (AVG)			
1	2455.12	4105.2	21.02	98.52	98.43	0.12	17.1	17.1	109.2	109.0	0.131	0.124	0.127	0.002	0.002	0.002	62000.0	39063	128159
2	2455.12	4250	20.99	73.36	73.1	0.50	18.7	18.6	118.7	118.1	0.200	0.200	0.200	0.009	0.009	0.009	21739.1	13697	44936
3	2455.12	4233.18	21	68.52	67.51	2.17	18.5	18.1	117.6	115.1	0.300	0.450	0.375	0.100	0.110	0.105	3571.4	2250	7382
4	2455.12	4294.31	21.03	61.15	59.71	3.72	19.1	18.4	121.7	117.3	0.370	0.400	0.385	0.210	0.200	0.205	1878.0	1183	3882
5	2455.12	4355.64	20.99	85.66	82.06	5.89	19.8	18.7	125.7	118.7	0.420	0.480	0.450	0.311	0.350	0.331	1361.6	858	2814
6	2455.12	4420.51	20.78	79.72	75.31	8.09	20.4	18.9	130.0	120.3	0.480	0.380	0.430	0.450	0.380	0.415	1036.1	653	2142
7	2455.12	4447.1	21	80.18	75.09	9.4	20.7	18.9	131.8	120.4	0.600	0.610	0.605	0.710	0.710	0.710	852.1	537	1761
8	2455.12	4460.7	20.94	76.67	71.08	11.1	20.8	18.8	132.7	119.4	0.61	0.63	0.620	1	1.02	1.01	614	387	1269
9	2453.21	4480.4	20.96	83.01	75	14.8	21.1	18.3	134.1	116.8	0.666	0.7	0.683	1.42	1.41	1.415	483	304	998

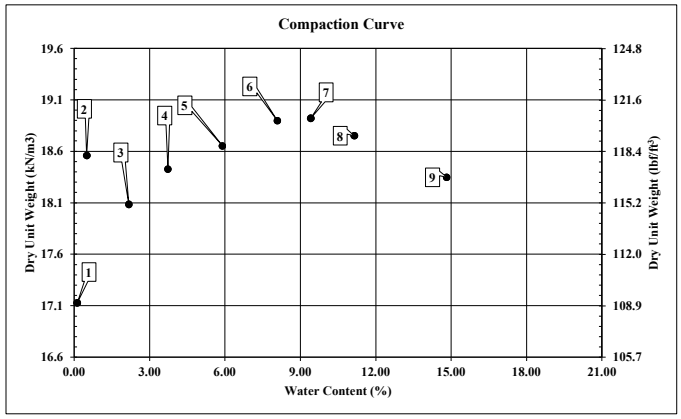

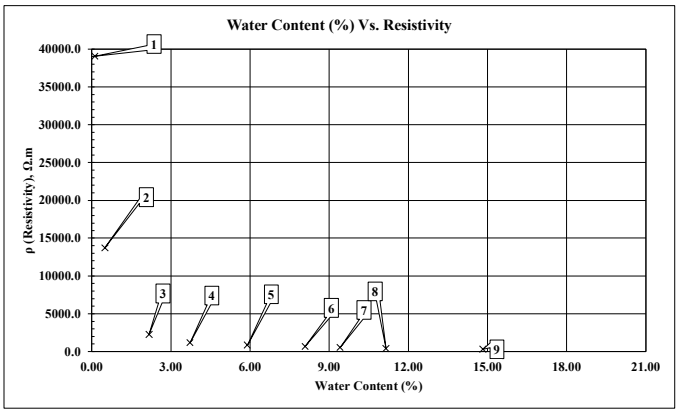

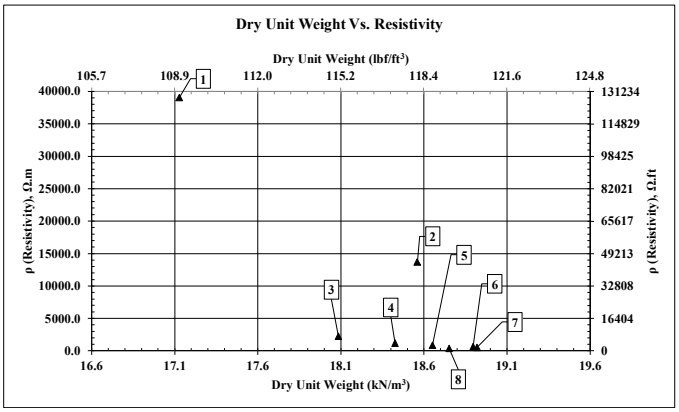

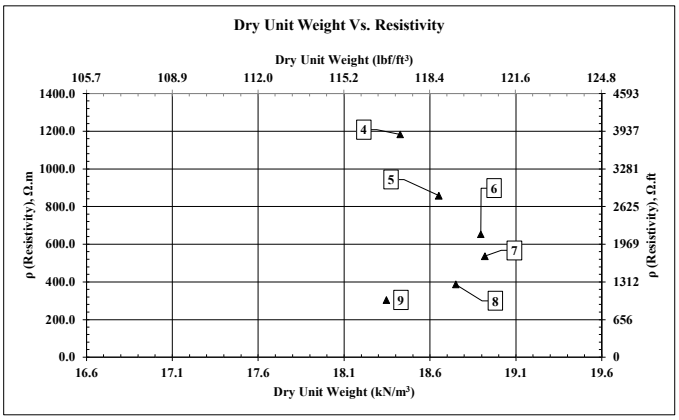

Plastic Mold Test (Compaction and ER Testing for 35 Drops) – Poorly Graded Sand

Test #	Weight (g)		Weight (g)			ω (%)	γ (kN/m³)	γd (kN/m³)	γ (lb/ft³)	γd (lb/ft³)	VDC			mADC			Resistance	ρ(Resistivity) Ω.m	ρ (Resistivity) Ω.ft
	(Mold)	(Mold + Moist Soil)	(Can)	(Can + Moist Soil)	(Can + Dry Soil)						VDC (Side 1)	VDC (Side 2)	VDC (AVG)	mADC (Side 1)	mADC (Side 2)	mADC (AVG)			
1	2455.12	4109	21	98.52	98.5	0.03	17.2	17.2	109.4	109.4	0.133	0.133	0.133	0.002	0.002	0.002	61860.5	38975	127870
2	2455.12	4255.6	20.99	73.36	73.1	0.50	18.7	18.6	119.1	118.5	0.220	0.200	0.210	0.009	0.009	0.009	22826.1	14381	47183
3	2455.12	4268.42	21	68.52	67.51	2.17	18.8	18.4	120.0	117.4	0.410	0.390	0.400	0.115	0.090	0.103	3902.4	2459	8067
4	2455.12	4300.7	21.03	61.15	59.71	3.72	19.2	18.5	122.1	117.7	0.387	0.380	0.384	0.205	0.185	0.195	1966.7	1239	4065
5	2455.12	4363.86	20.99	85.66	82.06	5.89	19.8	18.7	126.3	119.2	0.425	0.490	0.458	0.326	0.360	0.343	1333.8	840	2757
6	2455.12	4434.25	20.78	79.72	75.31	8.09	20.6	19.0	130.9	121.1	0.495	0.444	0.470	0.550	0.485	0.518	907.2	572	1875
7	2455.12	4462.6	21	80.18	75.09	9.41	20.9	19.1	132.8	121.4	0.630	0.670	0.650	0.770	0.777	0.774	840.3	529	1737
8	2455.12	4475.72	20.94	76.67	71.08	11.15	21.0	18.9	133.7	120.3	0.650	0.700	0.675	1.100	1.110	1.200	562.5	354	1163
9	2455.12	4490.54	20.89	83.24	75.5	14.17	21.2	18.5	134.7	117.9	0.650	0.675	0.663	1.400	1.390	1.395	474.9	299	982

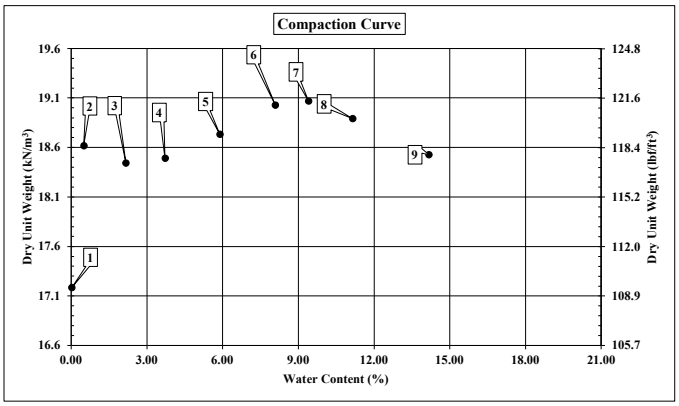
Compaction Curve
Dry Unit Weight (kN/m³)
Dry Unit Weight (lbf/ft³)
Water Content (%)
19.6
19.1
18.6
18.1
17.6
17.1
16.6
124.8
121.6
118.4
115.2
112.0
108.9
105.7
0.00
3.00
6.00
9.00
12.00
15.00
18.00
21.00
1
2
3
4
5
6
7
8
9

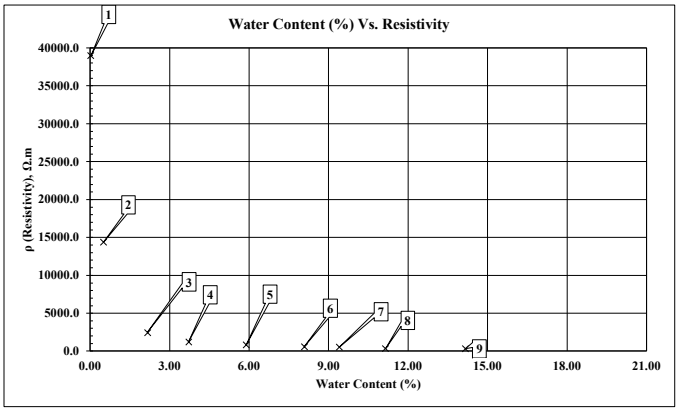
Water Content (%) Vs. Resistivity
ρ (Resistivity), Ω.m
Water Content (%)
40000.0
35000.0
30000.0
25000.0
20000.0
15000.0
10000.0
5000.0
0.0
0.00
3.00
6.00
9.00
12.00
15.00
18.00
21.00
1
2
3
4
5
6
7
8
9

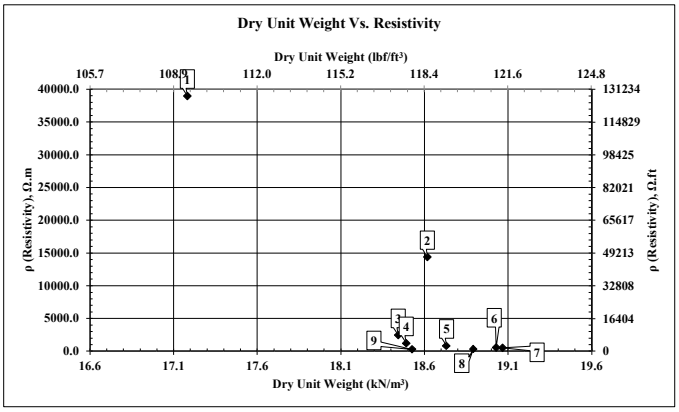
Dry Unit Weight Vs. Resistivity
Dry Unit Weight (lbf/ft³)
Dry Unit Weight (kN/m³)
ρ (Resistivity), Ω.m
ρ (Resistivity), Ω.ft
105.7
108.9
112.0
115.2
118.4
121.6
124.8
16.6
17.1
17.6
18.1
18.6
19.1
19.6
40000.0
35000.0
30000.0
25000.0
20000.0
15000.0
10000.0
5000.0
0.0
131234
114829
98425
82021
65617
49213
32808
16404
0
1
2
3
4
5
6
7
8
9

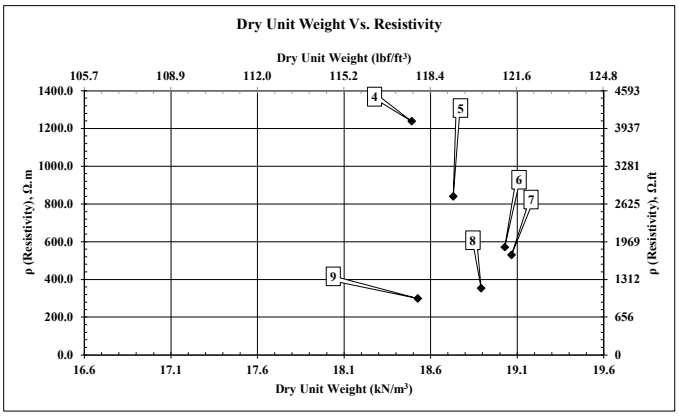

Plastic Mold Test (Compaction and ER Testing for 45 Drops) – Poorly Graded Sand

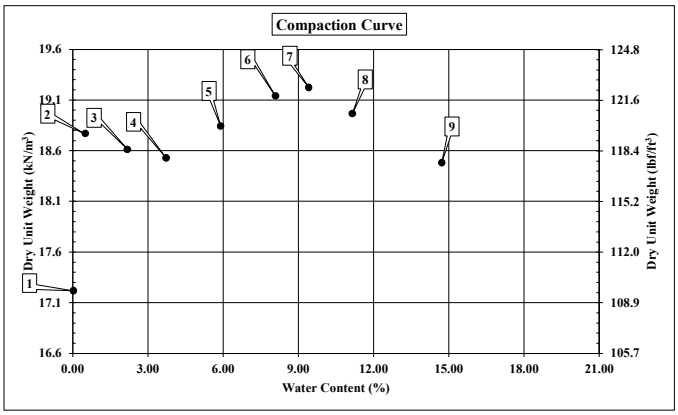

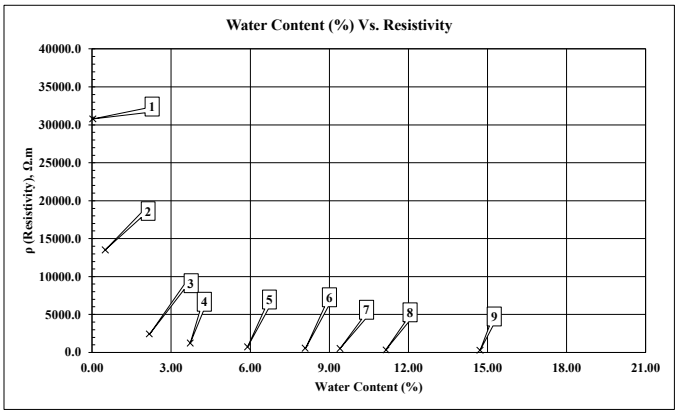

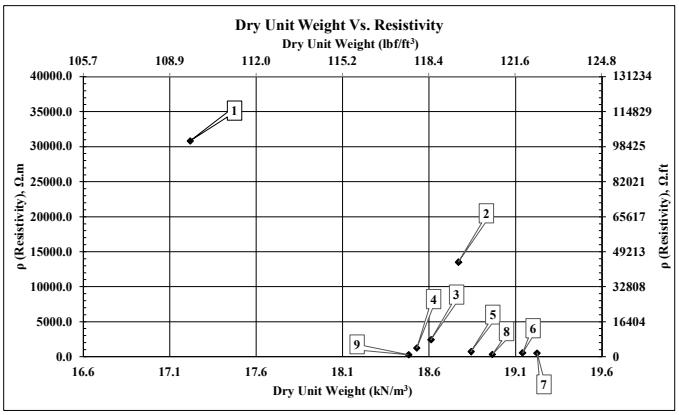

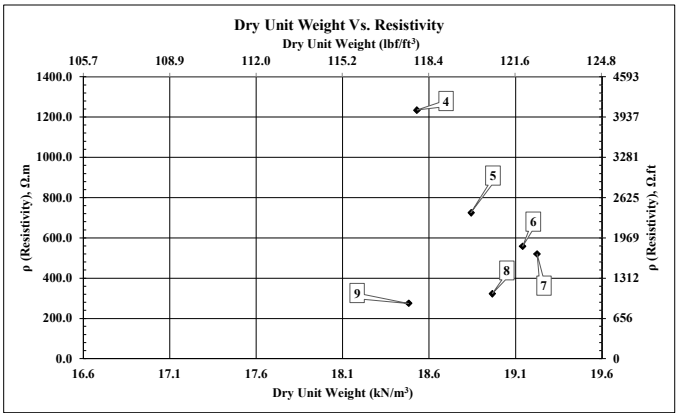

Plastic Mold Test (Compaction and ER Testing for 56 Drops) – Poorly Graded Sand

Test #	Weight (g)		Weight (g)			ω (%)	γ (kN/m³)	γd (kN/m³)	γ (lb/ft³)	γd (lb/ft³)	VDC			mADC			Resistance	ρ(Resistivity) Ω.m	ρ (Resistivity) Ω.ft
	(Mold)	(Mold + Moist Soil)	(Can)	(Can + Moist Soil)	(Can + Dry Soil)						VDC (Side 1)	VDC (Side 2)	VDC (AVG)	mADC (Side 1)	mADC (Side 2)	mADC (AVG)			
1	2455.12	4100	21	98.52	98.43	0.12	17.1	17.1	108.8	108.7	0.131	0.124	0.127	0.002	0.002	0.002	55260.9	34817	114228
2	2455.12	4280.31	20.99	73.36	73.1	0.50	19.0	18.9	120.7	120.1	0.223	0.206	0.215	0.010	0.010	0.010	21450.0	13514	44339
3	2455.12	4250	21	68.52	67.51	2.17	18.7	18.3	118.7	116.2	0.412	0.400	0.406	0.010	0.030	0.020	20300.0	12790	41962
4	2455.12	4319.1	21.03	61.15	59.71	3.72	19.4	18.7	123.3	118.9	0.400	0.400	0.400	0.200	0.230	0.215	1860.5	1172	3846
5	2455.12	4375.93	20.99	85.66	82.06	5.89	20.0	18.8	127.1	120.0	0.380	0.475	0.428	0.400	0.360	0.380	1125.0	709	2325
6	2455.12	4455.15	20.78	79.72	75.31	8.09	20.8	19.2	132.3	122.4	0.610	0.510	0.560	0.675	0.600	0.638	878.4	553	1816
7	2455.12	4472.99	21	80.18	75.09	9.41	21.0	19.2	133.5	122.0	0.670	0.675	0.673	0.830	1.000	1.000	672.5	424	1390
8	2455.12	4494.5	20.94	76.67	71.08	11.15	21.2	19.1	134.9	121.4	0.710	0.730	0.720	1.410	1.460	1.435	501.7	316	1037
9	2455.12	4500.38	21.01	95.15	86	14.08	21.3	18.6	135.3	118.6	0.800	0.800	0.800	2.000	2.000	2.000	400.0	252	827

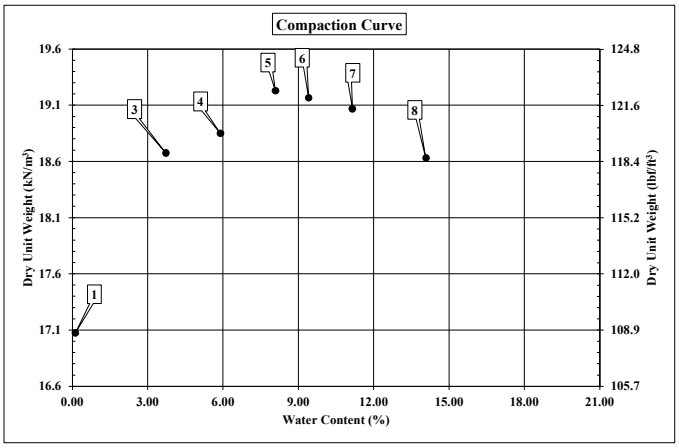

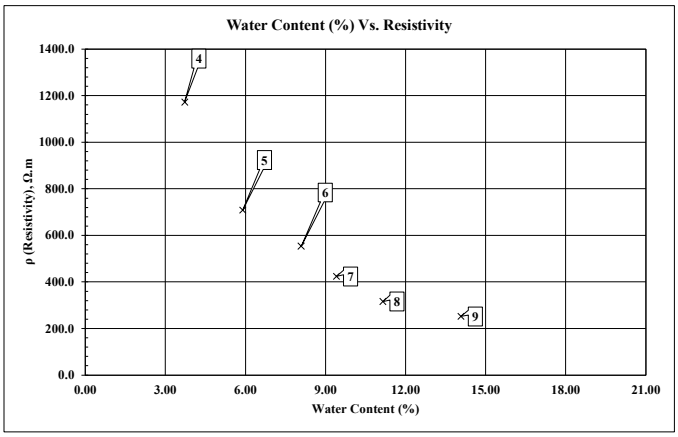

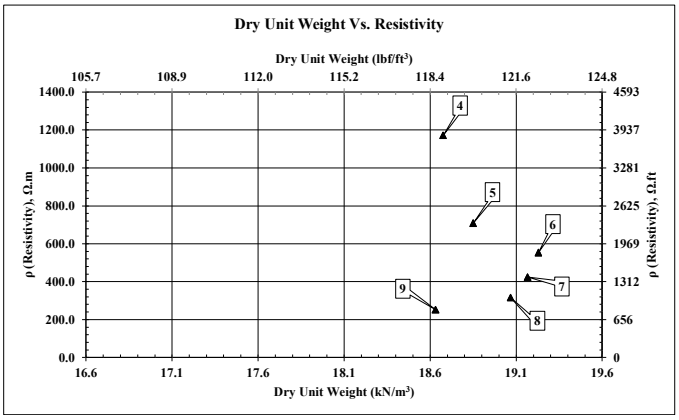

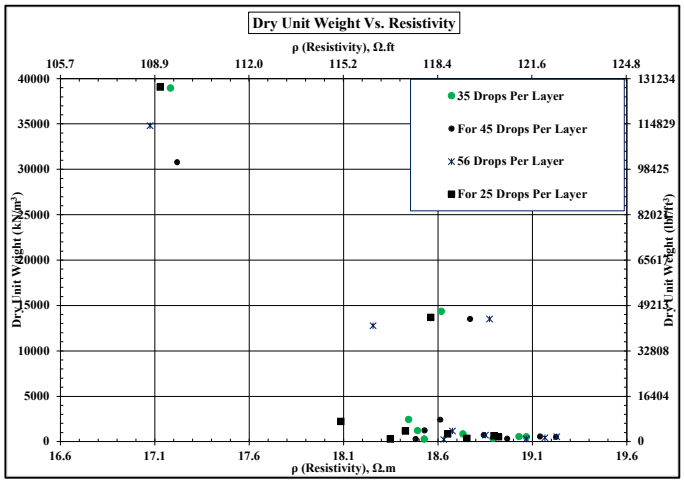

Standard Proctor Mold ASTM (Compaction and ER Testing for 25 Drops) – Fat Caly

Test.#	Weight (g)		Weight (g)			ω (%)	γ (kN/m³)	γd (kN/m³)	γ (lb/ft³)	γd (lb/ft³)	VDC			mADC			Resistance	ρ (Resistivity) Ω.m	ρ (Resistivity) Ω.ft
	(Mold)	(Mold + Moist Soil)	(Can)	(Can + Moist Soil)	(Can + Dry Soil)						VDC (Side 1)	VDC (Side 2)	VDC (AVG)	mADC (Side 1)	mADC (Side 2)	mADC (AVG)			
1	2473.31	4436.22	21.01	94.25	90.76	5.00	20.6	19.7	131.4	125.1	0.470	0.450	0.460	1.160	1.360	1.260	365.1	230	755
2	2473.31	4545.21	21.02	91.31	86.77	6.90	21.8	20.4	138.7	129.7	0.470	0.460	0.465	1.420	1.890	1.655	281.0	177	581
3	2460.01	4599.43	21	83.4	78.01	9.45	22.5	20.6	143.2	130.8	0.600	0.650	0.625	2.640	2.930	2.785	224.4	141	464
4	2460.01	4644.89	20.94	69.53	64.14	12.48	23.0	20.4	146.2	130.0	0.550	0.650	0.600	3.480	3.060	3.270	183.5	116	379
5	2499.9	4630.22	20.98	84.57	76.7	14.12	22.4	19.6	142.6	124.9	0.500	0.550	0.525	3.860	4.000	3.930	133.6	84	276
6	2499.9	4590.76	21.05	87.69	78.45	16.10	22.0	18.9	139.9	120.5	0.354	0.412	0.383	4.160	4.120	4.140	92.5	58	191
7	2499.9	4530.74	21.04	87.51	77.25	18.25	21.4	18.1	135.9	115.0	0.250	0.400	0.325	6.500	6.450	6.475	50.2	32	104

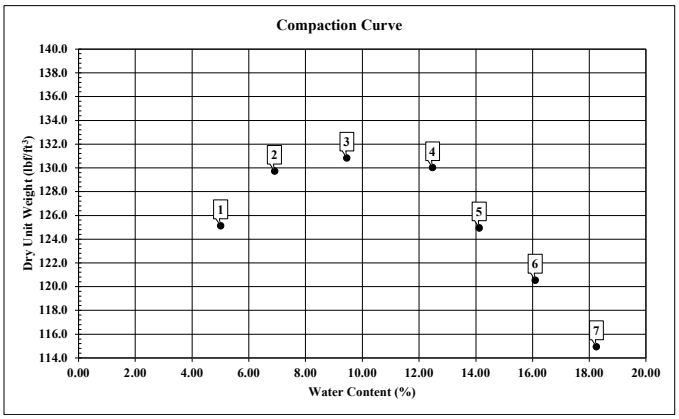

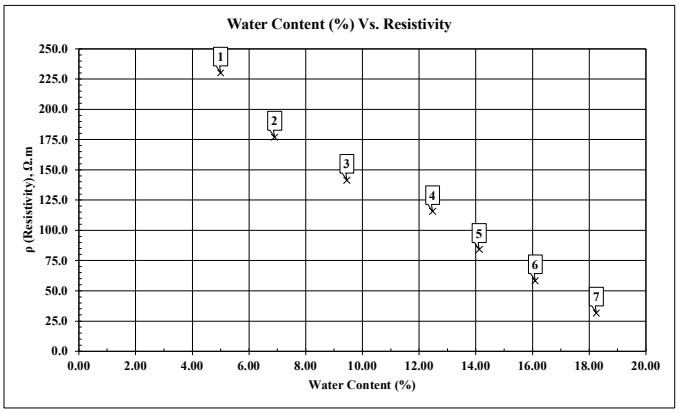

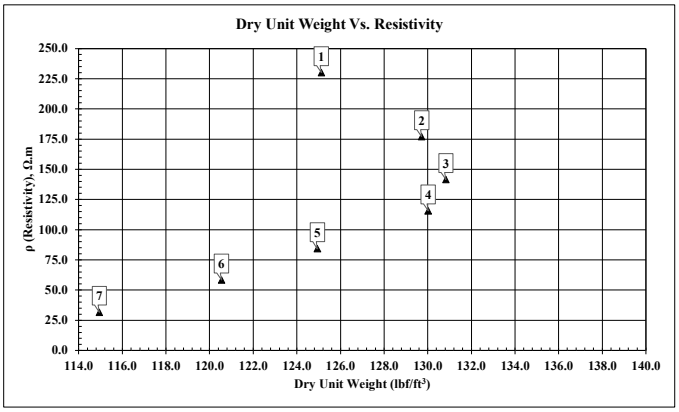

Modified Proctor Mold ASTM (Compaction and ER Testing for 56 Drops) – Fat Caly

Test #	Weight (g)		Weight (g)			ω (%)	γ (kN/m³)	γd (kN/m³)	γ (lb/ft³)	γd (lb/ft³)	VDC			mADC			Resistance	ρ(Resistivity) Ω.m	ρ (Resistivity) Ω.ft
	(Mold)	(Mold + Moist Soil)	(Can)	(Can + Moist Soil)	(Can + Dry Soil)						VDC (Side 1)	VDC (Side 2)	VDC (AVG)	mADC (Side 1)	mADC (Side 2)	mADC (AVG)			
1	2473.31	4520.22	21.01	94.25	90.76	5.00	21.5	20.5	137.0	130.5	0.570	0.520	0.545	1.650	1.730	1.690	322.5	203	667
2	2473.31	4642.4	21.02	91.31	86.77	6.90	22.8	21.3	145.2	135.8	0.670	0.700	0.685	2.900	3.000	2.950	232.2	146	480
3	2460.01	4697.16	21	83.4	78.01	9.45	23.5	21.5	149.7	136.8	0.870	0.850	0.860	4.330	4.250	4.290	200.5	126	414
4	2460.01	4720.38	20.94	69.53	64.14	12.48	23.8	21.1	151.3	134.5	0.670	0.750	0.710	4.700	4.930	4.815	147.5	93	305
5	2499.9	4650.34	20.98	84.57	76.7	14.12	22.6	19.8	143.9	126.1	0.550	0.620	0.585	5.340	5.780	5.560	105.2	66	217
6	2499.9	4629.76	21.05	87.69	78.45	16.10	22.4	19.3	142.6	122.8	0.410	0.425	0.418	6.250	6.650	6.450	64.7	41	134
7	2499.9	4580.64	21.04	87.51	77.25	18.25	21.9	18.5	139.3	117.8	0.300	0.320	0.310	7.200	7.450	7.325	42.3	27	87

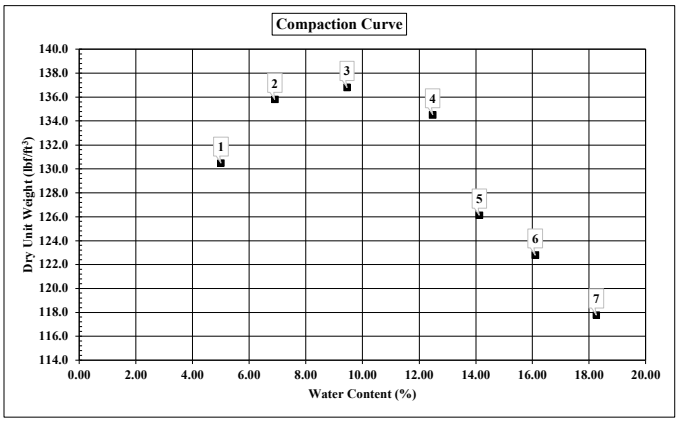
Compaction Curve
Dry Unit Weight (lbf/ft³)
Water Content (%)
140.0
138.0
136.0
134.0
132.0
130.0
128.0
126.0
124.0
122.0
120.0
118.0
116.0
114.0
0.00
2.00
4.00
6.00
8.00
10.00
12.00
14.00
16.00
18.00
20.00
1
2
3
4
5
6
7

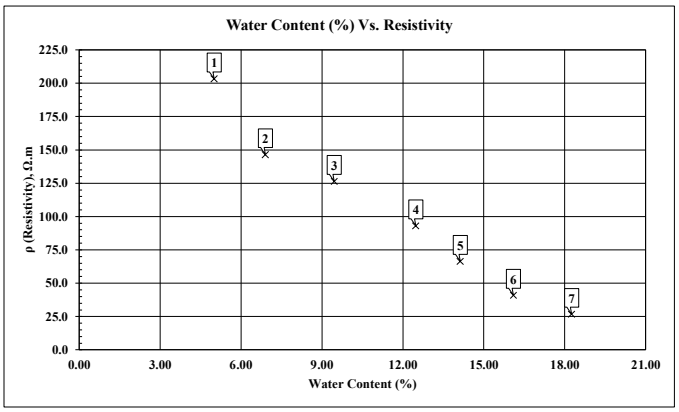
Water Content (%) Vs. Resistivity
ρ (Resistivity), Ω.m
Water Content (%)
225.0
200.0
175.0
150.0
125.0
100.0
75.0
50.0
25.0
0.0
0.00
3.00
6.00
9.00
12.00
15.00
18.00
21.00
1
2
3
4
5
6
7

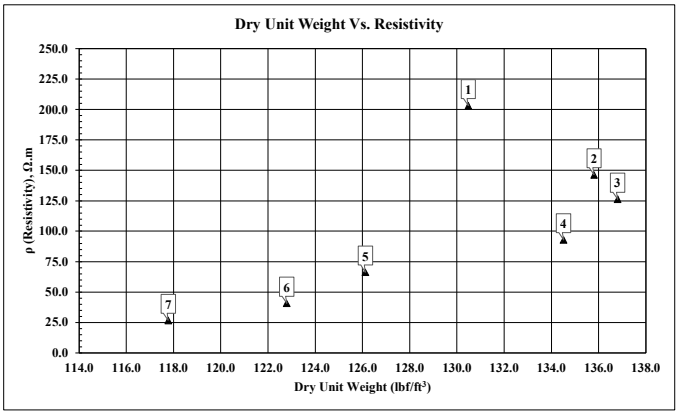
Dry Unit Weight Vs. Resistivity
ρ (Resistivity), Ω.m
Dry Unit Weight (lbf/ft³)
250.0
225.0
200.0
175.0
150.0
125.0
100.0
75.0
50.0
25.0
0.0
114.0
116.0
118.0
120.0
122.0
124.0
126.0
128.0
130.0
132.0
134.0
136.0
138.0
1
2
3
4
5
6
7

Test #	Weight (g)		Weight (g)			ω (%)	γ (kN/m³)	γd (kN/m³)	γ (lb/ft³)	γd (lb/ft³)	VDC			mADC			Resistance	ρ (Resistivity) Ω.m	ρ (Resistivity) Ω.ft
	(Mold)	Mold + Moist So	(Can)	Can + Moist Soil	Can + Dry Soil						VDC (Side 1)	VDC (Side 2)	VDC (AVG)	mADC (Side 1)	mADC (Side 2)	mADC (AVG)			
1	2455.12	4233.18	21	68.52	67.51	2.17	18.5	18.1	117.6	115.1	0.300	0.450	0.375	0.100	0.110	0.105	3571.4	872	2862
2	2455.12	4294.31	21.03	61.15	59.71	3.72	19.1	18.4	121.7	117.3	0.370	0.400	0.385	0.210	0.200	0.205	1878.0	459	1505
3	2455.12	4355.64	20.99	85.66	82.06	5.89	19.8	18.7	125.7	118.7	0.420	0.480	0.450	0.311	0.350	0.331	1361.6	333	1091
4	2455.12	4420.51	20.78	79.72	75.31	8.09	20.4	18.9	130.0	120.3	0.480	0.380	0.430	0.450	0.380	0.415	1036.1	253	830
5	2455.12	4447.1	21	80.18	75.09	9.4	20.7	18.9	131.8	120.4	0.600	0.610	0.605	0.710	0.710	0.710	852.1	208	683
6	2455.12	4460.7	20.94	76.67	71.08	11.1	20.8	18.8	132.7	119.4	0.61	0.63	0.620	1	1.02	1.01	614	150	492
7	2453.21	4480.4	20.96	83.01	75	14.8	21.1	18.3	134.1	116.8	0.666	0.7	0.683	1.42	1.41	1.415	483	118	387
1	2455.12	4250	21	68.52	67.51	2.17	18.7	18.3	118.7	116.2	0.412	0.400	0.406	0.100	0.100	0.100	4060.0	992	3254
2	2455.12	4319.1	21.03	61.15	59.71	3.72	19.4	18.7	123.3	118.9	0.400	0.400	0.400	0.200	0.230	0.215	1860.5	454	1491
3	2455.12	4375.93	20.99	85.66	82.06	5.89	20.0	18.8	127.1	120.0	0.380	0.475	0.428	0.400	0.360	0.380	1125.0	275	902
4	2455.12	4455.15	20.78	79.72	75.31	8.09	20.8	19.2	132.3	122.4	0.610	0.510	0.560	0.675	0.600	0.638	878.4	215	704
5	2455.12	4472.99	21	80.18	75.09	9.41	21.0	19.2	133.5	122.0	0.670	0.675	0.673	0.830	1.000	1.000	672.5	164	539
6	2455.12	4494.5	20.94	76.67	71.08	11.15	21.2	19.1	134.9	121.4	0.710	0.730	0.720	1.410	1.460	1.435	501.7	123	402
7	2455.12	4500.38	21.01	95.15	86	14.08	21.3	18.6	135.3	118.6	0.800	0.800	0.800	2.000	2.000	2.000	400.0	98	321
1	2466.21	4375.45	21	57.3	56.55	2.11	19.4	19.0	123.4	120.9	0.510	0.510	0.510	0.146	0.136	0.141	3617.0	884	2899
2	2466.21	4459.32	20.84	62	60.35	4.18	20.2	19.4	128.8	123.7	0.525	0.530	0.528	0.482	0.520	0.501	1052.9	257	844
3	2466.21	4537.57	20.9	50.55	48.85	6.08	21.0	19.8	133.9	126.2	0.525	0.535	0.530	0.820	0.850	0.835	634.7	155	509
4	2466.21	4600.06	21.08	57.36	54.67	8.01	21.7	20.1	137.9	127.7	0.662	0.640	0.651	1.270	1.150	1.210	538.0	131	431
5	2466.21	4630.25	20.92	71.19	66.6	10.05	22.0	20.0	139.9	127.1	0.800	0.800	0.800	1.500	1.620	1.560	512.8	125	411
6	2466.21	4600.25	21	120	109.39	12.00	21.7	19.3	138.0	123.2	0.900	0.850	0.875	1.850	1.890	1.870	467.9	114	375
7	2466.21	4552.42	20.91	132.68	118.97	13.98	21.2	18.6	134.9	118.3	0.600	0.650	0.625	1.820	1.850	1.835	340.6	83	273
1	2466.21	4408.34	21	57.3	56.55	2.11	19.7	19.3	125.6	123.0	0.597	0.500	0.549	0.189	0.160	0.175	3143.3	768	2519
2	2466.21	4521	20.84	62	60.35	4.18	20.9	20.0	132.8	127.5	0.495	0.490	0.493	0.580	0.600	0.590	834.7	204	669
3	2466.21	4600	20.9	50.55	48.85	6.08	21.7	20.4	137.9	130.0	0.588	0.573	0.581	1.020	0.970	0.995	583.4	143	468
4	2466.21	4680	21.08	57.36	54.67	8.01	22.5	20.8	143.1	132.5	0.800	0.800	0.800	1.500	1.620	1.560	512.8	125	411
5	2466.21	4680.69	20.92	71.19	66.6	10.05	22.5	20.4	143.2	130.1	0.660	0.820	0.740	1.720	1.700	1.710	432.7	106	347
6	2466.21	4640.34	21	120	109.39	12.00	22.1	19.7	140.6	125.5	0.760	0.760	0.760	1.800	1.830	1.815	418.7	102	336
7	2466.21	4590.22	20.91	132.68	118.97	13.98	21.6	18.9	137.3	120.5	0.600	0.650	0.625	2.000	2.000	2.000	312.5	76	250

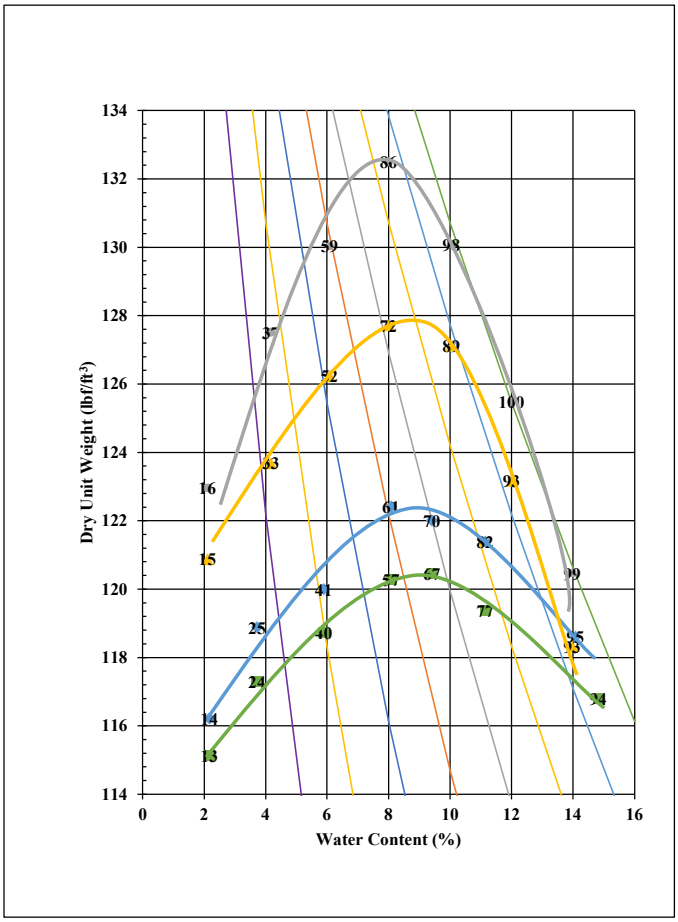

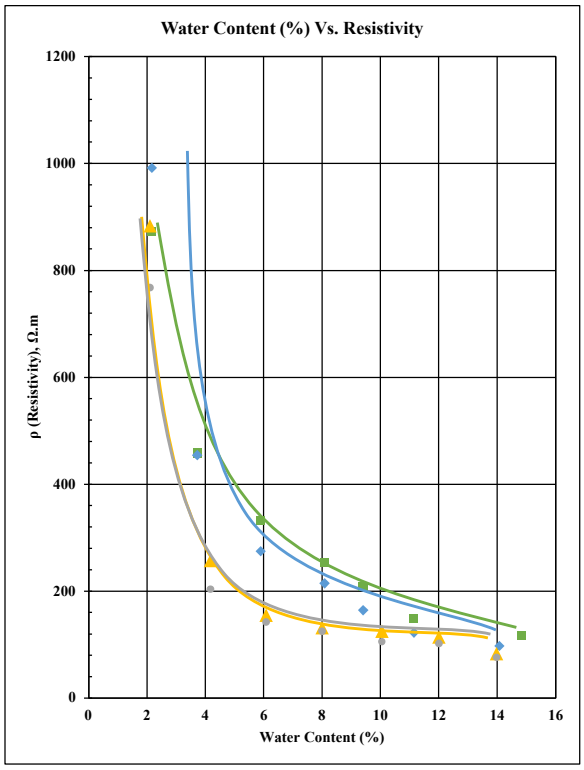
Water Content (%) Vs. Resistivity
ρ (Resistivity), Ω.m
1200
1000
800
600
400
200
0
0
2
4
6
8
10
12
14
16
Water Content (%)

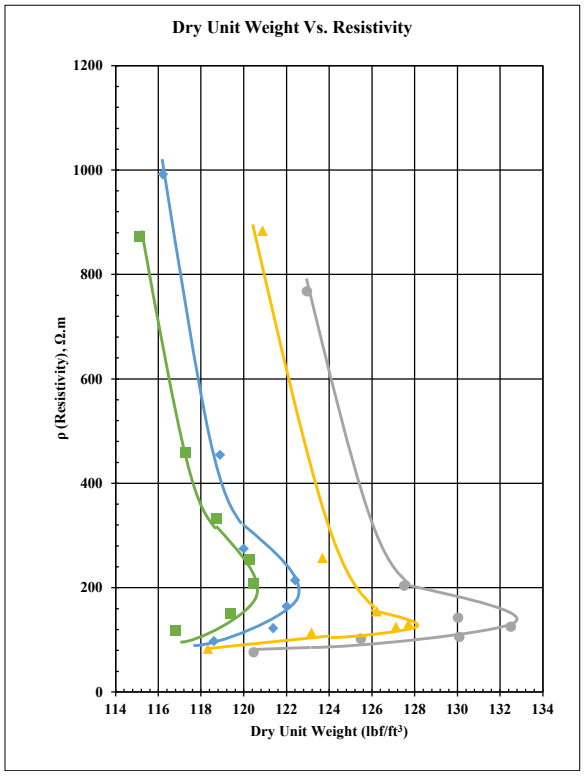
Dry Unit Weight Vs. Resistivity
ρ (Resistivity), Ω.m
1200
1000
800
600
400
200
0
114
116
118
120
122
124
126
128
130
132
134
Dry Unit Weight (lbf/ft³)

Laboratory SP/MP and Soil Strip Testing Results

	SAMPLE #	WEIGHT OF CAN (g)	WEIGHT OF CAN AND	WEIGHT OF CAN AND DRY SOIL(g)	WEIGHT OF MOLD (kg)	WEIGHT OF MOLD AND SOIL	CD (slide	VCD (slide 1)	mACD (slide 1)	mACD (slide 2)	ω (%)	γ (kN/m³)	γd (kN/m³)	γ (lb/ft³)	γd (lb/ft³)	Resistance	ρ (Resistivity) Ω.m	ρ (Resistivity) Ω.ft	Saturation (%)
Standard Proctor N=25	S-1-25	20.87	59.3	58.3	4.35	6.27	0.395	0.5	0.4	0.35	2.67	20.19	19.67	128.5	125.2	1193.33	335	1098	20
	S-2-25	20.92	85.39	82.47	4.35	6.37	0.49	0.36	0.79	0.69	4.74	21.24	20.28	135.2	129.1	574.32	161	528	41
	S-3-25	20.94	46.08	44.33	4.35	6.47	0.5	0.536	1.39	1.61	7.48	22.30	20.74	141.9	132.1	345.33	97	318	71
	S-4-25	20.94	36.01	34.72	4.35	6.45	0.71	0.7318	3.33	3.243	9.36	22.09	20.20	140.6	128.6	219.35	62	202	80
Standard Proctor N=56	S-1-56	20.71	53.25	52.49	4.35	6.32	0.436	0.456	0.4	0.45	2.39	20.72	20.23	131.9	128.8	1049.41	294	965	20
	S-2-56	20.77	59.05	57.33	4.35	6.43	0.42	0.47	0.83	0.85	4.70	21.88	20.89	139.3	133.0	529.76	149	487	46
	S-3-56	20.95	53.83	51.7	4.35	6.51	0.5	0.59	1.54	1.7	6.93	22.72	21.25	144.6	135.2	336.42	94	309	74
	S-4-56	20.83	70.38	66.16	4.35	6.47	0.68	0.64	3.03	3.4	9.31	22.30	20.40	141.9	129.8	205.29	58	189	82
Modified Proctor N=25	M-1-25	21	54.25	53.57	6.04	10.1	0.32	0.21	0.25	0.23	2.09	20.96	20.53	133.4	130.7	1104.17	310	1016	19
	M-2-25	20.85	75.02	72.47	6.04	10.37	0.46	0.4623	0.89	0.8	4.94	22.36	21.30	142.3	135.6	545.74	153	502	53
	M-3-25	20.98	82.42	78.21	6.04	10.57	0.47	0.38	1.48	1.283	7.36	23.39	21.79	148.9	138.7	307.64	86	283	89
	M-4-25	20.75	62.79	59.33	6.04	10.5	0.74	0.62	3.2	3.152	8.97	23.03	21.13	146.6	134.5	214.11	60	197	93
Modified Proctor N=56	M-1-56	20.79	67.37	66.32	6.04	10.27	0.405	0.289	0.34	0.33	2.31	21.84	21.35	139.0	135.9	1035.82	290	953	25
	M-2-56	20.7	83.43	80.58	6.04	10.49	0.41	0.42	0.81	0.79	4.76	22.98	21.93	146.3	139.6	518.75	145	477	60
	M-3-56	20.72	75.95	72.29	6.04	10.64	0.62	0.4922	1.8	1.92	7.10	23.75	22.18	151.2	141.2	298.98	84	275	95
	M-4-56	21.01	68.54	64.71	6.04	10.54	0.72	0.81	3.9314	4.28	8.76	23.23	21.36	147.9	136.0	194.59	55	179	96

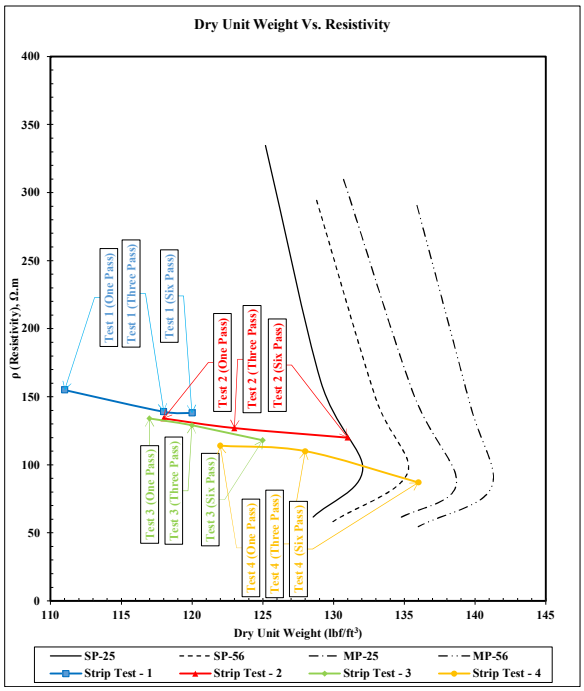

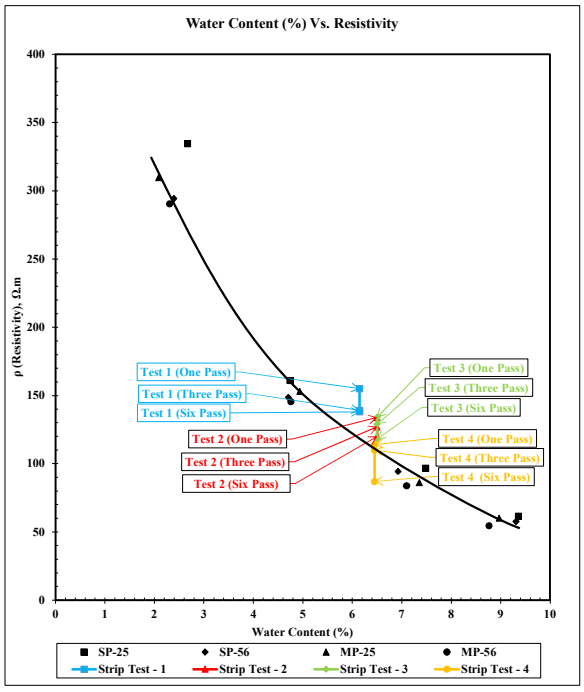
Water Content (%) Vs. Resistivity
ρ (Resistivity), Ω.m
Water Content (%)
Test 1 (One Pass)
Test 1 (Three Pass)
Test 1 (Six Pass)
Test 2 (One Pass)
Test 2 (Three Pass)
Test 2 (Six Pass)
Test 3 (One Pass)
Test 3 (Three Pass)
Test 3 (Six Pass)
Test 4 (One Pass)
Test 4 (Three Pass)
Test 4 (Six Pass)
SP-25
SP-56
MP-25
MP-56
Strip Test - 1
Strip Test - 2
Strip Test - 3
Strip Test - 4

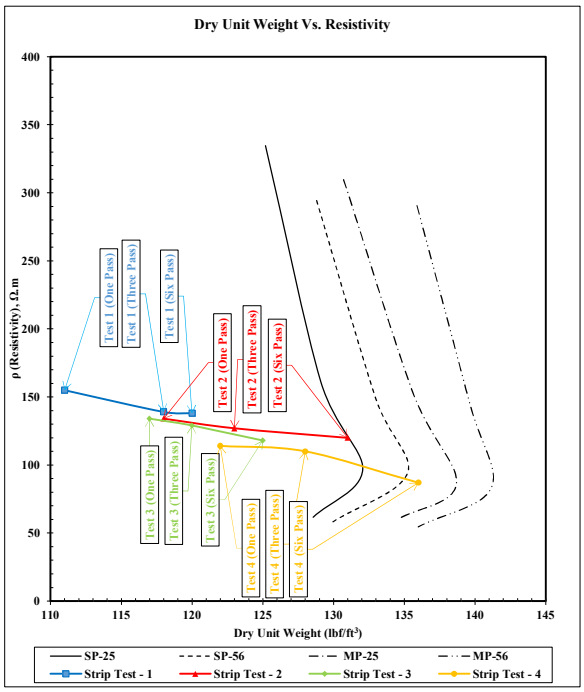
Dry Unit Weight Vs. Resistivity
ρ (Resistivity), Ω.m
Dry Unit Weight (lbf/ft³)
Test 1 (One Pass)
Test 1 (Three Pass)
Test 1 (Six Pass)
Test 2 (One Pass)
Test 2 (Three Pass)
Test 2 (Six Pass)
Test 3 (One Pass)
Test 3 (Three Pass)
Test 3 (Six Pass)
Test 4 (One Pass)
Test 4 (Three Pass)
Test 4 (Six Pass)
SP-25
SP-56
MP-25
MP-56
Strip Test - 1
Strip Test - 2
Strip Test - 3
Strip Test - 4

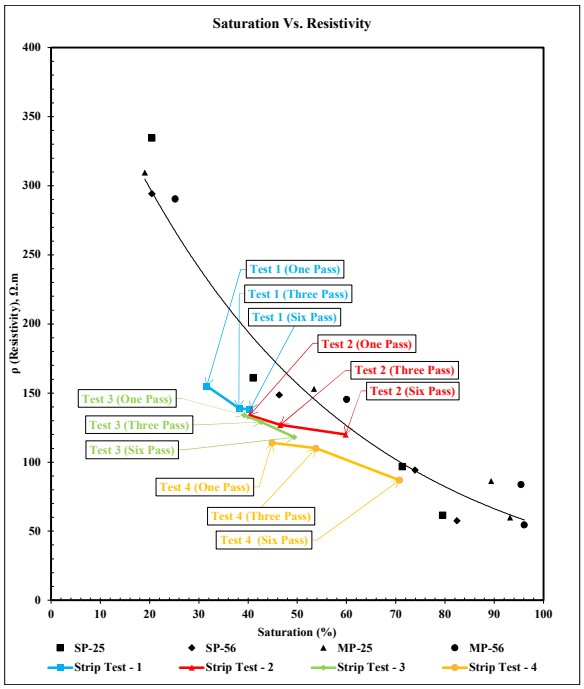

	ω (%)	γd (lb/ft^3)	ρ (Resistivity) Ω.m	Saturation (%)
Standard Proctor N=25	2.67	125.2	335	20
	4.74	129.1	161	41
	7.48	132.1	97	71
	9.36	128.6	62	80
Standard Proctor N=56	2.39	128.8	294	20
	4.70	133.0	149	46
	6.93	135.2	94	74
	9.31	129.8	58	82
Modified Proctor N=25	2.09	130.7	310	19
	4.94	135.6	153	53
	7.36	138.7	86	89
	8.97	134.5	60	93
Modified Proctor N=56	2.31	135.9	290	25
	4.76	139.6	145	60
	7.10	141.2	84	95
	8.76	136.0	55	96

		γ_d (lb/ft^3)	ρ (Resistivity) Ω.m	ω (%)	S(%)	Relative Compaction (%)
test 1	One Pass	111	155	6.15	32	80.0
	Three Pass	118	139	6.15	38	85.1
	Six Pass	120	138	6.15	40	86.5
test 2	One Pass	118	134	6.5	40	85.1
	Three Pass	123	127	6.5	47	88.7
	Six Pass	131	120	6.5	60	94.4
test 3	One Pass	117	134	6.5	39	84.4
	Three Pass	120	129	6.5	43	86.5
	Six Pass	125	118	6.5	49	90.1
test 4	One Pass	122	114	6.45	45	88.0
	Three Pass	128	110	6.45	54	92.3
	Six Pass	136	87	6.45	71	98.1

Test Number	ω	γ_d (lb/ft^3) One Pass	γ_d (lb/ft^3) Three Pass	γ_d (lb/ft^3) Six Pass	ρ (Resistivity) Ω.m One Passes	ρ (Resistivity) Ω.m Three Passes	ρ (Resistivity) Ω.m Six Passes
Test 1	6.15	111	118	120	155	139	138
Test 2	6.5	118	123	131	134	127	120
Test 3	6.5	117	120	125	134	129	118
Test 4	6.45	122	128	136	114	110	87

Point		Segment	Depth (in)		Weidth (in)	γ (lb/ft^3)	γd (lb/ft^3)	γ (lb/ft^3)	γd (lb/ft^3)	γ (lb/ft^3)	γd (lb/ft^3)	VCD	mACD	VCD	mACD	VCD	mACD	Resistance	ρ (Resistivity) Ω.m	Resistance	ρ (Resistivity) Ω.m	Resistance	ρ (Resistivity) Ω.m
1	2	B1	14 1/4	14 1/8	13 1/4	117.5	110.7	124.7	117.5	127.3	120.0	-	-	-	-	-	-	-	-	-	-	-	-
3	4	B2	14 1/4	14 1/4	13 1/4	117.5	110.7	124.7	117.5	127.3	120.0	0.33	0.53	0.35	0.53	0.39	0.66	623	164	660	174	591	156
5	6	B3	14 3/8	14 3/8	13 1/4	117.5	110.7	124.7	117.5	127.3	120.0	0.36	0.72	0.37	0.69	0.44	0.81	500	132	536	141	543	143
7	8	B4	14 3/8	14 1/4	13 1/4	117.5	110.7	124.7	117.5	127.3	120.0	0.36	0.63	0.37	0.74	0.39	0.78	571	151	500	132	500	132
9	10	B5	14 1/6	14 1/4	13 1/4	117.5	110.7	124.7	117.5	127.3	120.0	0.39	0.65	0.38	0.75	0.39	0.68	600	158	507	134	574	151
11	12	B6	14 1/4	14 1/4	13 1/4	117.5	110.7	124.7	117.5	127.3	120.0	0.41	0.65	0.41	0.8	0.36	0.62	631	166	513	135	581	153
13	14	B7	14 1/4	14 1/4	13 1/4	117.5	110.7	124.7	117.5	127.3	120.0	0.41	0.81	0.44	0.84	0.48	0.97	506	133	524	138	495	130
15	16	B8	14 1/4	14 1/4	13 1/4	117.5	110.7	124.7	117.5	127.3	120.0	0.53	0.86	0.54	1.07	0.56	1.18	616	162	505	133	475	125
17	18	B9	14 3/8	14 3/8	13 1/4	117.5	110.7	124.7	117.5	127.3	120.0	0.57	0.82	0.48	0.93	0.48	1	695	183	516	136	480	127
19	20	B10	14 1/4	14 1/4	13 1/4	117.5	110.7	124.7	117.5	127.3	120.0	0.36	0.63	0.44	0.9	0.47	0.96	571	151	489	129	490	129
21	22	B11	14 5/32	14 1/4	13 1/4	117.5	110.7	124.7	117.5	127.3	120.0	0.48	0.82	0.5	0.98	0.51	1.02	585	154	510	134	500	132
23	24	B12	14 1/4	14 3/16	13 1/4	117.5	110.7	124.7	117.5	127.3	120.0	-	-	-	-	-	-	-	-	-	-	-	-
		Avg	14 1/4	14 1/4	13 1/4	117	111	125	118	127	120	0.42	0.71	0.43	0.82	0.45	0.87	590	155	526	139	523	138

Location						1 pass	3 pass	6 pass	1 pass		3 pass		6 pass		1 pass		3 pass		6 pass		1 pass		3 pass		6 pass	
Point		Segment	Depth (in)		Weidth (in)	Layer 1 Depth	Layer 1 Depth	Layer 1 Depth	γ (lb/ft^3)	γd (lb/ft^3)	γ (lb/ft^3)	γd (lb/ft^3)	γ (lb/ft^3)	γd (lb/ft^3)	VCD	mACD	VCD	mACD	VCD	mACD	Resistance	ρ (Resistivity) Ω.m	Resistance	ρ (Resistivity) Ω.m	Resistance	ρ (Resistivity) Ω.m
1	2	B1	14 3/8	14 1/8	13 1/4	-	-	-	-	-	-	-	-	-	-	-	-	-	-	-	-	-	-	-	-	-
3	4	B2	14 1/2	14 1/4	13 1/4	9 7/8	9 8/9	10	141.6	133.0	142.1	133.5	146.7	137.8	0.38	0.81	0.43	0.87	0.37	1.12	469.14	124	494.25	130	330.36	87
5	6	B3	14 3/8	14 3/8	13 1/4	9 3/4	9 7/8	10	137.8	129.4	141.6	133.0	146.7	137.8	0.44	0.99	0.4	0.8	0.35	1.04	444.44	117	500.00	132	336.54	89
7	8	B4	14 3/8	14 1/4	13 1/4	9 3/8	9 3/4	10	129.1	121.2	139.7	131.2	148.3	139.3	0.43	0.96	0.41	0.91	0.34	1.1	447.92	118	450.55	119	309.09	81
9	10	B5	14 1/4	14 1/4	13 1/4	9 4/9	9 5/9	9 7/8	132.4	124.4	135.5	127.3	145.7	136.8	0.42	0.92	0.4	1.07	0.37	1.05	456.52	120	373.83	99	352.38	93
11	12	B6	14 3/8	14 1/4	13 1/4	9 1/4	9 1/2	9 3/4	125.9	118.3	132.8	124.8	139.7	131.2	0.42	0.97	0.45	1.18	0.4	1.06	432.99	114	381.36	101	377.36	99
13	14	B7	14 1/4	14 1/4	13 1/4	9 1/6	9 1/4	9 3/4	125.5	117.9	127.5	119.7	141.6	133.0	0.41	0.99	0.43	1.05	0.36	1.12	414.14	109	409.52	108	321.43	85
15	16	B8	14 1/4	14 1/4	13 1/4	9 1/6	9 1/3	9 7/8	125.1	117.5	129.1	121.2	145.7	136.8	0.41	0.97	0.45	1.16	0.36	1.21	422.68	111	387.93	102	297.52	78
17	18	B9	14 3/8	14 3/8	13 1/4	9 1/6	9 1/2	9 3/4	122.1	114.7	130.7	122.8	137.8	129.4	0.41	0.99	0.44	1.16	0.4	1.25	414.14	109	379.31	100	320.00	84
19	20	B10	14 5/16	14 1/4	13 1/4	9 1/4	9 3/4	9 7/8	126.7	119.0	140.6	132.1	144.6	135.9	0.4	1.03	0.45	1.17	0.41	1.28	388.35	102	384.62	101	320.31	84
21	22	B11	14 5/16	14 1/4	13 1/4	9 1/2	9 3/4	10	133.3	125.2	140.6	132.1	149.4	140.3	0.36	0.8	0.44	1.05	0.41	1.2	450.00	119	419.05	110	341.67	90
23	24	B12	14 5/16	14 3/16	13 1/4	-	-	-	-	-	-	-	-	-	-	-	-	-	-	-	-	-	-	-	-	-
		Avg	14 1/3	14 1/4	13 1/4	-	-	Avg	130	122	136	128	145	136	0.408	0.943	0.430	1.042	0.377	1.143	434	114	418	110	331	87

Location						1 pass	3 pass	6 pass	1 pass		3 pass		6 pass		1 pass		3 pass		6 pass		1 pass		3 pass		6 pass	
Point		Segment	Depth (in)		Weidth (in)	Layer 1 Depth	Layer 1 Depth	Layer 1 Depth	γ (lb/ft^3)	γd (lb/ft^3)	γ (lb/ft^3)	γd (lb/ft^3)	γ (lb/ft^3)	γd (lb/ft^3)	VCD	mACD	VCD	mACD	VCD	mACD	Resistance	ρ (Resistivity) Ω.m	Resistance	ρ (Resistivity) Ω.m	Resistance	ρ (Resistivity) Ω.m
1	2	B1	14 3/8	14 1/8	13 1/4	-	-	-	-	-	-	-	-	-	-	-	-	-	-	-	-	-	-	-	-	-
3	4	B2	14 1/2	14 1/4	13 1/4	9 7/8	9 8/9	10	136.7	128.4	137.1	128.8	141.6	133.0	0.4	0.78	0.43	0.83	0.38	0.8	513	135	518	137	475	125
5	6	B3	14 3/8	14 3/8	13 1/4	9 3/4	9 7/8	10	133.0	124.9	136.7	128.4	141.6	133.0	0.45	0.94	0.43	0.92	0.39	0.9	479	126	467	123	433	114
7	8	B4	14 3/8	14 1/4	13 1/4	9 3/8	9 3/4	10	124.6	117.0	134.8	126.6	143.1	134.5	0.41	0.87	0.45	0.98	0.43	1.03	471	124	459	121	417	110
9	10	B5	14 1/4	14 1/4	13 1/4	9 4/9	9 5/9	9 7/8	127.8	120.1	130.8	122.9	140.6	132.1	0.43	0.92	0.43	0.89	0.38	0.89	467	123	483	127	427	113
11	12	B6	14 3/8	14 1/4	13 1/4	9 1/4	9 1/2	9 3/4	121.5	114.1	128.2	120.5	134.8	126.6	0.45	0.94	0.39	0.89	0.41	0.92	479	126	438	115	446	117
13	14	B7	14 1/4	14 1/4	13 1/4	9 1/6	9 1/4	9 3/4	121.1	113.8	123.0	115.6	136.7	128.4	0.46	0.89	0.44	0.89	0.42	0.87	517	136	494	130	483	127
15	16	B8	14 1/4	14 1/4	13 1/4	9 1/6	9 1/3	9 7/8	120.7	113.4	124.6	117.0	140.6	132.1	0.41	0.79	0.43	0.84	0.41	0.93	519	137	512	135	441	116
17	18	B9	14 3/8	14 3/8	13 1/4	9 1/6	9 1/2	9 3/4	117.8	110.7	126.2	118.5	133.0	124.9	0.44	0.86	0.42	0.86	0.37	0.85	512	135	488	129	435	115
19	20	B10	14 5/16	14 1/4	13 1/4	9 1/4	9 3/4	9 7/8	122.2	114.8	135.7	127.5	139.6	131.1	0.48	0.86	0.46	0.85	0.45	0.98	558	147	541	143	459	121
21	22	B11	14 5/16	14 1/4	13 1/4	9 1/2	9 3/4	10	128.6	120.8	135.7	127.5	144.2	135.5	0.47	0.81	0.36	0.86	0.46	0.87	580	153	419	110	529	139
23	24	B12	14 5/16	14 3/16	13 1/4	-	-	-	-	-	-	-	-	-	-	-	-	-	-	-	-	-	-	-	-	-
		Avg	14 1/3	14 1/4	13 1/4	-	-	Avg	125	118	131	123	140	131	0.440	0.866	0.424	0.881	0.410	0.904	509	134	482	127	455	120

Location					1 pass	3 pass	6 pass	1 pass		3 pass		6 pass		1 pass		3 pass		6 pass		1 pass		3 pass		6 pass	
Point		Segment	Depth (in)	Weidth (in)	Layer 1 Depth	Layer 1 Depth	Layer 1 Depth	γ (lb/ft³)	γ± (lb/ft³)	γ (lb/ft³)	γ± (lb/ft³)	γ (lb/ft³)	γ± (lb/ft³)	VCD	mACD	VCD	mACD	VCD	mACD	Resistance	ρ (Resistivity) Ω.m	Resistance	ρ (Resistivity) Ω.m	Resistance	ρ (Resistivity) Ω.m
1	2	B1	-	13 1/4	-	-	-	-	-	-	-	-	-	-	-	-	-	-	-	-	-	-	-	-	-
3	4	B2	9 8/9	9 8/9	13 1/4	5	5 1/4	5 1/3	125.8	118.1	132.5	124.5	134.3	126.2	1.91	3.38	1.83	3.71	1.54	3.25	565.09	149	493.26	130	473.85	125
5	6	B3	9 7/8	9 7/8	13 1/4	4 3/4	5	5 1/8	120.0	112.7	127.8	120.1	129.5	121.6	1.83	3.91	1.78	3.84	1.64	3.83	468.03	123	463.54	122	429.20	113
7	8	B4	9 3/4	9 3/4	13 1/4	4 5/8	4 7/9	5	120.0	112.7	123.8	116.3	129.5	121.6	1.77	3.4	1.88	4.28	1.89	4.55	520.59	137	439.25	116	415.38	109
9	10	B5	9 5/9	9 5/9	13 1/4	4 3/8	4 5/8	4 7/8	118.9	111.7	125.0	117.4	131.6	123.7	1.79	3.9	1.71	3.77	1.52	3.64	458.97	121	453.58	120	417.58	110
11	12	B6	9 1/2	9 1/2	13 1/4	4 1/2	4 5/8	4 7/9	122.6	115.2	125.8	118.1	129.9	122.0	1.9	4.01	1.53	3.37	1.72	4	473.82	125	454.01	120	430.00	113
13	14	B7	9 1/4	9 1/4	13 1/4	4 5/8	4 5/8	4 7/9	133.0	124.9	133.0	124.9	137.6	129.3	1.89	3.77	1.73	3.31	1.71	3.7	501.33	132	522.66	138	462.16	122
15	16	B8	9 1/3	9 1/3	13 1/4	4 3/4	4 2/3	4 7/9	134.8	126.6	133.0	124.9	135.7	127.5	1.72	3.36	1.72	3.54	1.73	4.04	511.90	135	485.88	128	428.22	113
17	18	B9	9 1/2	9 1/2	13 1/4	5	4 3/4	5	136.7	128.4	129.5	121.6	134.8	126.6	1.76	3.66	1.67	3.27	1.49	3.5	480.87	127	510.70	135	425.71	112
19	20	B10	9 3/4	9 3/4	13 1/4	4 3/4	4 7/8	5	123.0	115.6	126.2	118.5	127.8	120.1	2.01	3.75	1.83	3.51	1.89	4.12	536.00	141	521.37	137	458.74	121
21	22	B11	9 3/4	9 3/4	13 1/4	4 3/8	4 7/9	5 1/5	114.4	107.5	123.8	116.3	134.8	126.6	1.85	3.37	1.76	3.15	1.88	3.52	548.96	145	558.73	147	534.09	141
23	24	B12		13 1/4	-	-	-	-	-	-	-	-	-	-	-	-	-	-	-	-	-	-	-	-	-	-
		Avg	9 3/5	9 3/5	13 1/4	-	-	Avg	125	117	128	120	133	125	1.843	3.651	1.744	3.575	1.701	3.815	507	134	490	129	447	118

Field Unit Weight-Sand Cone Method		
Item	Quantity	Unit
Calibration of Unit Weight of Ottawa Sand		
. Weight of Proctor mold, W_1	9.40	lb
. Weight of Proctor mold + Sand, W_2	12.69	lb
. Volume of the mold, V_1	0.03294	ft^3
. Dry Unit Weight, $\gamma_{d(Sand)}$	99.9	lb/ft^3
Calibration Cone		
. Weight of bottle + Cone + Sand (before use), W_3	16.23	lb
. Weight of bottle + Cone + Sand (after use), W_4	12.72	lb
. Weight of Sand to Fill Cone, W_c	3.51	lb
Result from Field Tests		
. Weight of bottle + Cone + Sand (before use), W_6	12.34	lb
. Weight of bottle + Cone + Sand (after use), W_8	6.52	lb
0. Volume of hole, V_2	0.0231336	ft^3
1. Weight of Can, W_5	0.14	lb
2. Weight of Can +moist soil, W_7	0.307	lb
3. Weight of Can +dry soil, W_9	0.298	lb
4. Weight of Extracted Soil, W_{10}	3.14	lb
5. Moisture Unit Weight of Soil in Field, γ	135.7	lb/ft^3
6. Moisture Content in field, ω	6.14	%
7. Dry Unit Weight, γ_d	127.9	lb/ft^3

Field Unit Weight-Sand Cone Method		
Item	Quantity	Unit
Calibration of Unit Weight of Ottawa Sand		
. Weight of Proctor mold, W_1	9.40	lb
. Weight of Proctor mold + Sand, W_2	12.69	lb
. Volume of the mold, V_1	0.03294	ft^3
. Dry Unit Weight, $\gamma_{d(Sand)}$	99.9	lb/ft^3
Calibration Cone		
. Weight of bottle + Cone + Sand (before use), W_3	16.26	lb
. Weight of bottle + Cone + Sand (after use), W_4	12.62	lb
. Weight of Sand to Fill Cone, W_c	3.64	lb
Result from Field Tests		
. Weight of bottle + Cone + Sand (before use), W_6	13.45	lb
. Weight of bottle + Cone + Sand (after use), W_8	7.5	lb
0. Volume of hole, V_2	0.023133581	ft^3
1. Weight of Can, W_5	0.14	lb
2. Weight of Can +moist soil, W_7	0.320	lb
3. Weight of Can +dry soil, W_9	0.310	lb
4. Weight of Extracted Soil, W_{10}	3.23	lb
5. Moisture Unit Weight of Soil in Field, γ	139.6	lb/ft^3
6. Moisture Content in field, ω	6.15	%
7. Dry Unit Weight, γ_d	131.5	lb/ft^3

Field Unit Weight-Sand Cone Method		
Item	Quantity	Unit
Calibration of Unit Weight of Ottawa Sand		
1. Weight of Proctor mold, W_1	9.40	lb
2. Weight of Proctor mold + Sand, W_2	12.69	lb
3. Volume of the mold, V_1	0.03294	ft^3
4. Dry Unit Weight, $\gamma_{d(Sand)}$	99.9	lb/ft^3
Calibration Cone		
5. Weight of bottle + Cone + Sand (before use), W_3	16.26	lb
6. Weight of bottle + Cone + Sand (after use), W_4	12.56	lb
7. Weight of Sand to Fill Cone, W_c	3.70	lb
Result from Field Tests		
8. Weight of bottle + Cone + Sand (before use), W_6	12.56	lb
9. Weight of bottle + Cone + Sand (after use), W_8	6.74	lb
10. Volume of hole, V_2	0.0212308	ft^3
11. Weight of Can, W_5	0.14	lb
12. Weight of Can +moist soil, W_7	0.320	lb
13. Weight of Can +dry soil, W_9	0.309	lb
14. Weight of Extracted Soil, W_{10}	3.14	lb
15. Moisture Unit Weight of Soil in Field, γ	147.9	lb/ft^3
16. Moisture Content in field, ω	6.45	%
17. Dry Unit Weight, γ_d	138.9	lb/ft^3